ROLES OF TMIGD3 AND A3AR IN SUPPRESSION OF OSTEOSARCOMA MALIGNANCY

By

SWATHI V. IYER

Submitted to the graduate degree program in Molecular and Integrative Physiology with an emphasis in Cancer Biology and the Graduate Faculty of the University of Kansas in partial fulfillment of the requirements for the degree of Doctor of Philosophy.

_____

Co-chair: Tomoo Iwakuma, M.D. Ph.D.

_____

Co-chair: David F. Albertini, Ph.D.

_____

Shrikant Anant, Ph.D.

_____

Fariba Behbod, PharmD, Ph.D.

_____

James P. Calvet, Ph.D.

Date Defended: 24th March 2016

The dissertation committee for Swathi V Iyer certifies that this is the approved version of the following dissertation:

ROLES OF TMIGD3 AND A3AR IN SUPPRESSION OF OSTEOSARCOMA MALIGNANCY

_____

Co-Chair: Tomoo Iwakuma, M.D. Ph.D.

_____

Co-Chair: David F. Albertini, Ph.D.

Date Approved: 4/22/16

ABSTRACT

Osteosarcoma (OS) is the second leading cause of cancer-related death in children and young adults. Despite advances in the treatment for OS, the survival rate of high-grade OS has reached a plateau and remains at 50-80% for the past three decades due to its highly metastatic and drug resistant nature. However, the crucial players that regulate malignant properties of OS and the underlying mechanisms are unclear. Towards this goal we attempted to identify factors whose knockdown could overcome cell death and proliferation arrest induced by anchorage-independence, serum-free conditions, leading to sphere formation. Thus, we screened a human whole-genome shRNA library using SJSA-1 OS cells harboring poor sphere forming potential. This screening led to the identification of an uncharacterized gene, namely "transmembrane and immunoglobulin domain containing 3 (TMIGD3)". Our *in vitro* and *in vivo* experiments successfully revealed that downregulation of TMIGD3 using two independent shRNAs significantly increased sphere formation, cell migration, tumor formation, and metastases of multiple OS cells. Interestingly, overexpression of TMIGD3 isoform1 (i1) significantly suppressed cell proliferation, sphere formation and tumor formation, whereas its isoform 3 (i3) sharing the C-terminal region with i1 failed to do so. Since the N-terminal region consisting of 117 amino acids of TMIGD3 i1 is shared with the N-terminal region of adenosine A3 receptor (A3AR), we also overexpressed A3AR in OS cells and found that A3AR overexpression suppressed proliferation, migration, and tumor formation of OS cells as well. These results suggest that the N-terminal region plays a crucial role in the suppression of OS malignancy. We furthermore found that TMIGD3 downregulation, similar to A3AR knockdown led to an

increase in the activity of NF-κB, a well-characterized downstream signaling of A3AR. Subsequent knockdown of NF-κB in cells downregulated for TMIGD3 abrogated their enhanced malignant properties. Analysis of human OS tissues revealed low expression of both TMIGD3 and A3AR when compared to normal bone and lung tissues. Additionally, we questioned the role of TMIGD3 in influencing stem-like properties of OS, since TMIGD3 knockdown in OS cells increased sphere formation, a hallmark of stem-like properties *in vitro*. We found that downregulation of TMIGD3 increased stem cell transcription factor expression, tumor initiation potential, and activity of aldehyde dehydrogenase (ALDH). These data suggest the potential role of TMIGD3 as a novel regulator of stem-like properties of OS.

In summary, our study identified TMIGD3 i1 and A3AR as novel suppressors of OS malignancy and suggests that signaling regulated by TMIGD3 i1 and A3AR could serve as a potential targets for treatment of high grade OS.

ACKNOWLEDGEMENTS

I would like to take this opportunity to express my sincere gratitude for my mentor, Dr. Tomoo Iwakuma. It has been a very exciting and memorable experience of my life for the past 6 years. I would like to thank him for being my unfaltering coach, for being my guiding light, and teaching me the great aspects of being a successful scientist. This is just the beginning of my journey and I am very glad to have started the climb to scientific achievement as his student. His utmost priority on performing exemplary research and the success of his lab members kept me always heading in the right direction and enabled me to raise my standards of research to a high level. The weekly scientific meetings and discussions, personal meetings, besides long discussions on pertinent scientific questions has been the central tenet to my development as a novice critical thinker. I would also like to thank all present and past lab members of Dr. Iwakuma's lab. They have been more than just colleagues and encouraged me, supported me, and guided me through these years as my genuine well-wishers.

I would also like to express my deepest appreciation for each of my committee members, Dr. David Albertini, Dr. Shrikant Anant, Dr. Fariba Behbod and Dr. James Calvet for providing me with guidance and scientific expertise for the improvement of my study. They also played a tremendous role in shaping my scientific acumen as a graduate student. I greatly appreciate their time, advice, constructive criticism, patience and support through the entire course of my project.

I also want to extend my gratitude to the Department of Physiology, for giving me the chance of being a part of your Department and making my transfer process so

smooth. I fit right into my Graduate responsibilities with ease following my transfer from LSU Health Sciences Center, and have to thank the Department of Physiology staff members especially the administrative staff, and Dr. Lane Christenson and Dr. Michael Wolfe for their support and help. Additionally, I would also like to thank Dr. Danny Welch for letting me share his excellent lab facilities that have been a key to the success of my project and giving me the pleasure of being a representative of the Cancer Biology Department.

I would like to take this opportunity to express my sincere thanks to the Department of Genetics of LSU Health Sciences Center especially Dr. Dipatsri Mandal, Dr. Jay Kolls, Dr. Andrew Hollenbach for satiating my scientific curiosity during my early years as a graduate student, and for supporting me and helping me cope with the plethora of experiences in a new environment.

Most of all, I am greatly indebted to my family- my parents and my sister for their support and belief in me. My parents have provided me with the best of the education that gave me immense opportunities and has led me to the place I am today. I still have a long way to go, but my success today is greatly dependent on their support and encouragement through my formative years. In spite of being the first biologist in my entire family, my parents never faltered in encouraging me with my career decisions and I am greatly thankful to them and my sister in particular, for being my emotional and mental pillars of strength.

Also, this memorable journey would not have been successful without the support from my ever-encouraging friends here in Kansas City as well as in New Orleans. My anxieties of adjusting to a new country and to then a new city, KC were lost

immediately when my friends welcomed me with open arms. Special thanks to Harold Elias for your inundating support, encouragement, optimism, strength and affection.

Last but not the least, I would also like to thank the financial support provided for my study through the National Institutes of Health, American Cancer Society (awarded to Dr. Iwakuma), and the University of Kansas Medical Center Biomedical Research Training Program (BRTP).

TABLE OF CONTENTS

LIST OF ABBREVIATIONS

A3AR	Adenosine Receptor 3
aa	Amino acids
AC	Adenylyl cyclase
ADA	Adenosine deaminase
ADP	Adenosine diphosphate
ALDH	Aldehyde Dehydrogenase
ALP	Alkaline phosphatase
AMP	Adenosine monophosphate
AR	Adenosine receptors
ATP	Adenosine triphosphate
BMP-2	Bone morphogenetic protein
cAMP	cyclic AMP
CDK	Cyclin dependent kinase
CDK4	Cyclin dependent kinase 4
CNT	Concentrative nucleoside transporter
CSCs	Cancer stem cells
DAG	Diacylglycerol
DEAB	Diethylaminobenzaldehyde
DMEM	Dulbecco’s Modified Eagle’s Medium
ENT	Equilibrative nucleoside transporter
ER	Estrogen receptor
Erk	Extracellular Receptor Kinase

FACS	Fluorescence activated cell sorting
GDP	Guanosine diphosphate
GEFs	Guanine nucleotide exchange factors
GIRKs	G-protein regulated inward rectifying K+ channels
GPCR	G-protein coupled receptor
GRKs	G-protein coupled receptor kinases
GSK3β	Glycogen synthase kinase 3β
HBSS	Hank's balanced salt solution
i1	Isoform 1
i3	Isoform 3
IgG	Immunoglobulin G
IHC	Immunohistochemistry
IP_3	Inositol 1,4,5 triphosphate
LDH	lactate dehydrogenase
LOH	Loss of heterozygosity
MAPK	Mitogen-Activated Protein Kinase
MDM2	Mouse double minute 2 homolog
MEK	MAPK/Erk Kinase
MOI	Multiplicity of infection
NGF	Nerve growth factor
NSG	NOD-scid IL2Rγ^{null}
OPG	Osteoprotegin
OS	Osteosarcoma

OSX	Osterix
pErk	Phospho- Extracellular Receptor Kinase
PI3K	Phophoinositide 3- kinase
PI3K	Phosphatidylinositol 3-kinase
PIP_2	Phosphatidylinositol-4,5-bisphosphate
PKB/AKT	Protein kinase B
PKC	Protein kinase C
PLC	Phospholipase C
PLCβ	Phospholipase Cβ
qRT-PCR	Quantitative reverse transcription PCR
RANKL	Receptor activator of nuclear factor-κB ligand
RB	Retinoblastoma
RECQL4	RecQ protein like-4
RGS	Regulators of G-protein signaling
RPMI	Roswell Park Memorial Institute
RTS	Rothmund-Thomson syndrome
RUNX2	RUNX-related transcription factor 1
S.D	Standard deviation
shRNA	small hairpin or short hairpin ribonucleic acid
SP	Side population
SPATC1	Spermatogenesis and centriole associated 1
TICs	Tumor-initiating cells
TMIGD3	Transmembrane and Immunoglobulin Domain containing 3

UTR	Untranslated region
WB	Western Blot
WRN	Werner’s syndrome

LIST OF FIGURES AND TABLES

LIST OF FIGURES

CHAPTER 1: BACKGROUND AND INTRODUCTION

CHAPTER 2: GENOME-WIDE SCREENING TO IDENTIFY FACTORS THAT REGULATE SPHERE FORMATION OF OS CELLS

CHAPTER 3: ROLE OF TMIGD3 AND A3AR IN MALIGNANT PROPERTIES OF OS

CHAPTER 4: SIGNALING PATHWAYS REGULATED BY TMIGD3 AND A3AR

CHAPTER 5: PRELIMINARY RESULTS ELUCIDATING THE ROLE OF TMIGD3 IN STEM-LIKE PROPERTIES OF OS

LIST OF TABLES

CHAPTER 1

BACKGROUND AND INTRODUCTION

1.1 Osteosarcoma- An unsolved deadly malignancy

Sarcomas account for ~1% of all malignancies, however they occur with a high frequency in children, comprising of ~15% of all childhood cancers[1]. Osteosarcoma (OS) is a primary mesenchymal tumor characterized by the production of osteoid by malignant cells[2]. French surgeon Alexis Boyer coined the term OS as early as 1805. It is a relatively rare malignancy with approximately 800 cases diagnosed per year in the US[3]. Despite the rarity, OS is the most common primary malignancy of the bone that accounts for approximately 3.4% of all childhood cancers and 56% of malignant bone tumors in children[4,5]. The mainstay of treatment includes primary tumor surgical resection and/or radiation therapy combined with systemic chemotherapy (doxorubicin and cisplatin with or without methotrexate). Many patients develop resistance to the treatment and relapse. While the five-year survival rates for localized disease have stayed at 70%, patients who manifest micrometastases, which are observed in 80% of cases and those who have disease relapse, continue to have dismal outcomes with survival rates of about 20%[6]. Targeted therapy that aims at developing treatments directed towards molecular anomalies essential for tumorigenesis is an exciting and hopeful development in cancer treatment for the past 10 years. However, as of now, no such targeted therapy is available for OS, and there is a great need for developing new therapies, to improve the prognosis of patients with high grade OS.

1.2 Epidemiology

OS represents occurrence at two distinct stages in life: an initial peak at adolescent age and the second peak during or after the 6th decade of life[7]. An association between rapid bone growth and occurrence of the disease is debated, owing to the tumor's typical metaphyseal location and the peak incidence during adolescence and early childhood. The observation that large breed canines have a 185-fold risk compared to small breed canines supports this theory[8]. In humans, as well, OS does occur in patients significantly taller than the general population[9,10]. The incidence is slightly higher in men when compared to women (male/female ratio, ~1.6), but peaks earlier among females (age 12 years / age 16 years), which may be attributed to differences in growth spurt between the two sexes[10]. The incidence rates for OS for all races and both sexes, in children and adolescents in the US are 4.5 cases per million people per year[11]. Age standardized incidence rates for OS in both males and females does not appear to differ significantly between Asian countries and the US[1]. Overall, the incidence rates for OS seem to be quite comparable throughout the world. However, there are some reports of notable differences such as the increase in incidence rates observed amongst Japanese males living in the state of California (1.3 per 100,000 males), which is considered to be relatively high compared to rates throughout the world, and in Japan in particular[12]. Similarly, high incidence rates are also observed in Japanese males living in Hawaii, suggesting that Japanese migrants may be subjected to a higher risk of OS due to environmental influences or lifestyle[12]. These data suggest that there might be a geographic or ethnic influence on OS incidence.

1.3 Clinical presentation

Patients present with localized pain at rest and swelling of the affected area. Diagnostic lab values are not very useful with the exception of alkaline phosphatase (ALP)[13], which is elevated in approximately 40% of cases, and lactate dehydrogenase (LDH)[14], which is elevated in 30% of cases. Although, these markers have some prognostic information[15], their significance as biomarkers for OS is questionable.

Metastatic disease is presented as macrometastases in 10-20% of patients and micrometastases in 80% of patients at the time of diagnosis. The most common sites include lungs followed by other bones. The presence of metastases is considered to be the most potent and reliable prognostic indicator that reduces survival from 70% to less than 20%.

1.4 Pathogenesis

1.4.1 Bone growth and tumorigenesis

Development of OS has been associated with a preference for rapidly growing bone. Rapid bone growth observed during puberty is well correlated with OS growth. There is a slightly higher incidence in boys (57%) when compared with girls (44%)[11], though the peak age for OS development is slightly earlier in females than in males, owing to the differences in their respective skeletal growth[16]. Bone is composed of two cell types, which are responsible for bone formation (osteoblast) or resorption (osteoclast). Osteoblasts, the bone forming cells, arise from mesenchymal stem cells expressing markers such as RUNX-related transcription factor 1 (RUNX2), Osterix (OSX), Osteopontin, Bone sialoprotein and Ostecalcin[17]. These cells synthesize type I

collagen which comprises 95% of the bone matrix, called osteoid. OS share many characteristics of immature osteoblasts[18]. The other type of cells present in the bone is the osteoclasts that are responsible for bone resorption, hence considered to be highly specialized macrophages. Osteoclasts are derived from the monocyte lineage, and have phagocytic-like mechanisms like macrophages[19]. Osteoclast differentiation and function are tightly regulated by osteoblasts that secrete local signals, of which the most important are receptor activator of nuclear factor-κB ligand (RANKL) and osteoprotegin (OPG). RANKL mediates differentiation of osteoclasts and activity through binding to its receptor RANK, present on the surface of osteoclasts [20]. On the other hand, OPG is a decoy receptor for RANKL, and inhibits the differentiation of osteoclasts [21]. Increased osteoclast activity is directly correlated with enhanced osteolytic activity of bone matrix exhibited by OS, aiding in the process of invasion [22].

1.4.2 Environmental factors

Many physical, chemical, and biological factors have been suggested as carcinogens for OS. Ionizing radiation and UV exposure are very well correlated with OS development. Most of the secondary OS cases are attributed to ionizing radiation regardless of chemotherapy treatment. Radiation-induced OS account for 3%, appearance of which is reported almost 30 years following radiation exposure [23]. OS caused by radiation is dose-dependent and its incidence is increasing in patients following irradiation for the treatment of other primary tumors [24]. Chemical agents such as methylchlanthrene and chromium salts[25], beryllium oxide [26] and asbestos [27] may also be associated with OS development.

1.4.3 Bone diseases

Paget's disease of the bone is characterized by abnormal bone turnover, associated with extensive bone remodeling resulting in weakened bone tissue and affects patients generally over 40 years of life [28,29]. This disease was discovered in 1877 by Sir James Paget and has been associated with defects in the genes *PDB2* (18q) and *SQSTM1* (5q) [30]. This disease is associated with high level of osteoclastic bone resorption, resulting in increase in osteoblast proliferation thus accelerating OS development. Approximately, 1% of individuals with Paget's disease develop OS [31].

Heritable multiple osteochondromas are characterized by multiple osteochondromas that are bone tumors comprised of cartilage and bone. The age of diagnosis is 3 years, and almost all individuals affected by this disease are diagnosed by age 12. The two most prominent gene mutations linked to this disease are *EXT1* and *EXT2* ; mutations are detected in almost 70-95% of affected individuals [32]. These patients carry a low risk of developing sarcomas of the bone- most frequently chondrosarcoma (0.5-20%) than OS. The risk of developing a sarcoma is directly related to the number of osteochondrosarcomas present in the individual [32].

1.4.4 Heritable syndromes linked to OS

Patients with Li-Fraumeni syndrome, a rare autosomal dominant disorder carry a germline mutation in the tumor suppressor TP53, of which 12% develop OS [33]. The strongest incidence of genetic predisposition to OS exists in patients carrying germline mutations in the retinoblastoma gene (RB), a key regulator of cell cycle progression [34]. The incidence of OS in patients with retinoblastoma is increased several hundred-fold

[35]. Patients with rare autosomal recessive disorders caused by mutations in the RecQ DNA helicase family members, which are necessary to maintain genome integrity, also have predisposition to OS. One such syndrome, the Rothmund-Thomson syndrome (RTS), is caused by mutations in the helicase RecQ protein like-4 (RECQL4) which is the most strongly associated with OS (32% of individuals develop OS) amongst other syndromes associated with RecQ helicases [36,37]. Another syndrome which has mutations in the RECQL4 is RAPADILINO syndrome, a very rare disorder, of which approximately 10% of cases develop OS [38]. Werner's syndrome (WRN; progeria) is also caused by mutations in the WRN helicase RECQL2 which is characterized by abnormal telomere maintenance and chromosomal rearrangements [39]. Approximately 10% of these patients diagnosed with WRN develop OS[40]. Bloom's syndrome patients have mutations in the BLM DNA helicase, also belonging to the RecQ family[41]. These patients have extremely short stature, and approximately 3% of the patients develop OS.

1.5 Genetics of OS

A variety of alterations including several complex chromosomal rearrangements have been detected using molecular and cytogenetic analyses in OS[42]. However, none of these pathways has been implicated as hallmarks of OS development[43]. Genomic hybridization studies comparing human OS tumors to human osteoblasts identified several areas of DNA gain or loss, and mutations of oncogenes such as MYC, FOS, MDM2 as well as RECQ helicase mutations were found to be associated with a small proportion of OS. Some of these recurrent alterations may have prognostic value [44].

Despite the extensive analyses, the common underlying genetic alterations responsible for disease development and progression still remain obscure [45]. The retinoblastoma (RB) and the TP53 tumor suppressor pathways are the only known strongest genetic associations for sporadic and hereditary OS. As previously stated, Li Fraumeni syndrome patients with a hereditary TP53 mutation are predisposed to OS while patients with RB mutations have a 500-fold increase in the incidence of OS.

Genetic alterations of RB1 are found in 70% of sporadic OS. Loss of heterozygosity (LOH) of the RB locus occurs in 60-70% of OS tumors, which also serves as a poor prognostic factor. RB1 regulates the G1/S transition of the cell cycle, which is hyperphosphorylated, thereby leading to E2F activation and cell cycle progression[46]. The phosphorylation of RB1 is regulated by cyclin dependent kinase 4 (CDK4). The CDKs are in turn regulated by a series of inhibitory proteins, including $p16^{INK4a}$. Loss of $p16^{INK4a}$ is also observed in OS with RB1 alterations [47].

TP53 encodes a transcription factor that regulates genes involved in cell cycle, apoptosis and DNA damage response. Genetic alterations in TP53 observed in OS accounts for 22%[48]. It is observed that inactivation of RB and TP53 in conditional knockout mice leads to spontaneous metastatic OS, in which cells are disrupted in their differentiation processes[49,50]. However, TP53 mutation is not correlated with prognosis of human OS development and/or metastasis [33].

Thus, it is surprising that only few predisposing mutations have been identified for OS progression. Also, the disease processes and key players involved in the malignant properties including metastasis and chemoresistance are not well

established. These concerns need to be addressed towards development of novel promising therapeutic strategies for OS.

1.6 Tumor initiating cells (TICs) and cancer

It is a well-accepted view that tumors comprise a heterogeneous mass comprising a hierarchy of cells. Human OS tumors exhibit osteoblast-like features, and are arrested at different stages of differentiation ranging from highly differentiated to poorly differentiated or undifferentiated subtypes[51]. Increasing evidence suggests that the heterogeneous composition of the tumor may be one of the reasons for the ineffectiveness of the standard radiation and chemotherapeutic regimens [52,53]. Most of these treatments are based on the view that all cancer cells are fast dividing and are tumorigenic, and all cells have the ability to regenerate the entire tumor[54]. This model called the clonal evolution or stochastic model is based on initial studies on the clonal origin of leukemia and oncogenic viruses [55,56]. In contrast, the cancer stem cell (CSC) model proposes that within the heterogeneous tumor mass, there exists a small subpopulation of cells called CSCs that are responsible for the most aggressive properties of the tumor including drug resistance and metastasis [54]. This subpopulation also referred to as tumor initiating cells (TICs), maintains the unique and exclusive capacity to regenerate the bulk of the tumor after chemotherapy or at secondary sites [57](Fig 1.1). A number of studies suggest that OS conforms to a hierarchical CSC model rather than a stochastic model [58-61]. Accumulating evidence has supported the CSC/TIC hypothesis and shown that CSCs/TICs have biological and molecular similarities to somatic stem cells that maintain normal tissues. Numerous reports have

demonstrated that CSCs/TICs possess high tumor initiating potential, as well as other stem-like properties, including high metastatic potential, multi-lineage differentiation, high expression levels of ABC transporters or stem cell transcription factors (e.g. Oct-4, Sox-2, Nanog), stem cell surface markers (e.g. CD133, CD44), aldehyde dehydrogenase (ALDH) activity, and drug resistant properties [62-65]. However, the most important property of CSCs/TICs is the capability of self-renewal, just like normal stem cells, which can be assessed by serial transplantability of selected cellular population. A deeper understanding of the mechanisms underlying generation, maintenance, and enhancement of these CSC/TIC-like properties would help in developing targeted cancer therapy that could aim at the deadly attributes of cancer, such as metastasis and drug resistance.

The first proof of concept study of CSC model came in 1994 in hematologic malignancies conducted by Dick and colleagues who showed that rare CD34+/CD38- cells derived from a leukemia patient gave rise to successful acute myeloid leukemia in transgenic immunocompromised mice demonstrating the ability of regeneration of a tumor from a single cell *in vivo* [66]. CSCs of solid cancers with epithelial, neuro-ectodermal, and mesenchymal origins are also identified as a subpopulation with high ALDH activity, present as side population (SP), or express stem cell surface markers [67]. Their properties are evaluated based on their abilities to grow clonally as spheres in serum- and anchorage-independent conditions, to initiate tumors from low numbers of cells in immunocompromised mice, to regenerate tumors following serial transplantation, and to differentiate into multiple lineages [67,68].

Figure 1.1 Stochastic model vs CSC/TIC model

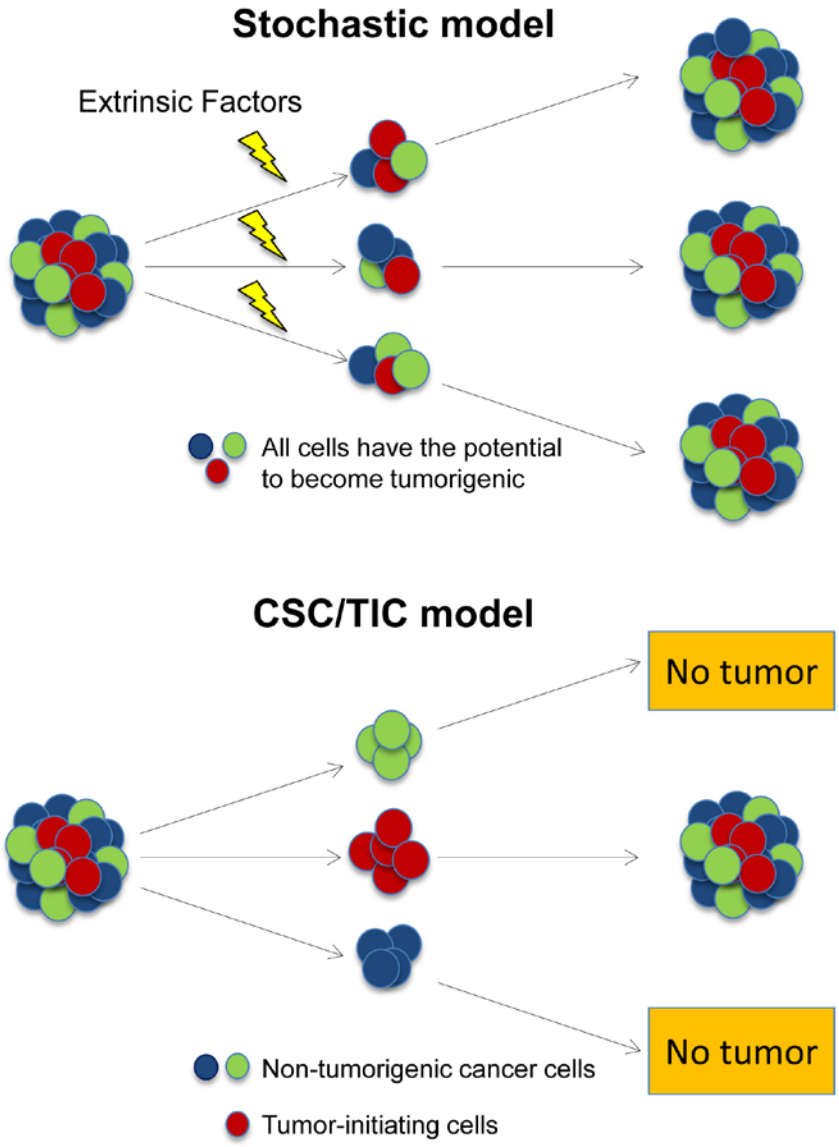

1.6.1 CSCs/TICs in OS

The first evidence of CSCs/TICs in OS was demonstrated by Gibbs and colleagues who showed that sarcospheres from OS cell lines and primary OS cells that were capable of growing in serum- and anchorage- independent conditions to form spheres, possessed the properties of self-renewal and multipotency [69]. Cells isolated from OS sarcospheres show high tumor initiating potential and drug-resistant properties [70]. Also, high expression of Oct-4 is observed in OS spheres, and cells engineered with an Oct-4 driven GFP reporter are capable of self-renewal of GFP positive population in xenografted tumors. The Oct-4 positive GFP cells are highly tumorigenic and successfully metastasized to the lungs and also express other mesenchymal stem cell markers [71]. Another important pluripotency factor associated with OS TICs is transcription factor Sox-2. Previous reports show enhanced expression of Sox-2 in human OS cell lines and patient tissue samples. Also sphere-forming ability relies on expression of Sox-2 while loss of Sox-2 leads to inhibition of sphere formation as well as tumorigenic potential [72].

Apart from that several studies have also isolated cells with stem-like properties in OS using stem cell surface markers such as CD133 (prominin), CD117 (c-kit), and Stro-1 [73,74]. Specifically, cells doubly positive for CD117 and Stro-1 ($CD117^{+}Stro\text{-}1^{+}$) successfully give rise to tumors exhibiting higher metastatic potential in immunocompromised mice. $CD117^{+}Stro\text{-}1^{+}$ cells also show increased drug resistance when compared to $CD117^{-}Stro\text{-}1^{-}$ cells. These malignant properties are due to enrichment of subcellular population of OS cells expressing a metastasis associated marker CXCR4 and a drug transporter marker ABCG2 [73]. Other methods to identify OS

CSCs/TICs include use of mouse stem cell surface antigen Sca-1, ability to efflux rhodamine 123 or Hoechst 33342 dyes, or high ALDH activity [49,72,75,76]. In particular, ALDHs comprise a group of cytosolic enzymes that convert intracellular aldehydes into carboxylic acids through oxidation and increased expression of ALDH1, which is a drug detoxification enzyme, is a property associated with normal stem cells including hematopoietic stem cells and neural progenitors[77]. Not surprisingly though, CSCs/TICs in different types of cancer are associated with high expression of ALDH1, as it is well known that TICs adapt several properties from normal stem cells [78]. Cells sorted for ALDH1 from OS99-1, based on the Aldeflour assay, from tumor xenografts, show enhanced proliferation, colony formation, and express stem cell related transcription factors including Oct-4, Nanog and Sox-2 [79]. These $ALDH^{high}$ cells are capable of self-renewal when serially transplanted in mice and successfully reforms the bulk of the tumor. Honoki *et al* show that MG63 OS cells exhibits a high percentage of cells positive for ALDH, and the spheres from these cells are also enriched for ALDH1 expression [76].

However, even though the presence of OS CSCs/TICs is well corroborated with many reports, the mechanisms behind their regulation or maintenance remain largely unknown.

1.7 Objective of our research

The molecular mechanisms that contribute to the most aggressive properties of OS, such as metastasis and drug resistance, remain to be elucidated. Since the prognosis for OS patients who manifest metastases are bleak, and the current chemotherapeutic regimen is not efficient against metastatic and recurrent OS, there is an urgent need for discovering new therapies. The key to these therapies may lie at a detailed and precise understanding of the molecular determinants governing the malignant properties of OS, since they can be crucial targets of OS therapy. Given that the ability of cancer cells to form spheres in anchorage- and serum-independent conditions is well correlated to malignant properties, our study which identifies and characterizes factors regulating sphere formation of OS cells would greatly improve our understanding of the mechanistic process of OS progression and hence ultimately accelerate the development of novel therapeutic strategies that target the most malignant properties of OS.

1.8 Specific Aims

OS, the most common bone cancer, is the second highest cause of cancer-related death in children and adolescents[80]. Despite major advances in the treatments of this disease, the long-term survival rates for patients with high-grade OS have reached a plateau for the past three decades and remain at approximately 50-80% [72,81,82]. The major reasons for the stagnation of the survival rates are attributed to its highly metastatic and drug resistant nature [83]. The ***long-term goal of this study*** aims at understanding the molecular mechanisms behind the malignant properties of high-grade OS and discovering novel therapeutic targets to improve the prognosis of patients suffering from high-grade OS.

The ability to survive and proliferate in serum-deprived and anchorage-independent conditions to form spheres is considered to be a hallmark of malignant properties. However, the underlying molecular framework contributing towards sphere formation is unclear. Identification and characterization of factors that contribute to sphere formation of OS cells would greatly help us understand the mechanistic process through which OS cells gain or enhance malignant properties.

Our ***central hypothesis*** is that genes that suppress sphere formation inhibit malignant properties of OS. The ***objective of this study*** is to identify and characterize factors that regulate sphere forming potential of OS cells. Towards this goal and to test our hypothesis, we screened a human whole-genome shRNA library using SJSA-1 OS cells harboring poor sphere forming potential. Our screening identified a novel gene "transmembrane and immunoglobulin containing domain 3 (TMIGD3)" whose knockdown enhanced sphere formation of OS cells. TMIGD3 is located on chromosome

1p13.2 (Gene ID: 57413, NCBI), and is found to be deleted in some malignancies including pheochromocytoma, OS, and meningioma. Intriguingly, the N-terminal region of 117 amino acids of TMIGD3 is shared with the N-terminal region of adenosine A3 receptor (A3AR) located on the same chromosome locus 1p13.2 (Gene ID: 140, NCBI), a Gi-protein that is well established to suppress inflammation and cancer through the NF-κB and β-catenin pathways. We ***hypothesize*** that TMIGD3 suppresses malignant properties of OS via overlapping pathways with A3AR. To test this hypothesis, we have achieved the following Specific Aims.

Aim 1: Identify factors that suppress sphere formation using a human whole-genome shRNA library.

Aim 2: Determine the roles of TMIGD3 in malignant properties of OS, in comparison with A3AR.

Aim 3: Determine the mechanisms behind TMIGD3 mediated OS suppression, and identify overlapping pathways altered by TMIGD3 in comparison with A3AR.

Aim 4: Determine the roles of TMIGD3 in stem-like properties of OS.

Results for Aims 1, 2, 3, and 4 are presented in Chapter 2, 3, 4, and 5 respectively.

This study has delineated the novel suppressive roles of TMIGD3 and A3AR in the regulation of malignant properties of OS, which would significantly increase our understanding of the mechanisms underlying malignant progression of OS. Therefore, TMIGD3 and A3AR could become potential pharmaceutical targets for therapy-resistant malignant OS, which might contribute to the improvement of the survival and quality of life in patients with OS.

1.9 Significance

This study is ***significant*** because it is has identified TMIGD3 and A3AR as novel factors crucial to the suppression of malignant properties of OS, including proliferation, migration, tumor formation, and metastasis. Detailed analyses identified the TMIGD3 isoform 1 (i1), but not TMIGD3 i3, as the important factor involved in the suppression of OS malignancy. This is the first study demonstrating the biological function of TMIGD3. We also further elucidated the underlying mechanisms by which TMIGD3 keeps a check on the aggressive properties of OS via the suppression of the NF-κB activity. Additionally, we delineated the role of A3AR, in OS malignancy which was not previously characterized. Our immunohistochemistry analyses using human OS tissues revealed decreased expression of both TMIGD3 and A3AR, compared to normal bone and lung tissues raising the question of the significance of the usage of A3AR agonists for the treatment of OS. Meanwhile, this leads the way for exploring the mechanisms underlying the reduced expression levels of TMIGD3 and A3AR.

Our data further suggests the role of TMIGD3 in stem-like properties of OS, which are also partly attributed to impart malignant characteristics to the tumor. Thus, the dissection of TMIGD3 as a novel regulator of OS progression would help us target the most lethal characteristics of this disease, metastasis and chemoresistance. It is also possible that TMIGD3 may be responsible for the malignant and stem cell-like properties not only of OS, but also of other types of sarcomas, since all sarcomas are of mesenchymal origin [84-86]. Therefore, TMIGD3 could become a potential biomarker or a pharmaceutical target for many types of sarcomas, and hence our study might have a significant impact on the survival and quality of life in these sarcoma patients.

1.10 Innovation

- Our study is the first to perform a whole-genome shRNA library screening to identify novel regulators that influence sphere forming potential of OS using an unbiased approach.
- This is the first study examining the clinical significance of TMIGD3 and A3AR in OS, as well as their functions as crucial players that suppress OS tumorigenesis.
- Our study is also the first to describe the differential roles of isoforms of TMIGD3 in cancer or A3AR in OS.
- Our study is the first to delineate the role of TMIGD3 in the NF-κB pathway, hence opening up avenues for the use of NF-κB inhibitors to target OS malignancy.
- We are the first to study the potential significance of TMIGD3 as a novel regulator of stem-like properties of OS.
- Our study delineating the roles of TMIGD3 and A3AR as novel tumor suppressors in OS thus providing new therapeutic interventions to target OS malignancy.

CHAPTER 2

GENOME-WIDE SCREENING TO IDENTIFY FACTORS THAT REGULATE SPHERE FORMATION OF OS CELLS

2.1 Introduction

The survival rate for metastatic OS remains at 20% for the past 30 years[87,88]. This is mainly because the factors and mechanisms by which aggressive characteristics of OS are regulated remain unclear. A deeper understanding of the molecular mechanisms behind the malignant properties and discovering novel therapeutic regimens to target these malignant properties are required to improve the prognosis of patients suffering from high-grade OS.

Cancer cells which can grow in serum- and anchorage-independent conditions to form spheres must have the abilities to overcome cell death (anoikis: anchorage-dependent cell death) and proliferation arrest induced by low-attachment and nutrition deprived conditions, and hence sphere forming potential is well correlated with high malignant properties of cancer cells [89,90]. Indeed, cells within spheres derived from primary and established cancer cells including OS frequently show high tumor initiating and metastatic potential, as well as resistance to chemotherapeutic drugs, with high expression of factors associated with self-renewability, thus possessing stem-like properties [69,73,91-94]. We hypothesized that factors that suppress sphere forming potential of OS cells inhibit the aggressive characteristics of this disease.

To test this hypothesis, we first tested several OS cell lines for their inherent abilities of sphere forming potential. We chose SJSA-1 OS cell line, since it had low sphere forming potential (in size and in percentage). We infected SJSA-1 cells with a human whole-genome short hairpin RNA (shRNA) lentiviral library at a low (0.2) multiplicity of infection (MOI) and performed sphere formation assays. After validation, 9 clone-derived cells showed the abilities to form spheres with sizes greater than 75μm at

more than 2% of frequency. Genomic sequencing identified candidate shRNAs in these clones, and 7 shRNAs for 7 genes were present in these clones since 3 were for the same gene: a novel uncharacterized protein, called transmembrane and immunoglobulin containing domain 3 (TMIGD3). Since 3 clones contained shRNAs for TMIGD3 and because infection of parental SJSA-1 cells with a lentiviral vector encoding the identified shRNA for TMIGD3 consistently increased sphere forming potential, we pursued TMIGD3 for our further analysis of its roles in OS malignancy. The reason we think that relatively higher number of clones had the shRNA for TMIGD3 is because, during the selection process before performing sphere assays, the knockdown of TMIGD3 may provide with a growth advantage that may increase the number of cells that express the shRNA for TMIGD3, Thus, our screening strategy identified a potential novel player that could play a crucial role in the suppression of aggressive properties of OS.

2.2 Materials and Methods

shRNA library

The human whole-genome shRNA library was purchased from Open Biosystems Inc. The library consists of 21,416 genes in total, 75,000 shRNAs (approximately 3.5 shRNAs per gene) divided into 7 pools of lentiviral particles. The cells were infected at a low multiplicity of infection (0.2 MOI) to ensure that a single cell did not have more than a single copy of virus.

Sphere formation assays

Sphere formation assays were performed as previously described [73]. Briefly, cells (20 cells per well) were plated on 96-well ultra-low attachment plates. (Corning Inc., Corning) (without the presence of extracellular matrix components, thus leading to formation of spheres in free floating conditions) in DMEM F12 serum free medium containing 10mM HEPES, 50 µM of putrescine, 20nM of progesterone, ITS (insulin 25 mg/ml, sodium selenite 25 µg/ml, transferrin 25 mg/ml), EGF (10 ng/ml), and FGF (10 ng/ml) for 10-14 days and numbers of spheres with sizes over 30 µm were counted. Sphere forming potential was calculated as the percentage of # of spheres formed/# of cells seeded.

2.3 Results

2.3.1 Identification of a suitable OS cell line to perform screening

Sphere forming ability is considered to be a hallmark of aggressive properties of cancer cells *in vitro*. We hence hypothesized that factors that regulate sphere formation would play roles in malignant properties of OS. To test this hypothesis, we performed sphere formation assays by screening a human whole-genome shRNA lentiviral vector library. First, to determine the appropriate cell lines to be used for the screening where downregulation of a gene would allow a single OS cell to form a sphere, we tested sphere forming potential of several OS cell lines, including U2OS, SJSA-1, Saos2, and MG63, in anchorage- and serum-independent sphere specific conditions in ultra-low attachment 96-well plates (Table 1). We seeded 20 cells per well so that single spheres were derived from single cells without forming aggregates. To measure the sphere forming potential, we only counted spheres with sizes >30 μm in diameter and categorized the formed spheres into two groups by sizes: 30-75 μm and >75 μm. We observed no sphere formation from U2OS and Saos2 cells, low potential in SJSA-1 cells, and high potential in MG63 cells. We chose SJSA-1 cells for further screening purposes, since it retained its sphere forming potential even though it was considerably low.

Table 1. Sphere forming potential of OS cell lines.

Different OS cell lines including U2OS, SJSA-1, Saos2, and MG63 were examined for their sphere forming potential (% sphere formation= percentage of # of spheres formed/# of cells seeded) for two weeks in sphere specific conditions. The sphere forming potential was classified into two different categories based on their diameters: 30-75 μm and >75 μm. Spheres with less than 30 μm in diameter were not counted as spheres. Data are presented as average +/- standard deviation (S.D.) from at least four independent experiments.

Table 1. Sphere forming potential of OS cell lines.

Cell line	Total cell # examined	% sphere formation (average +/- S.D.) 30-75 μm, >75 μm
U2OS	140,000	0+/-0, 0+/-0
SJSA-1	140,000	0.5+/-0.5, 0+/-0
Saos2	140,000	0+/-0, 0+/-0
MG63	2,160	7.7+/-1.5, 4.5+/-2.1

2.3.2 TMIGD3 as a factor that suppresses sphere formation of OS cells

SJSA-1 cells were infected with the shRNA library at 0.2 MOI, so that single shRNA was present per cell. After selection with puromycin, the infected cells were subjected to sphere assays (1st screening, Fig 2.1A). Spheres formed with sizes >75 μm in diameter were isolated, cultured for expansion, and then subjected to secondary sphere assays to further confirm their increased sphere forming potential (2nd sphere assays, Fig. 2.1A). Nine (9) clones were selected, since they formed spheres greater than 75 μm in diameters at more than 2% of frequency. These 9 clones were expanded, followed by genomic DNA isolation. PCR was performed using specific PCR primers flanking the shRNA site, and the PCR products were further sequenced to identify the target sequences within the shRNAs (Fig. 2.1A). Out of the 9 clones, 7 target sequences for 7 genes were identified (Table 2), since 3 of the 9 clones were identical, which was for transmembrane and immunoglobulin domain containing 3 (TMIGD3) (the same shRNA for TMIGD3 was present in each of the 3 clones). To further validate the effects of these 7 shRNAs on sphere forming potential of SJSA-1 cells, we infected SJSA-1 cells with lentiviral vectors encoding each shRNA identified for these 7 genes (Fig. 2.2A). Of these 7 genes, SJSA-1 cells infected with lentiviral vectors encoding shRNAs for *TMIGD3* and *spermatogenesis and centriole associated 1* (*SPATC1)* showed higher sphere forming abilities (Fig. 2.2B). We decided to pursue TMIGD3 for further characterization due to the following reasons: 1) 3 of the 9 clones contained the shRNA for TMIGD3 targeting the 3'UTR. 2) It had a higher frequency of sphere

formation (both primary and secondary sphere assay) than all clones. 3) The sizes of the spheres were bigger than all the clones.

Figure 2.1 Screening strategy and results

(A) SJSA-1 cells infected with a human whole-genome shRNA library at 0.2 MOI were selected with puromycin for 48 hours and subjected to sphere formation assays (1^{st} screening) in sphere specific conditions where 20 cells/well were plated in 96-well ultra-low attachment plates with serum-free sphere media. Sizes of spheres were determined 2 weeks later, and spheres with sizes greater than 75 μm in diameter were isolated and expanded in monolayer culture. These sphere-derived cells were further subjected to 2^{nd} sphere assays, where spheres with sizes greater than 75 μm at >2% of frequency were further analyzed for identification of the respective shRNA using genomic PCR and sequencing.

(B) Summary of screening results is presented below the schematic strategy. Of the 9 sphere-derived clones, 7 genes were identified, since 3 clones contained the same shRNA for TMIGD3.

Figure 2.1 Screening strategy and results

A

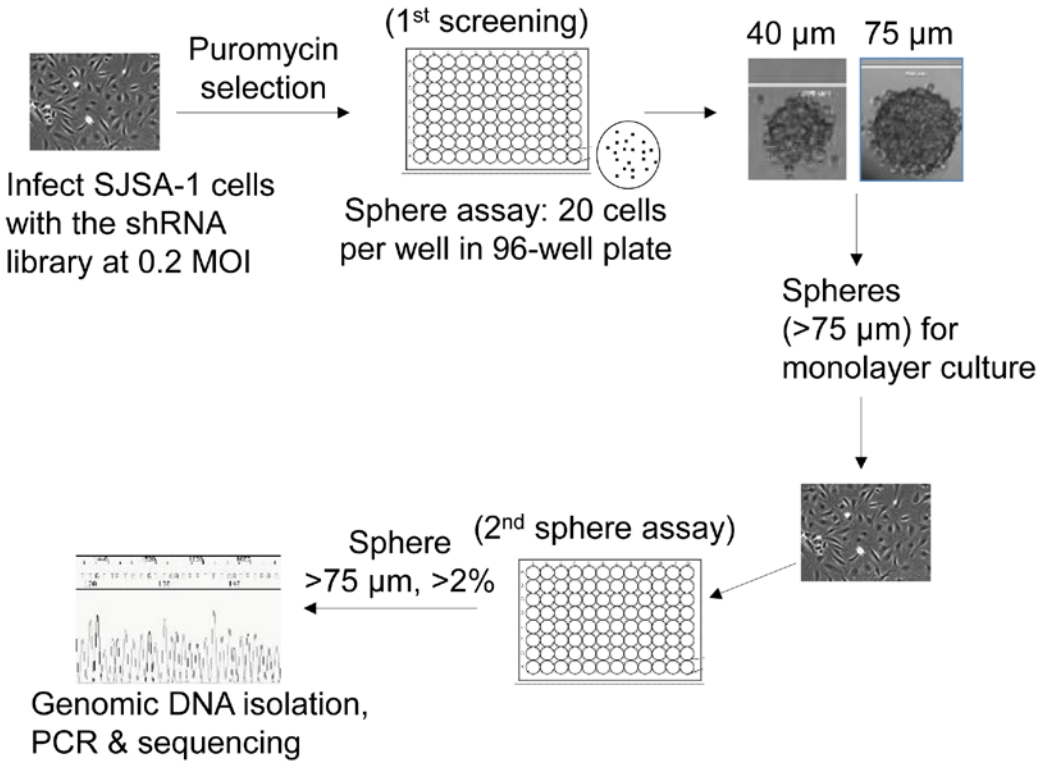

B

# of genes in the library	# of cell tested	# of clones that formed spheres (>75µm, >2%) in second screening	Genes identified
21,416	140,000	9	7

Figure 2.2 Validation of candidate genes

(A) The pGIPZ lentiviral vectors containing each identified shRNA for 7 genes were infected into SJSA-1 cells, followed by puromycin selection and sphere formation assays.

(B) Results of sphere assays. Total number of cells examined was 2,000 per clone. Graph showing percentage of sphere formation (percentage of # of sphere formed/# of cells seeded) from at least 3 independent experiments.

Figure 2.2 Validation of candidate genes

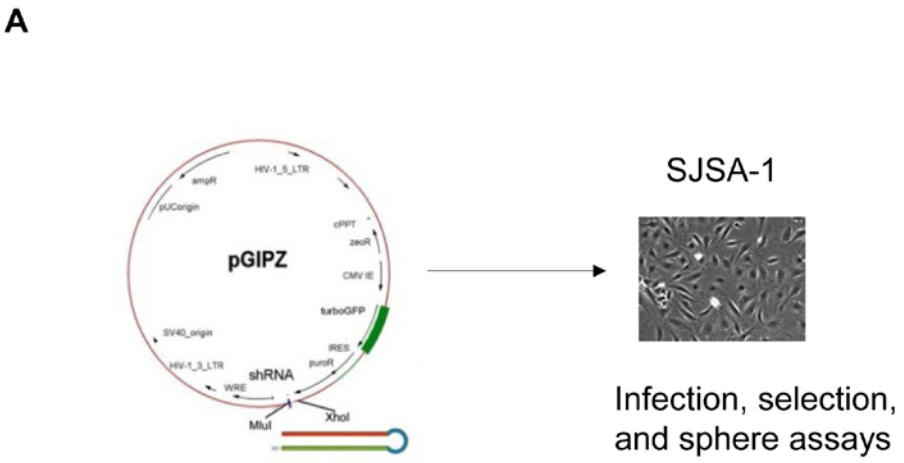

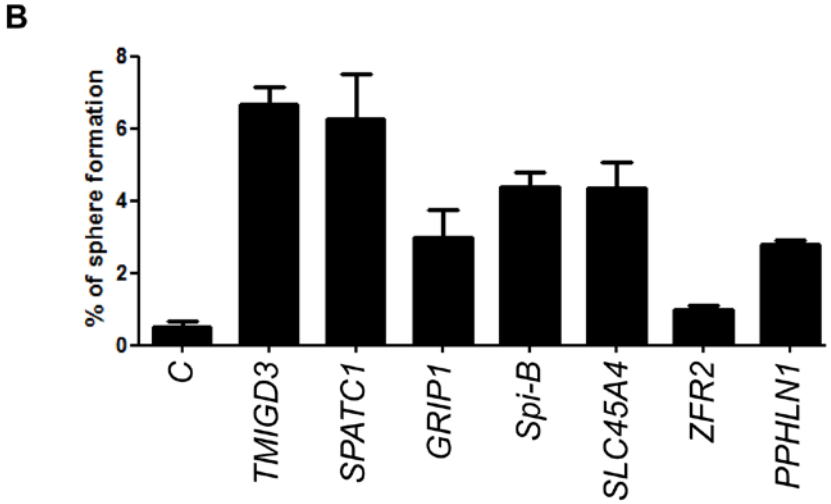

Table 2 Functions of candidates.

Candidate genes identified in the screening and their known functions.

Table 2. Functions of candidates.

Gene name (abbreviation)	Function
Transmembrane and immunoglobulin domain containing 3 (TMIGD3)	Unknown. Ig-like fold containing proteins. TMIGD3 i1 is an alternative splicing form of adenosine A3 receptor (A3AR), whereas TMIGD3 i3 has no overlap with A3AR.
Solute carrier family 45-4 (SLC45A4)	Unknown. No reference.
Spi-B (Spi-B)	Ets family transcription factor implicated in B cell lymphoma suppression.
Glutamate Receptor Interacting Protein 1 (GRIP1)	Cytoplasmic multi-PDZ scaffolding protein implicated in neuronal synaptic function.
Zinc finger RNA binding Protein 2 (ZFR2)	Unknown. No reference.
Spermatogenesis and Centriole associated 1 (SPATC1)	Centrosomal protein implicated in zygotic cell division (Y chromosome).
Periphilin-1 (PPHLN1)	Gastric cancer antigen Ga50 involved in epithelial differentiation.

2.4 Discussion

One of the hallmarks of malignant properties of cancer cells is the ability to survive in serum- and anchorage-independent conditions to form spheres. Our sphere assays involve culture of cells in 3 dimensional conditions, similar to other assays including 3D organoid cultures however the differences include: 1. low numbers of cells that prevent cell to cell contact and adhesion 2. Anchorage–independence that prevents cell-matrix attachment. Thus, these strict conditions wherein most of normal cells as well as most of cancer cells die, could be considered to be a true test for the survival of the most transformed or aggressive population of cells.

Our screening identified a novel uncharacterized protein, TMIGD3, whose downregulation increased sphere formation of OS cells. This has opened up new avenues to further expand the role of TMIGD3 in malignancy of OS, which is further illustrated in Chapters 3, 4 and 5. Sphere forming potential is considered to be a hallmark of malignancy as well as stem-like properties. Hence, we have elaborated on the role of TMIGD3 as a crucial player in the regulation of malignant properties and stem-like properties of OS. . Also, TMIGD3 shares its N-terminal region with adenosine A3 receptor (A3AR). Though the role of TMIGD3 in cancer is completely unknown, the role of A3AR as a suppressor of cancer progression is well established. Additionally, this study can be further extended to examine the roles of TMIGD3 in other sarcomas of mesenchymal origin as OS.

Cell density is considered to be the most crucial and determining factor in the efficiency of the sphere formation assay. The maintenance of clonality of the spheres is

the central tenet of these assays, meaning every sphere is derived from a single cell. We performed preliminary sphere formation assays with varying number of cells/well to determine an ideal condition, where the cells were well distributed, to avoid clusters of cells that could eventually give rise to aggregate based spheres, one of the major drawbacks associated with the sphere formation assay. Our conditions wherein 20 cells/well were seeded minimized aggregate formation and allowed spheres to be formed from a single cell. We confirmed this by performing preliminary experiments where we seeded one RFP-positive cell with high sphere forming potential and 19 GFP-positive cells with low sphere forming potential in a single well and we found that at the end of 2 weeks, only RFP-positive spheres with no contamination of GFP cells were present (data not shown). Indeed, the results of our screening analyses elucidated that the clonality of spheres was maintained, since only a single shRNA was identified in each of the 9 clones.

Amongst the other genes identified, knockdown of *SPATC1* (also known as *speriolin*) gave rise to a significant increase in sphere forming potential. However, its role in cancer malignancy is unclear. Interestingly, protein expression studies in different malignancies show moderate to high staining intensities in multiple cancer tissues (http://www.proteinatlas.org/ENSG00000186583-SPATC1/cancer). It would be interesting to characterize the role of *SPATC1* in malignant properties of OS in the future. It would also be interesting to study if there is a correlation between the other candidates identified through the screening and TMIGD3 and their combined effects on OS malignancy.

CHAPTER 3

ROLES OF TMIGD3 AND A3AR IN MALIGNANT PROPERTIES OF OS

3.1 Introduction

The mechanisms by which aggressive characteristics of OS are regulated are poorly understood. The ability of cells to survive under nutrient-deprived, anchorage-independent conditions, defines a symbol of malignant properties. We identified an uncharacterized protein, namely transmembrane and immunoglobulin domain containing 3 (TMIGD3), as a factor that suppressed sphere formation of SJSA-1 cell line through screening of a human whole-genome short hairpin RNA (shRNA) lentiviral library.

TMIGD3 knockdown enhanced other malignant properties including proliferation, migration, tumor formation, and metastases of multiple OS cells. TMIGD3 has mainly two isoforms: i1 and i3 which have unique first exons but share the rest of the exons and the 3' untranslated region (UTR). Interestingly, the first exon of *TMIGD3 i1* gene, consisting of 117 amino acids (aa), is shared with the first exon of A3AR, and hence TMIGD3 i1 is like a fusion protein of A3AR and TMIGD3 i3 (Fig 3.2) [95]. A3AR is a Gi protein associated G-protein coupled receptor (GPCR) and implicated in the suppression of immunological response and tumorigenesis of multiple cancers including hepatocellular carcinoma, prostate cancer, pancreatic carcinoma via inhibition of adenylyl cyclase and cyclic adenosine monophosphate (cAMP) signaling and hence downregulation of the activities of NF-κB and β-catenin [96-99]. Elevated cAMP levels is well correlated with increased malignancy of different cancers including brain and thyroid tumorigenesis[100] [101]. However, opposite effects of cAMP on hematologic malignancies have been reported in some rare cases wherein inhibition of cAMP through decrease in expression of adenylyl cyclase could provide growth advantage

and hence promote tumorigenesis [102]. Interestingly, overexpression of TMIGD3 i1 suppressed sphere formation, proliferation, and tumor formation of OS cells, similar to A3AR, whereas TMIGD3 i3 did not alter these phenotypes. The expression of both TMIGD3 and A3AR was lower in human OS tissues when compared to normal bone and lung tissues. This is the first report demonstrating the roles of TMIGD3 i1 in cancer suppression, and A3AR, specifically in the suppression of OS progression, thus opening new avenues as therapeutic targets for multiple cancers as well as OS.

3.1.1 A3AR, a G-protein coupled receptor and its role in tumor malignancy

3.1.1.1 G protein coupled receptors

G protein coupled receptors (GPCRs) comprise of a significant class of transmembrane proteins, which consist of seven transmembrane domains hence referred to as 7TM or heptahelical receptors. The transmembrane sequences are spread across the plasma membrane in the form of α-helices forming the receptor unit [103]. These receptors are a superfamily of receptors that have been a focus of drug intervention accounting for 50% of all modern-day medicine targets [104]. Hence, GPCR's are of great interest in pharmaceutical and academic research, focused on their function and malfunction in various human systems.

GPCRs are activated by a wide variety of ligands including photons, amines, hormones, neurotransmitters, and proteins. They have single polypeptide chains with seven hydrophobic transmembrane–spanning segments that couple with an intracellular effector molecule through a trimeric G protein complex [105]. The G protein name

originates from its interaction with guanine nucleotide binding proteins (α, β, γ subunits), which then initiate crucial signaling pathways in the cell [103,106].

GPCRs follow a simple, yet elegant mechanism of linking the presence of an extracellular signaling molecule to an intracellular cascade of responses, which has been well conserved through evolution. Hence, through repeated gene duplication, recombination and gene mutations over time, GPCRs are present in abundance in most animal organisms. Based on degree of sequence homology and functional similarity, GPCRs are divided into different subfamilies: Family A receptors are related to the rhodopsin and the β2-adrenergic receptor, family B are related to glucagon receptors, family C receptors are related to the metabotropic glutamate receptors, family D and family E receptors (STE2 and STE3 receptors) are related to yeast pheromone receptors, and family F includes four different cAMP receptors.

The signal transduction pathway of GPCR is performed through activation of heterotrimeric G proteins comprised of α, β, and γ subunit. In an inactive state, the Gα subunit is bound with guanosine diphosphate (GDP), and the Gαβγ heterotrimer is not associated with a GPCR [107]. Upon ligand activation, a subsequent conformational change occurs in the GPCR that increases its affinity for G proteins [107]. The G-proteins interact with the C terminus of the GPCR, which then catalyzes the release of GDP from the Gα subunit in exchange for GTP thereby destabilizing the trimeric complex [106,107]. The Gα (GTP) complex and the dimeric Gβγ once activated will interact with intracellular downstream effector proteins. The activation of the Gα (GTP) complex and the Gβγ are completed with subsequent hydrolysis of GTP into GDP and the

reassociation of the subunits into an inactive Gαβγ heterotrimer regulated by the RGS (Regulators of G-protein signaling) proteins [108,109].

There are four main classes of Gα proteins, $G\alpha_s$, $G\alpha_i$, $G\alpha_q$ and $G\alpha_{12}$. Each class has its own downstream effector. $G\alpha_s$ class of proteins couple with adenylyl cyclase to stimulate an increase in cAMP [108]. The $G\alpha_i$ family primarily acts through inhibition of adenylyl cyclase and hence cAMP, however its known to trigger other signaling events as well [107,108]. The $G\alpha_q$ subfamily uses phospholipase Cβ (PLCβ) as its primary effector [110]. Active PLCβ catalyzes the hydrolysis of phosphatidylinositol-4,5-bisphosphate (PIP_2) to inositol 1,4,5 triphosphate (IP_3) and diacylglycerol (DAG), both of which act as secondary messengers causing the release of Ca^{2+} from intracellular stores and hence activating protein kinase C (PKC) [108]. The $G\alpha_{12}$ subfamily regulates the activation of Rho-guanine nucleotide exchange factors (GEFs)[108,111].

Apart from the Gα (GTP) subunits, the Gβγ subunit also acts as an effector by activating a number of downstream targets including ion channels, G-protein regulated inward rectifying K+ channels (GIRKs), phosphatidylinositol 3-kinase (PI3K), phospholipases and adenylyl cyclase [107].

Once activated, the desensitization of the GPCR occurs through two families of proteins, the G-protein coupled receptor kinases (GRKs) and the arrestins. GRKs phosphorylate the agonist-bound activated GPCRs, thus leading to the binding of the inhibitory proteins, the arrestins [112]. There are currently seven known GRKs (GRK 1-7) [113]. The primary function of arrestins is to bind phosphorylated GPCRs, blocking further G protein binding, and hence blocking signaling through steric inhibition [114]. There are four members of the arrestin family; cone arrestin, rod arrestin (exclusively found in

retinal cells), and β-arrestin-1 (arrestin-2) and β-arrestin-2 (arrestin-3) ubiquitously present in all cells [115]. In addition to their roles in GPCR desensitization, GRKs and arrestins also play a roles in receptor internalization (endocytosis) [116].

3.1.1.2 Adenosine receptors and physiology of adenosine signaling

Adenosine receptors are a part of the superfamily of GPCRs that have their effects on a wide range of responses, and have been classified based on their stimulatory or inhibitory actions on adenylyl cyclase and on selectivity of agonists and antagonists. The physiological ligand for these receptors is adenosine, the universal energy molecule. Adenosine acts as a signal molecule through these receptors thus eliciting a broad spectrum of physiological effects. Adenosine receptors belong to the subfamily of rhodopsin-like receptors, with its typical heptahelical structure.

There are four membrane spanning adenosine receptors that bind to extracellular adenosine; these include the A1 and A3 receptor subtypes, which couple to a $G\alpha_i$ thus inhibiting the intracellular adenylyl cyclase (AC) activity and thus leading to decrease of cAMP, and the A2a and A2b receptors, which couple with a $G\alpha_s$ thus stimulating the AC activity increasing levels of intracellular cAMP concentrations [117]. In addition to this A1 receptors have been shown to activate phospholipase C to open K_{ATP} channels [118-120]. On the other hand, A3 receptors are known to couple possibly with $G\alpha_q$ [121] and are involved with activation of phospholipase C and D [119].

Adenosine receptor signaling depends on the level of extracellular adenosine [122]. Extracellular concentrations of adenosine are sensed by complex ectoenzyme machinery, which includes CD39 and CD73. These ectoenzymes metabolize ATP and ADP to AMP, and AMP to adenosine, respectively, and hence form the sources of extracellular adenosine [122]. The catabolic enzyme adenosine deaminase (ADA) degrades extracellular adenosine, thereby decreasing the activity of the adenosine receptors and hence maintaining homeostasis [123]. Nucleoside transporters present on

the cell membrane including equilibrative nucleoside transporters (ENTs) and concentrative nucleoside transporters (CNTs), move extracellular adenosine into the intracellular space terminating the AR signaling [124]. ENTs are classified into four subtypes: ENT1, ENT2, ENT3, and ENT4, which carry nucleosides along their concentration gradients. On the other hand, CNTs namely, CNT1, CNT2, and CNT3, facilitate the intracellular influx of nucleosides against their concentration gradient across the cell membrane (Fig 3.1).

The four-adenosine receptors have been cloned from seven mammalian species, including human. There are extensive sequence similarities across species for the A1, A2a, and A2b, whereas the A3 receptors are more variable [125]. Each of the receptor has different yet overlapping functions. Each of these receptors has a different affinity for adenosine; and hence these receptor subtypes can also be characterized based on their potency for binding to adenosine A1≥A2A>>A3=A2B, thus meaning that the A1 and A2A subtypes are high affinity receptors activated by nanomolar concentrations of adenosine, while the A2B and the A3 receptors are low affinity activated by micromolar concentrations of adenosine [126]. Adenosine receptors are widely expressed; however, their distribution and expression are species-dependent [127,128]. For example, the rat adenosine A1 receptor is widely expressed in the brain, heart, aorta, liver, kidney, eye, and bladder [127]. The same group has also illustrated that A3AR is widely expressed in the heart, central nervous system, lung, uterus, and testis. A2A receptor subtypes were expressed in the lung, brain, and uterus, while the A2B are present in the jejunum and colon. The receptors were all localized to the plasma membrane. Evidence also suggests their presence specifically in lipid rafts of the plasma membrane [129].

The adenosine receptors consist of the classical seven transmembrane helices as any other GPCRs, forming the binding site for ligands. Three extracellular and three intracellular loops of unequal size of amino acids connect the helices. The N-terminal of the protein is extracellular, and the C-terminal side is intracellular (cytoplasmic) [128].

Adenosine receptors play important roles in several physiological processes. Some of these include their well-studied roles in the heart and the brain. The roles of all four receptor subtypes are implicated in regulating coronary flow in the heart. A2AR subtype, is mostly responsible for coronary vasodilation, A1AR and A3AR are responsible for restriction of coronary vasodilation. A1 and A3 receptors are also known to provide cardioprotection following cardiac ischemia[130].

A1AR stimulation is also associated with suppression of neuronal activity through inhibition of PKA signaling pathway at the pre-synaptic and post-synaptic sites. On the other hand, A2AR coupled to Gs- protein, stimulates the PKA signaling in postsynaptic neurons. Heterodimerization of A2AR receptors with other receptors including A1AR, dopamine D2 receptors, and group I metabotropic glutamate 5 receptors for signaling purposes have also been reported. A3AR found in the hippocampus, are known to signal through coupling with Gi protein thus, inhibiting adenylyl cyclase activity and reducing cAMP concentrations. However, Gq coupling related activation of phospholipase C that regulates calcium status is also reported as a potential signaling mechanism for A3AR in the brain. Thus, the roles of adenosine receptors are varied and are influenced through control of signaling pathways downstream of these receptors[131].

Figure 3.1 Adenosine receptors and physiology of adenosine signaling. Adenosine is released from metabolically active cells and the signaling depends on extracellular levels of adenosine. Extracellular concentrations of adenosine are sensed by ectoenzymes CD39 and CD73. These ectoenzymes metabolize Adenosine triphosphate (ATP) and Adenosine diphosphate (ADP) to Adenosine monophosphate (AMP), and AMP to adenosine respectively; which then binds to four adenosine receptors A1 and A3 (inhibit levels of cAMP), and the A2a and A2b (increase levels of cAMP) localized on the membrane. The catabolic enzyme adenosine deaminase (ADA) degrades extracellular adenosine. Nucleoside transporters including equilibrative nucleoside transporters (ENTs) and concentrative nucleoside transporters (CNTs), move extracellular adenosine into the intracellular space thus terminating adenosine receptor signaling.

Figure 3.1 Adenosine receptors and physiology of adenosine signaling

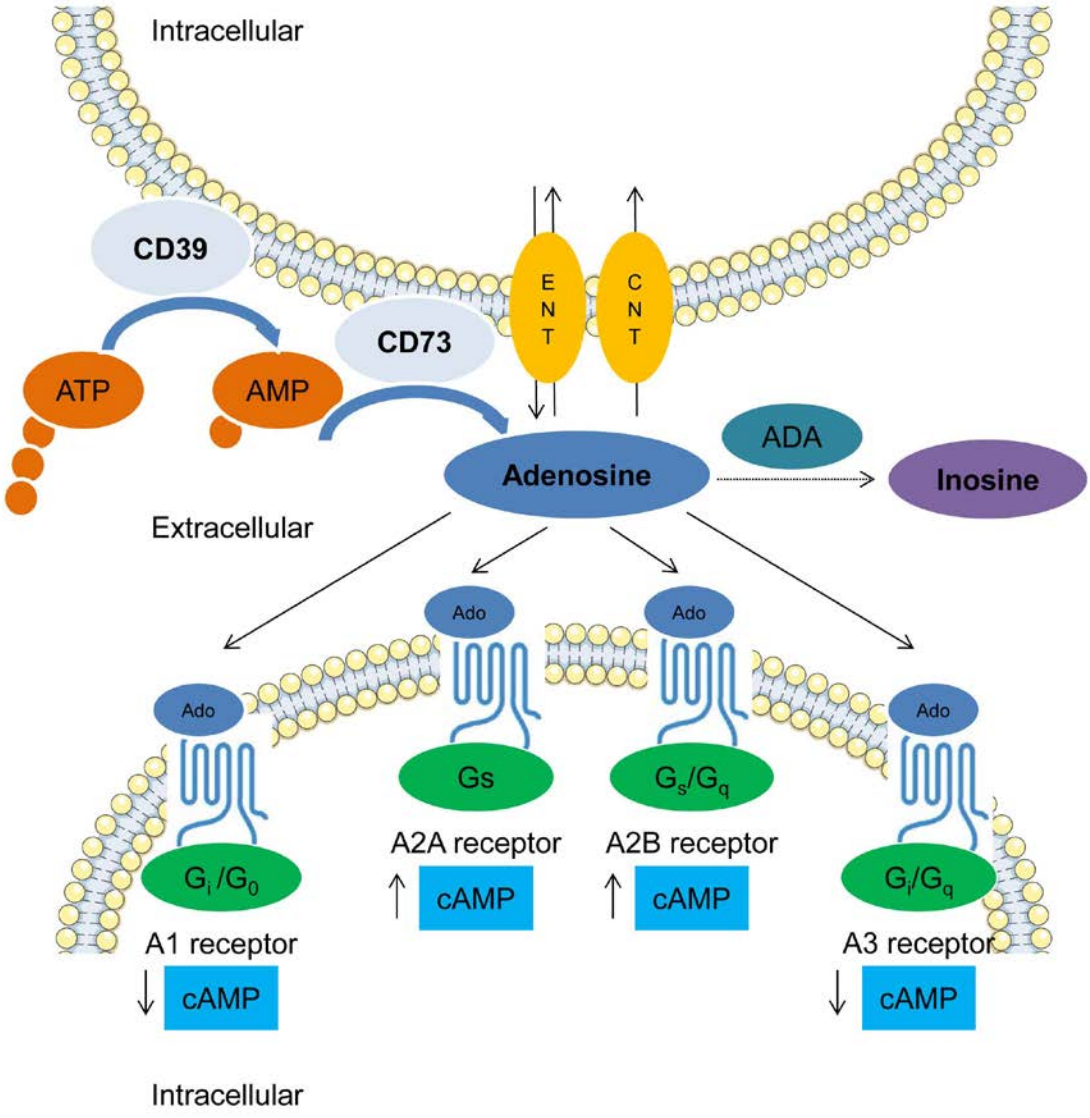

3.1.1.3 Adenosine receptors in cancer

Adenosine as a metabolite is released from metabolically active cells and is generated by degradation of ATP. The released adenosine binds to the four-adenosine receptors (ARs): A1, A2A, A2B, or A3 and causes effects that are widespread and pleiotropic. The cellular responses to adenosine depend on the expression of the particular receptor subtypes and serve as active modulators of signal transduction. Recent report shows that adenosine is a crucial factor in determining the cellular survival pathway towards the apoptotic or cytostatic state [132]. It is very well established that adenosine and ATP (i) are abundant in the tumor microenvironment, (ii) form potent modulators of the immune response and (iii) play key roles in host-tumor interaction. As adenosine receptors control cell survival pathways as a normal physiologic process, this mechanism is well adapted to directly affect tumor growth as well. Hence, ARs are becoming important drug targets for the treatment of various pathophysiological states including Parkinson's disease, schizophrenia, ischemia, asthma, and kidney failure. Several ligands (agonist and antagonists) are available for all four AR subtypes; however, few of these candidates are used in the fight against cancer.

ATP and adenosine accumulate in the tumor microenvironment, as a crucial autocrine and paracrine factor [133]. The levels of adenosine can rise to very high levels in response to pathophysiological conditions, such as hypoxia, inflammation, and trauma [134]. This increase in the levels of adenosine is suggested to be not just a mere coincidence, but is proven to be an active modulator of tumor progression. Adenosine activates the adenosine receptors and regulates proliferation, differentiation, and apoptosis of cancer cells, directly affecting neoplastic development, progression, and

metastasis. Adenosine receptors have been reported to directly affect angiogenesis (increase or decrease), which is of great importance for the survival of the tumor during hypoxic conditions [135]. Evidence suggests that several solid tumors express high levels of adenosine-sensing ectoenzymes, CD39 and CD73 [122]. These high levels regulate cancer cell proliferation and apoptosis by intratumoral adenosine generation[136]. It is also shown that genetic or pharmacological ablation of these ectoenzymes leads to defects in the tumor neovascularization[137,138]. Also, levels of ecto-ADA and its cofactor CD26 are deregulated in several cancers [122]. In addition to this, the expression of nucleoside transporters is also decreased in neoplastic tissues, thus causing deregulation of the adenosine signaling[139].

The role of adenosine on tumor growth is like a double-edged sword as both promotion and inhibition of proliferation have been reported. This complex mechanistic interplay of response is attributed to the engagement of different ARs, although these effects are not completely understood [140].

A1 receptors

The role of A1 receptors in tumor development is controversial. A1 receptors have been shown to regulate growth of breast cancer cells. Quantitative reverse transcription (qRT-PCR) analyses and western blot analyses reveal an increase in receptor expression in various cancer cell lines as well as primary tumor specimens of the breast[141]. Overexpression of these receptors has also been detected in colorectal adenocarcinoma and peritoneal colon tissues [142]. Activation of A1 receptors promotes cell proliferation by downregulating p27, a cyclin dependent kinase (CDK) inhibitor, and upregulating CDK4[141]. It has also been reported that estrogen receptor (ER)-mediated proliferation of breast cancer may also involve the A1 receptor, compounding the tumor-promoting role of ER independently[143]. Inhibition of A1 receptor attenuates MCF7 breast cancer cell proliferation[143]. However, anti-proliferative effects of A1 receptors have also been described. Following A1 stimulation, proliferation arrest is reported in human leukemic MOLT-4 cells, as well as breast cancer cell lines, T47D and HS578T [144]. Physiologically, high levels of A1 receptor are present in microglia and neurons in the central nervous system [145]. It is noted that A1AR- deficient mice show neuronal damage and lower survival rates when exposed to pathological states, such as hypoxia, whereas these mice show no obvious physiological deficiency in normal states [145] suggesting the importance of A1AR during pathophysiological conditions [145,146]. In fact, deletion of A1AR results in increased glioblastoma tumor growth[147], thus implying the anti-tumor effects of this receptor in brain tumors. The role of A1 receptors in tumor apoptosis is also controversial. It has also been reported that in rat astrocytoma cells caspase 9 followed by caspase 3 is activated through the A1AR pathway in the presence of

extracellular adenosine. This study presents a novel mechanism of cell death through caspase activation in response to adenosine[148]. More relevantly, apoptosis through activation of caspase-3, -8, and -9 in CW2 human colonic cancer cells can be inhibited by an A1AR antagonist both *in vitro* and *in vivo*[149]. However, in MDA-MB-431 cells, depletion of A1AR causes substantial cell death and apoptosis [148].

A2A receptors

A2A receptors have been detected on cell membranes of different tumor cells: SH-SY5Y neuroblastoma, NG108-15 neuroblastoma, U937 monocytic lymphoma, A375 melanoma, HT29 colon carcinoma, and human breast cancer MCF-7 [150-153]. The activation of A2A receptors following agonist stimulation increases proliferation of MCF-7 cells. Activation of A2A receptors inhibits apoptosis through alterations in the anti-apoptotic Bcl-2 and pro-apoptotic Bax proteins during reperfusion of the heart[154]. Also, activation of A2A using an agonist results in reduction in neuronal apoptosis during spinal cord reperfusion [155].

Though anti-apoptotic role of A2AR is seen in normal tissues, cell death by A2AR is observed in human A375 human melanoma cells[156]. Also, activation of caspase-9 and -3 is observed through A2AR in Caco-2 human colonic cancer cells[157].

A2B receptors

As previously stated, A2B receptor has the least affinity for adenosine, hence being activated only at exceptionally high levels of adenosine which is a phenomenon seen in pathological states rather than in normal physiological conditions[158]. Immunohistochemical analyses shows increased expression of A2B receptors in human colorectal carcinoma tissues and colon cancer cell lines when compared with normal colonic mucosa. Also, inhibition of A2B receptors using a specific antagonist (MRS1754) leads to reduced cell growth in a dose-responsive manner[159], suggesting cancer-favoring roles of A2B receptors. Real time qRT-PCR and western blot analyses also reveal high levels of this receptor subtype in both androgen-sensitive and androgen-insensitive prostate cancer cell lines, in which activation of A2B receptors leads to further increase in cellular proliferation, thus suggesting the use of A2B-specific antagonists for therapeutic intervention. However, the exact mechanisms underlying augmented proliferation by A2B receptors have to be investigated in detail before their translation into clinic.

A3 receptors

Tumor cell proliferation is also controlled through the A3 receptors[156,160-163]. . A3AR a Gi protein associated (GPCR) causes inhibition of adenylyl cyclase and cAMP signaling and hence activities of NF-κB and β-catenin, pErk pathways. Activation of A3 receptors inhibits growth of lymphoma cells, through inhibition of telomerase activity leading to G_0 or G_1 cell cycle arrest [163]. This mechanism is further confirmed in prostate cancer cell lines where A3 receptor activation induces G_0-G_1 cell cycle arrest [164] due to

downregulation of CDK4 and cyclin D1. Additionally, A3 receptor stimulation prevents entry of human melanoma cells into the G1 phase of cell cycle, thus inhibiting proliferation[156]. Activation of A3 receptor also suppresses proliferation of melanoma and colon cancer cell lines through downregulation of the β-catenin pathway. In both the cancers, activation of A3 receptor is followed by decreased expression of AKT (protein kinase B) leading to increase in levels of unphosphorylated glycogen synthase kinase 3 β (GSK3β)–which is the stable form of GSK3β thus leading to phosphorylation and subsequent degradation of β-catenin, and subsequent inhibition of gene expression of downstream targets, cyclin D1 and cMyc [161,162,165]. Treatment of breast cancer cell lines with A3AR agonists inhibits cell proliferation due to reduced expression of tyrosine kinase ERBB2 that leads to decrease in levels of its downstream effector Erk[166]. Furthermore, A3AR stimulation suppresses proliferation of human papillary carcinoma cells through reduced phospho-Erk (pErk) levels, causing G1 cell cycle arrest that is attributed to decreased expression of cyclin D1 and cyclin E2[167]. Activation of A3AR is also associated with reduction in the ability of prostate cancer cells to migrate *in vitro* and metastasize *in vivo* through inhibition of PKA-mediated ERK phosphorylation[168].

3.2 Materials and Methods

Cell lines

All the following human osteosarcoma cell lines including SJSA-1, U2OS, KHOS/NP, MG63, and Saos2 were maintained in Dulbecco's Modified Eagle's Medium (DMEM) or Roswell Park Memorial Institute (RPMI) medium with 10% fetal bovine serum (FBS) and 1% penicillin-streptomycin in a humidified incubator at 37^0C with 5% CO2.

shRNAs

The shRNAs used are as follows:

TMIGD3: *T6U*: AAGAACTAAGATCTTGAGATG (Catalog #: VGH5518-200202459, GE Healthcare, Dharmacon Inc)**,** *T3:* TAGTTGCAGATGGCAGAAG (Catalog #: HSH003091-3-HIVmH1, Genecopoeia, Inc.)**,** A3AR: *A2a*: TTCTTCTGTGAGTGGTGAC (Catalog #: VGH5518-200180351), *A2b*: TGATGATAGATAAAGGCAG (Catalog #: VGH5518-200176914, GE Healthcare, Dharmacon Inc.).

Western blotting

Cells were directly lysed in 1.5X SDS sample buffer and heated at 95°C for 10 minutes, followed by loading onto 4-12% tris-glycine gel (Bio-Rad Laboratories), separated by electrophoresis and transferred to polyvinylidene fluoride (PVDF) membrane (GE Healthcare Life Sciences). Blots were incubated with primary antibodies for A3AR (H-80, Santa Cruz Biotechnology), TMIGD3 (Pab128, generated against aa. 235 to aa.248 CGIQRDFARDDMDF by GenScript), FLAG (M2, Sigma-Aldrich), IκB (4814S, Cell Signaling), p65 (8242S, Cell Signaling), and GAPDH (H-12, Santa Cruz Biotechnology)

at 4°C overnight. After washing with TBS plus 0.1% Tween 20 (TBST), blots were incubated with appropriate secondary antibodies conjugated with fluorescence (IRDye 650CW goat anti-rabbit IgG, 800CW goat anti-mouse IgG, Li-COR), followed by analysis with the Li-COR Odyssey infra-red imaging systems (Lincoln, Nebraska).

Sphere formation assays

Sphere formation assays were performed as previously described [73]. Briefly, cells (20 cells per well) were plated on 96-well ultra-low attachment plates (Corning Inc., Corning) in DMEM/F12 medium containing 10mM HEPES, 50 µM of putrescine, 20 nM of progesterone, ITS (insulin 25 mg/ml, sodium selenite 25 µg/ml, transferrin 25mg/ml) , EGF (10 ng/ml), and FGF (10 ng/ml) for 10-14 days, and numbers of spheres with sizes over 30 µm were counted. Sphere forming potential was calculated as percentage of total # of spheres formed/ total # of cells seeded.

Cell proliferation assays

Cells ($1x10^4$) were seeded onto each well of 6-well plates (day 0). Live cell numbers were counted at days 2, 4, 6, and 8 following trypan-blue staining.

Transwell migration assays

Migration assays were performed with 24-well Transwell chambers (6.5 mm diameter, 8µm pore size, Corning) as previously described[169,170]. Cells ($1x10^4$) in 100 µl of 0.5% FBS-containing DMEM were seeded on the upper chamber, while 10% FBS-containing DMEM was added in the lower chamber as a chemoattractant. Cells were

allowed to migrate through the membrane for 10 hours. The non-migrating cells were removed from the upper face of the filters, and migrating cells to the lower face were stained with Diff-Quik Stain Set (Dade Behring, Newark, DE). Stained cells in the entire fields were counted under an inverted microscope.

In vivo tumor formations assays

For subcutaneous tumor growth assays, cells were dissociated into single-cell suspensions using nonenzymatic cell dissociation solution (Sigma Biochemicals), and numbers of live cells were counted following trypan blue staining (Thermo Fisher Scientific). Cell suspension in 50μl of 4.5 mg/mL Matrigel (BD Biosciences) in Hank's balanced salt solution (HBSS) was subcutaneously injected into flanks of NIH-III nude mice (Charles River). Tumors were measured three dimensionally 2-3 times a week for 18-21 days. For tail vein assays, 150 μl of cell suspension ($5x10^4$) was injected into the lateral veins of nude mice. Mice were monitored for labored breathing, and the numbers of pulmonary tumor nodules were evaluated 6 weeks after injections. For orthotopic injections, 15μl of cell suspension ($1x10^5$) was injected into femoral bone marrow space of anesthetized NOD-scid IL2Rγ^{null} (NSG) mice (The Jackson Laboratories) [171]. When the tumors reached ~2 cm in thigh diameter, the mice were euthanized. The weight of the primary tumors and numbers of tumor nodules in the lungs and liver (>0.5mm) were measured. All mice were maintained under specific pathogen free conditions, and experimental procedures were performed according to the protocol approved by Institutional Animal Care and Use Committee.

Immunohistochemistry (IHC) for human tissues

Formalin fixed paraffin-embedded tissues of 16 primary, 17 metastatic OS, as well as 10 normal lung tissues, were provided by Dr. Ossama Tawfik. All the samples were anonymous, and no patient information was given. All samples were collected during surgery for biopsy from patients admitted at the University of Kansas Medical Center [172]. We also purchased a tissue microarray (OS804a, US Biomax,) consisting of 38 primary OS and 10 normal bone tissues.

Sections (4 μm thick) from the aforementioned tissues were deparaffinized in xylene, rehydrated in grades of alcohol, rinsed in tap water, and blocked with 0.3 % hydrogen peroxide for 30 minutes. Antigen retrieval was performed in a steamer with sodium citrate buffer (10 mM sodium citrate, pH 6.0) for 20 minutes. After blocking in 2.5% normal horse serum for 30 minutes, sections were incubated with rabbit anti-human TMIGD3 (Ab128) and A3AR (A3R32-A, Alpha Diagnostics) antibodies for 30 minutes at room temperature. After washing in PBS, sections were incubated in anti-rabbit biotinylated secondary antibody for 30 minutes. The signal was detected using the Vectastain Elite ABC kit (Vector Laboratories). Pre-immune serum and/or normal rabbit immunoglobulin G (IgG, Vector Laboratories) were used as negative controls. Two independent investigators blindly evaluated all stained sections. Two independent investigators were blinded prior to evaluation of all stained sections. Scoring was based on intensity and extensity. The scoring was determined by assessing the whole tumor section, and each sample was scored on a scale of 0–3 for extensity with 0 corresponding to less than 25 % of positive tumor cells; 1 for 26–50 %; 2 for 51–75 %; and 3 for 76–100 %. The intensity of immunostaining was determined as 0 (negative

staining), 1 (weakly positive staining), 2 (moderately positive staining), and 3 (strongly positive staining). The immunoreactive score of each section was calculated by the sum of these two parameters and presented as a score ranging between 0-6 as described previously[173].

3.3 Results

3.3.1 *Gene structure of TMIGD3 and A3AR*

Our screening analyses of a human whole-genome shRNA-screening library identified TMIGD3 as a protein whose knockdown increased sphere formation of SJSA-1 OS cell line. TMIGD proteins are a group of proteins that contain an “immunoglobulin (Ig)-like fold”. TMIGD1 is implicated in cancer differentiation and adhesion [174,175], while TMIGD2 is implicated in cancer immunosuppression as a receptor of HHLA2, a B7 family member [176]. However, there is no report about TMIGD3. The *TMIGD3* gene has two splicing isoforms of i1 and i3 (Fig. 3.1). The C-terminal regions (exons T2-T6) of TMIGD3 i1 and i3 are overlapped. Intriguingly, the first exon (consists of three transmembrane helices) of the *TMIGD3 i1* gene is shared with the *adenosine A3 receptor (A3AR)* gene, one of the four adenosine G protein-coupled receptors, and hence TMIGD3 i1 is also called A3AR i1, while A3AR is precisely A3AR i2 [95]. On the other hand, TMIGD3 i3 does not have any overlapping region with A3AR, but it is still occasionally referred to as A3AR i3, likely because these genes are present in the same chromosomal locus (Fig. 3.2). To avoid confusion, we followed TMIGD3 i1 and i3 nomenclature, instead of using A3AR i1 and i3, since these proteins share an Ig-like domain in the common C-terminal region and their functions as adenosine receptors are unknown.

Figure 3.2 Structure of TMIGD3 and A3AR.

(A) Human *TMIGD3* and *A3AR* gene locus on chromosome 1. Gene structures of human *TMIGD3 i1*, *i3*, and *A3AR*. TMIGD3 comprises of two identified isoforms: i1 and i3, with exclusive first exons (A1/T1), while their C-terminal region (exons T2-T6) is overlapped. The first exon (A1) of *TMIGD3 i1* is shared with the first exon of *adenosine A3 receptor isoform2 (A3AR i2*-also commonly called A3AR*).* Thus, TMIGD3 i1 and A3AR are splicing variants. Black bars indicate: locations of the different shRNAs: *T6U, T3* (targeting TMIGD3 i1 and i3)*; A2a, A2b* (targeting A3AR). Green bar: Immunoglobulin (Ig)-like fold.

Figure 3.2 Structure of TMIGD3 and A3AR

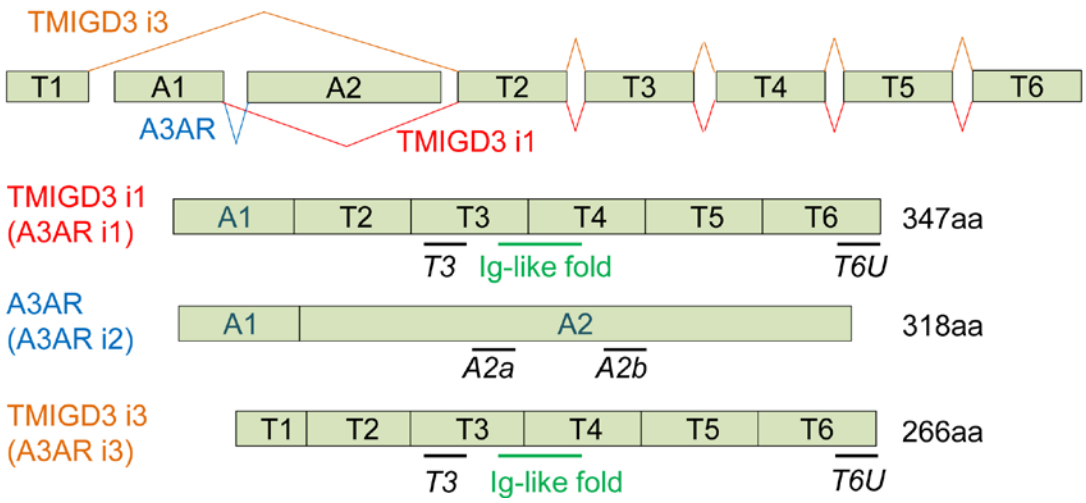

3.3.2 *Knockdown of TMIGD3 increases malignant properties of multiple OS cell lines*

Our identified shRNA is located in the 3' UTR region of TMIGD3 (*T6U*) which could target both TMIGD3 i1 and i3. To further confirm that TMIGD3 plays a role in the malignant properties of OS, we used another shRNA to downregulate the expression of TMIGD3 (*T3*). Knockdown of TMIGD3 with both shRNAs increased sphere formation of SJSA-1 and Saos2 OS cells (Fig. 3.3A). Since, TMIGD3 shares its N-terminal region with A3AR, we wanted to query the importance of A3AR in the sphere forming ability of OS cells. In fact, knockdown of A3AR with two different shRNAs (*A2a*, *A2b*) increased sphere forming ability of SJSA-1 OS cells (Fig. 3.3B). Moreover, knockdown of TMIGD3 and A3AR using different shRNAs increased cell proliferation (Fig. 3.3C) of SJSA-1 and migration of SJSA-1 and Saos2 cells (Fig. 3.4).These results suggest that both TMIGD3 and A3AR could be novel suppressors of malignant progression of OS cells.

Figure 3.3 Knockdown of TMIGD3 and A3AR increases sphere formation of multiple OS cells.

(A) Sphere formation assays using SJSA-1 (left) and Saos2 (right) cells with different shRNAs for TMIGD3. Error bars: means ± S.D. from 3 independent experiments. * $p<0.05$, ** $p<0.01$; Student's t-test.

(B) Sphere formation assays using SJSA-1 with different shRNAs for A3AR. Graphs showing percentage of sphere formation. Error bars: means ± S.D. from 3 independent experiments (n=1440). * $p<0.05$, ** $p<0.01$; Student's t-test.

(C) Proliferation assays following knockdown of TMIGD3 (*T6U, T3*) and A3AR (*A2a*, *A2b*) in SJSA-1 cells. Cells ($1x10^4$) were seeded on 6-well plates and numbers of cells were counted every 2 days following trypan blue staining.

Figure 3.3 Knockdown of TMIGD3 and A3AR increases sphere formation of multiple OS cells.

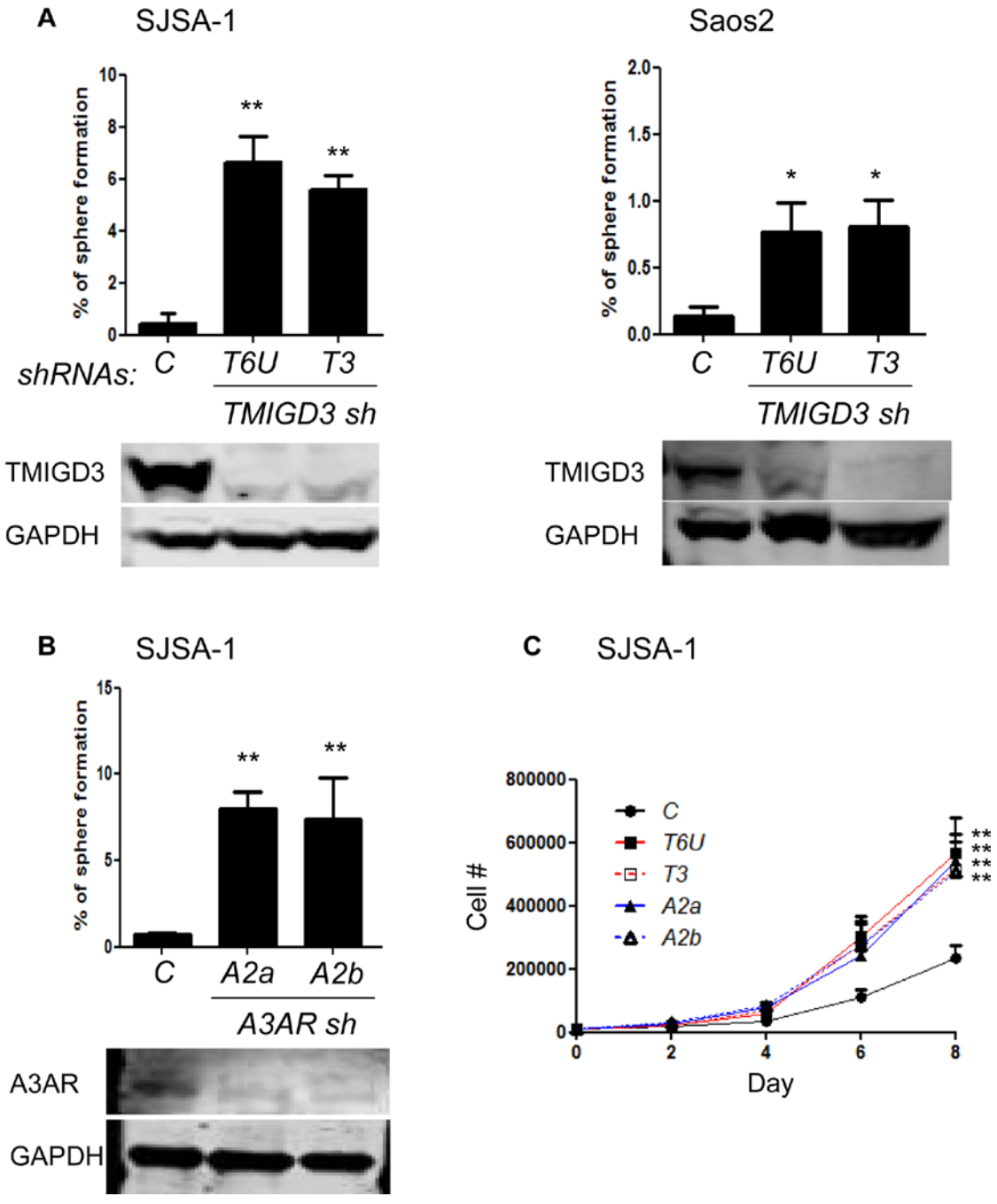

Figure 3.4 Knockdown of TMIGD3 and A3AR increases migratory potential of OS cells.

(A) Migration assays for 10 hours using cells downregulated for TMIGD3 in SJSA-1 (left) and Saos2 (right) cells.

(B) Migration assays using SJSA-1 cells downregulated for A3AR. Graphs showing the relative migration (top) compared with control and representative images (below). Error bars: means ± S.D. from 3 independent experiments. * $p<0.05$, ** $p<0.01$; Student's t-test.

Figure 3.4 Knockdown of TMIGD3 and A3AR increases migratory potential of OS cells

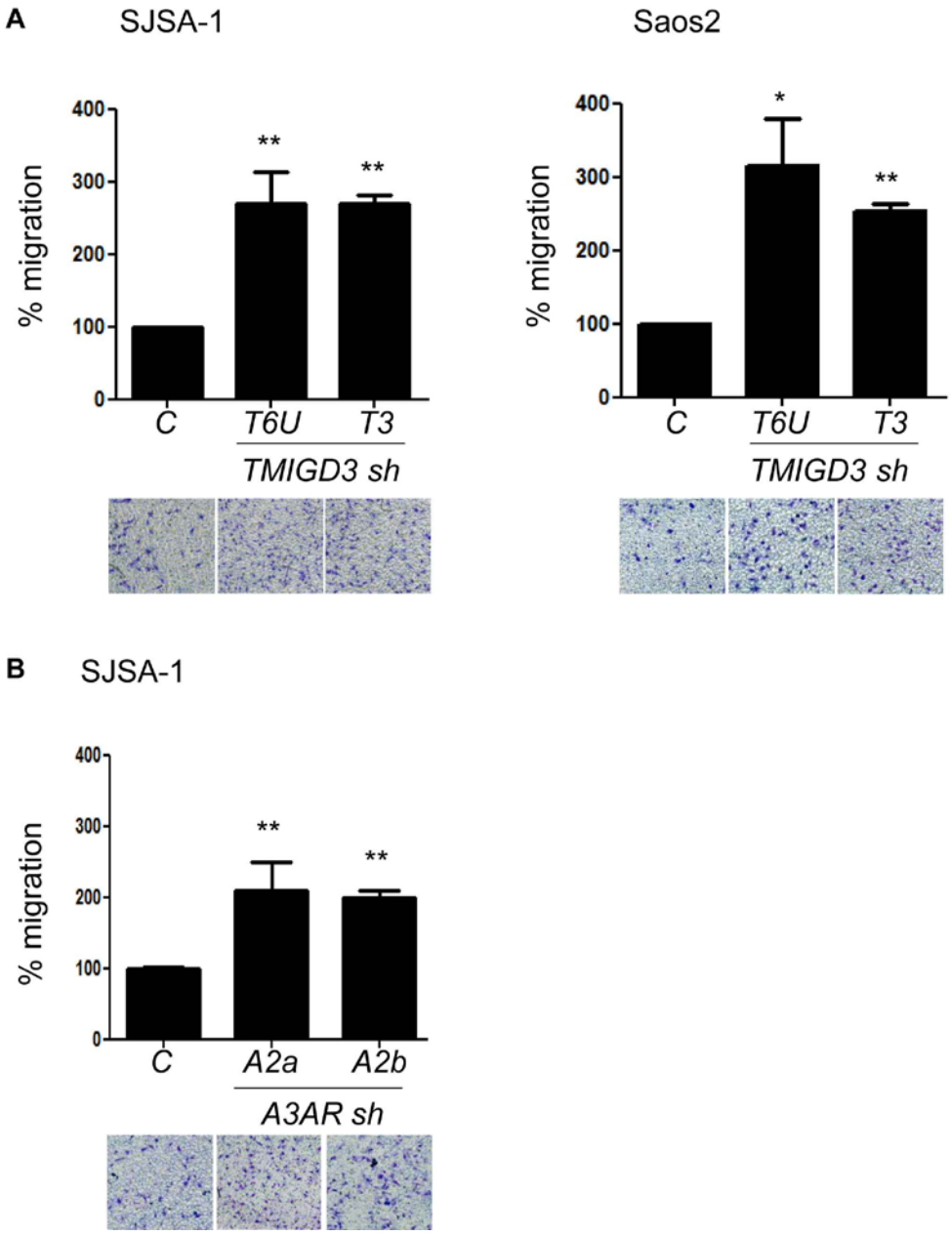

3.3.3 Knockdown of TMIGD3 and A3AR promote tumor formation and metastasis

To further address the effects of TMIGD3 and A3AR on OS malignancy *in vivo*, we performed subcutaneous tumor growth assays following knockdown of TMIGD3 and A3AR. We observed that downregulation of TMIGD3 and A3AR both led to increase in tumor growth in SJSA-1 (Fig. 3.5A). We also performed tail vein injection assays using SJSA-1 cells with or without knockdown of TMIGD3 by *T6U* and *T3* shRNAs. TMIGD3 knockdown by both shRNAs dramatically increased lung metastases of SJSA-1 cells (Fig. 3.5B).

For orthotopic injection assays, we directly injected SJSA-1 or Saos2 cells with or without knockdown of TMIGD3 into the femurs of mice. Knockdown of TMIGD3 significantly enhanced tumor establishment in femurs and metastases formation in the lungs or liver respectively (Fig. 3.6A). Similarly, knockdown of A3AR in SJSA-1 cells enhanced tumor establishment and lung metastases in orthotopic injection assays (Fig. 3.6B).

To further address the clinical significance of TMIGD3 and A3AR in OS, we wanted to examine protein expression of these proteins in human tissues. However, there was no available antibody for immunohistochemistry (IHC) that could discriminate TMIGD3 from A3AR. Hence, we generated a peptide antibody recognizing TMIGD3, namely Ab128 (located in exon T3, thus recognizing both TMIGD3 i1 and i3), and validated it for the use of IHC using tissues derived from tumors with or without knockdown of TMIGD3 (Fig. 3.7). Membrane distribution of the protein TMIGD3 was observed in the control tumor whereas in the TMIGD3-knockdown tumor (*T6U)*, the staining intensity was low, thus confirming the specificity of the generated Ab128

antibody. Using this antibody, we performed IHC for these proteins in primary and metastatic human OS tissues, as well as normal lung and bone tissues as controls (Fig. 3.8). We observed that expression of TMIGD3 and A3AR in both primary and metastatic human OS was significantly lower than that in normal bone and lungs. We did not see any significant differences between primary and metastatic tissues. It should be noted that this antibody detects both TMIGD3 i1 and i3 and cannot discriminate these isoforms. Nonetheless, our data suggest that reduced expression of TMIGD3 and A3AR is associated with malignant properties of OS *in vivo* and clinically.

Figure 3.5 Knockdown of TMIGD3 is associated with OS malignancy *in vivo*- subcutaneous and tail vein assays.

(A) Subcutaneous tumor formation assays using SJSA-1 cells ($5x10^5$) downregulated for TMIGD3 (*T6U*) and A3AR (*A2a*), or with non-silencing shRNA (*Control*). Tumors were measured twice a week until day 20 after injections. Error bars: means ± S.D. (n=5). ** $p<0.01$; Two-way ANOVA.

(B) Tail vein injection assays using SJSA-1 cells ($5x10^4$) infected with non-silencing (*control: GFP+, green*), *T6U (GFP+, green)*, or *T3 (DsRed+, red)* shRNAs. Mice (*Control:* n=7, *T6U:* n=7, *T3:* n=4) were euthanized 6 weeks later. Representative pictures of lungs (top) and images from a fluorescence dissecting stereo-microscope (bottom). Table represents average number of nodules observed.

Figure 3.5 Knockdown of TMIGD3 is associated with OS malignancy *in vivo*

A SJSA-1

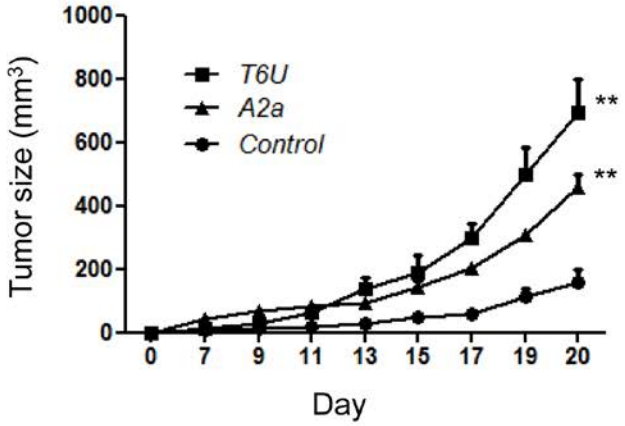

B SJSA-1

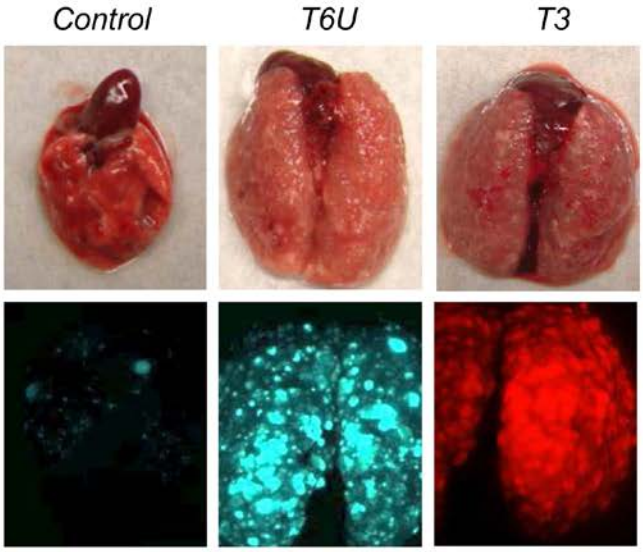

Cell line	Avr +/- SD
Control	8 +/- 7.7 (n=7, 4e5)
T6U	>100 (n=7, 4e5)
T3	>100 (n=4, 3e5)

Figure 3.6 Knockdown of TMIGD3 and A3AR is associated with OS malignancy *in vivo* orthotopic injection assays.

(A) Primary tumor and metastasis formation following orthotopic injections of SJSA-1 and Saos2 cells with (*T6U*) or without (*C*) TMIGD3 knockdown. Cells ($1x10^5$) were injected into femurs of NSG mice and mice were euthanized approximately 2 months (SJSA-1) and 5 months (Saos2) later when thigh diameter became ~2 cm in mice with TMIGD3 knockdown cells. Graphs showing primary tumor weight and number of metastatic nodules in the lungs (SJSA-1) or liver (Saos2) on the side of the graphs. (B) Primary tumor and metastasis formation following orthotopic injections of SJSA-1 cells ($1x10^5$) with (*A2a*) or without (*C*) A3AR knockdown. Mice were monitored as described above. Representative images of the primary tumor and metastatic nodules on the side of the graphs. Arrows indicate metastatic nodules. Error bars: means ± S.D. * $p<0.05$, ** $p<0.01$; Student t-test.

Figure 3.6 Knockdown of TMIGD3 and A3AR is associated with OS malignancy *in vivo*- orthotopic assays

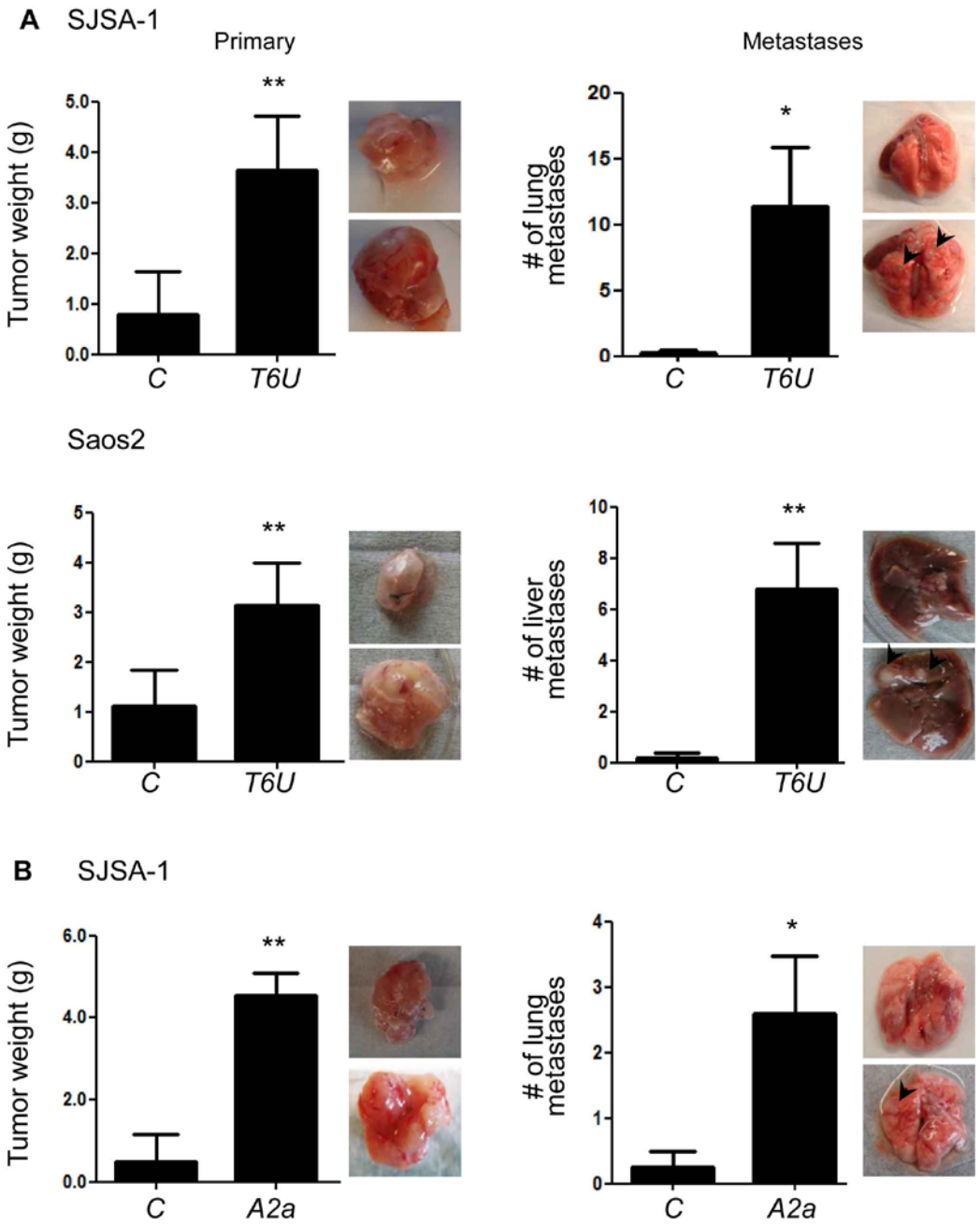

Figure 3.7 Generation of a peptide antibody for TMIGD3 and its validation.

(A) Structure of TMIGD3 i1 protein and location of peptides (aa. 235- aa. 248) of TMIGD3 i1 to generate a peptide antibody (Ab128).

(B) IHC for TMIGD3 with Ab128 using SJSA-1-derived tumors infected with lentiviral vectors encoding non-silencing control (*C*) or TMIGD3 (*T6U*) shRNAs.

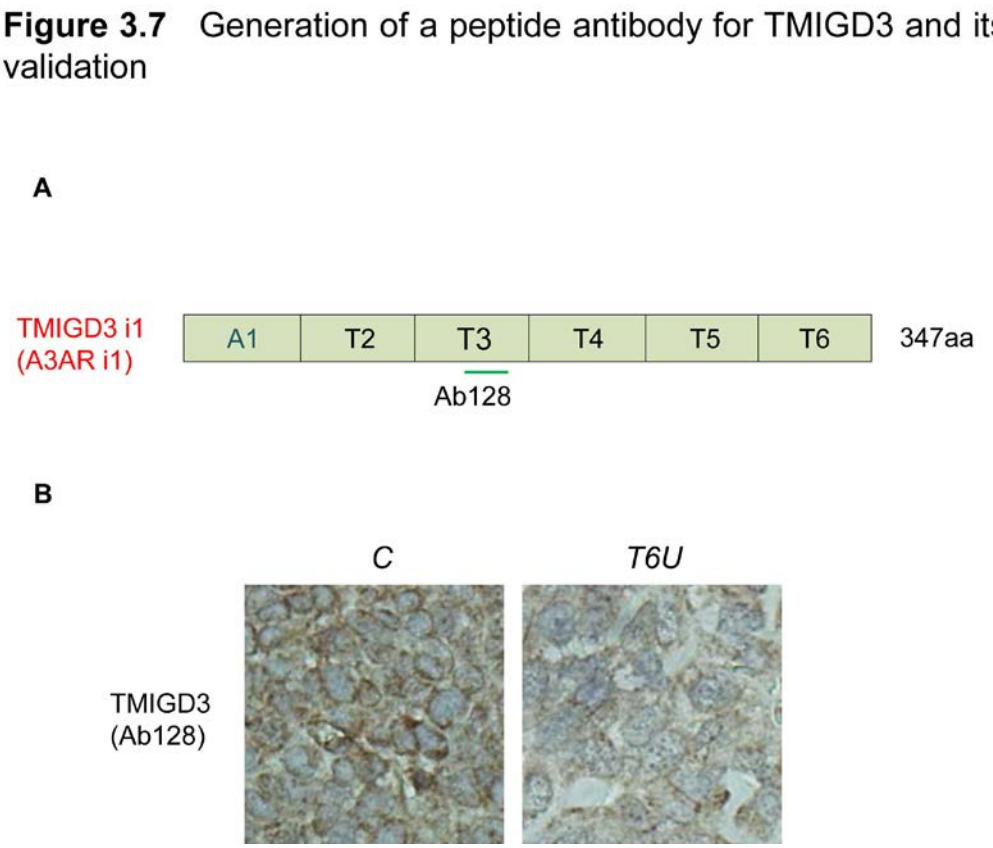

Figure 3.8 Clinical significance of TMIGD3 and A3AR.

IHC for TMIGD3 (A) and A3AR (B) in human OS and normal tissues. IHC analyses were performed using OS tissues (54 primary tissues and 17 metastases), as well as normal lung (n=10) and bone (n=10) tissues. Two independent investigators blinded prior to evaluation scored these samples. Scoring was based on intensity and extensity. The immunoreactive score of each section was calculated by the sum of these two parameters and presented as a score ranging between 0-6 (average of two reads). Representative images of IHC below the graphs. The horizontal lines in the plots represent the median. ** $p<0.01$; One way ANOVA.

Figure 3.8 Clinical significance of TMIGD3 and A3AR

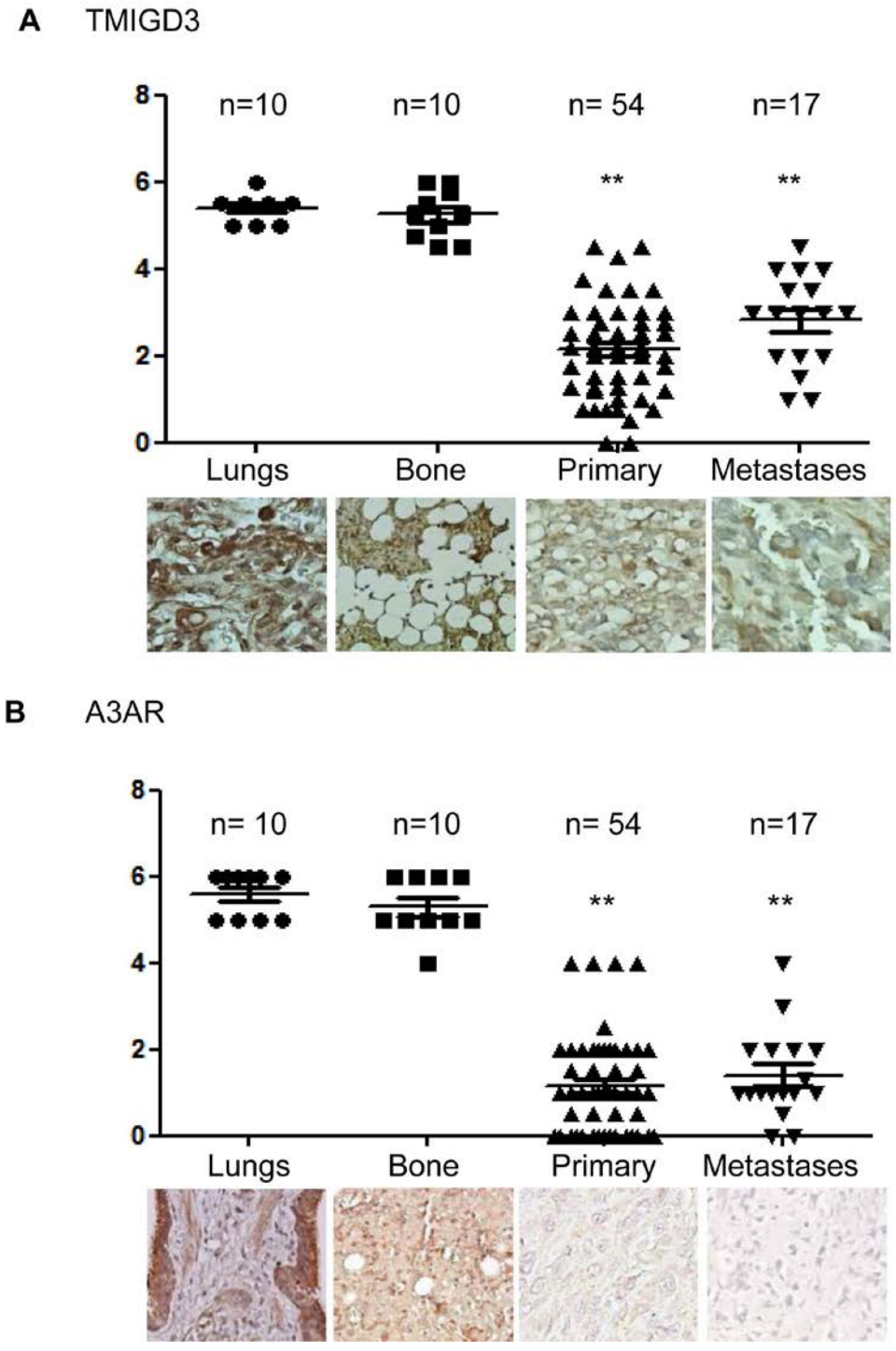

3.3.4 TMIGD3 i1 and A3AR, but not TMIGD3 i3, suppress malignant properties of OS

TMIGD3 gene has two splicing isoforms (Fig 3.2). We have demonstrated that knockdown of TMIGD3 plays roles in the suppression of OS progression. Since the used shRNAs (*T6U* and *T3*) target both TMIGD3 i1 and i3, our data does not delineate the isoform(s) that contributes to phenotypes associated with OS malignancy. To determine which isoforms of TMIGD3 suppress OS progression and compare their biological phenotypes with those of A3AR, we stably infected lentiviral vectors encoding the cDNA for empty vector (V), TMIGD3 i1 (cTi1), TMIGD3 i3 (cTi3), and A3AR (cA3) in SJSA-1 and KHOS/NP OS cell lines. Overexpression of TMIGD3 i1 and A3AR, but not TMIGD3 i3, significantly inhibited proliferation of both the cell lines (Fig. 3.9A). We further performed sphere formation assays using SJSA-1 and KHOS/NP cells with overexpression of TMIGD3 i1, i3, and A3AR. As expected, TMIGD3 i1 and A3AR, but not TMIGD3 i3, suppressed sphere formation of both cells (Fig. 3.9 B). These results suggest that TMIGD3 i1, but not i3, suppresses malignant properties of OS, similar to A3AR.

Intriguingly, western blotting for these proteins revealed that both TMIGD3 i1 and TMIGD3 i3 ran at almost the same size at ~54 kDa, higher than their predicted sizes of ~40 kDa and ~30 kDa, respectively (Fig. 3.9A). To confirm that, we performed western blotting using cells transfected with a FLAG tagged-TMIGD3 i3, together with non-tagged TMIGD3 i1 and i3, and found that even FLAG-tagged TMIGD3 i3 ran at similar size to TMIGD3 i1 and i3 (Fig 3.10). It should be noted that similar differences in predicted size vs actual size have been observed previously for TMIGD1 and TMIGD2, due to their post-translational modifications linked with N- glycosylation [174,177].

Nonetheless, these results suggest that TMIGD3 i1, but not i3 suppresses OS proliferation and sphere formation similar to A3AR, and the overlapping N-terminal region (consisting of the first 117 aa) may play a role in OS suppression.

We also performed rescue experiments to confirm whether overexpression of TMIGD3 i1 or TMIGD3 i3 could nullify increased sphere formation by TMIGD3 knockdown and to mitigate possible off-target effects of used shRNAs. Sphere formation assays using cells downregulated for TMIGD3 or A3AR by their shRNAs with or without overexpression of corresponding cDNAs for these proteins revealed that overexpression of TMIGD3 i1 rescued the increased sphere formation by TMIGD3 *T6U* and *T3* shRNAs, whereas TMIGD3 i3 overexpression failed to do so (Fig. 3.11A). Also, A3AR overexpression canceled the increased sphere formation by the *A2a* shRNA (Fig. 3.11B). Thus, sphere suppression effects by these shRNAs are not due to their off-target effects.

Also, the importance of TMIGD3 i1, TMIGD3 i3, and A3AR was questioned in other OS malignant properties including migration and tumor growth. Overexpression of TMIGD3 i1 and A3AR inhibited migratory potential (Fig. 3.12A) in SJSA-1 and KHOS/NP cells, as well as tumor formation of SJSA-1 cells (Fig. 3.12B). However, TMIGD3 i3 did not cause suppression of migration and tumor formation of OS cells. Thus, these data suggest that TMIGD3 i1, but not i3, suppresses malignant properties of OS cells *in vitro* and *in vivo*, similar to A3AR.

Figure 3.9 TMIGD3 i1, but not TMIGD3 i3, inhibits growth and sphere formation of OS, similar to A3AR.

(A) Proliferation assays using SJSA-1 (left) and KHOS/NP (right) cells overexpressing vector control (V), TMIGD3 i1 (cTi1), i3 (cTi3), and A3AR (cA3). Graphs represent data from 3 independent experiments, and representative immunoblots showing overexpression of each protein are present below the graphs. Error bars: means ± S.D. from 3 independent experiments.* $p<0.05$, ** $p<0.01$; Two-way ANOVA.

(B) Sphere formation assays using SJSA-1 and KHOS/NP cells overexpressing V, cTi1, cTi3, and cA3 as above. Graph showing % of sphere formation. Error bars: means ± S.D. * $p<0.05$, **$p<0.01$, n.s.: not significant; Student's t-test.

Figure 3.9 TMIGD3i1, but not TMIGD3i3, inhibits growth and sphere formation of OS, similar to A3AR

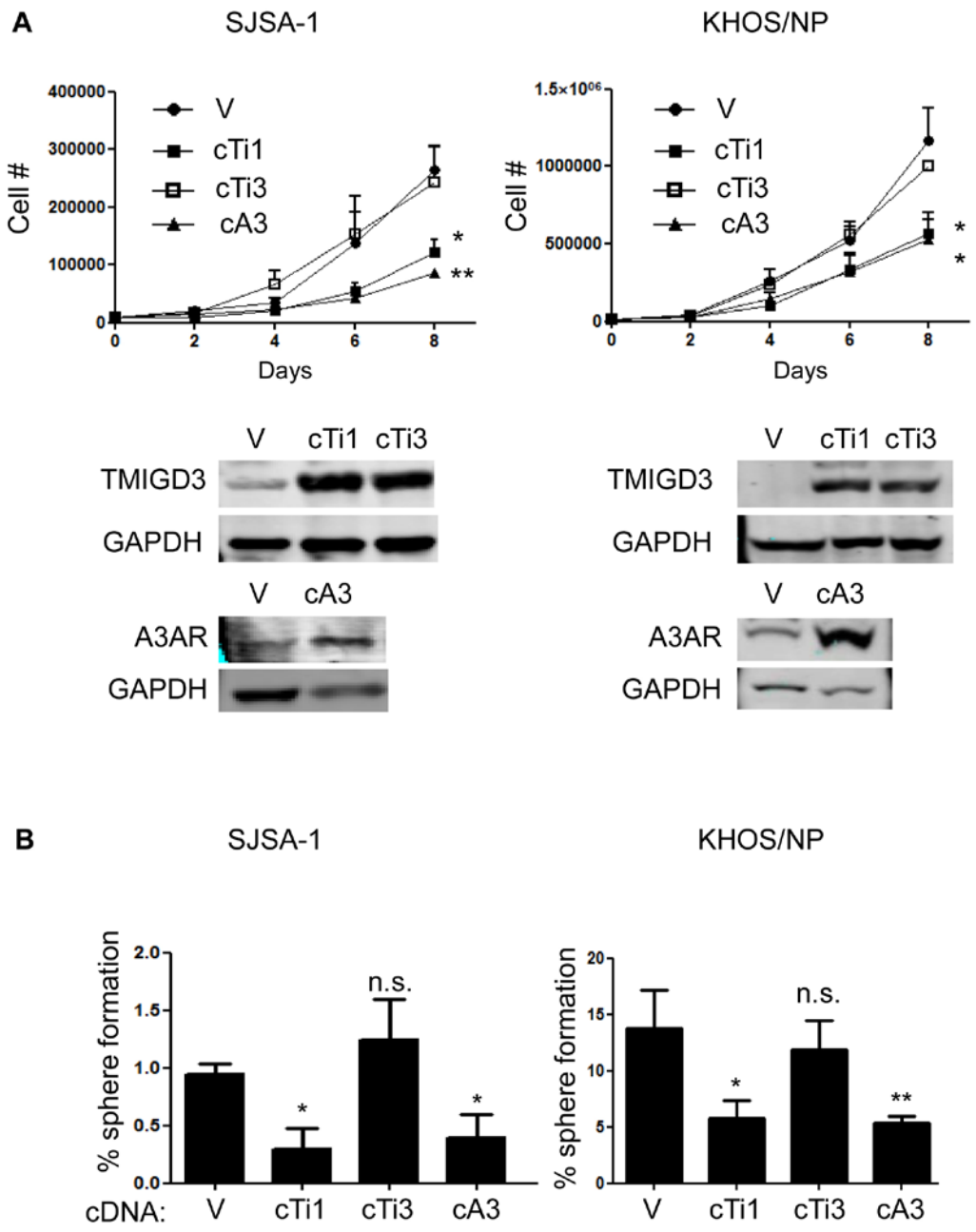

Figure 3.10 TMIGD3 i1 and i3 run at almost the same size.

Representative images of western blotting using SJSA-1 cells expressing V, cTi1, cTi3, and FLAG-tagged cTi3 (Fl-cTi3) for indicated proteins. To note, although the predicted size for TMIGD3 i1 is 54 kDa and that for TMIGD3 is 36 kDa, bands for these two isoforms were detected at almost the same size.

Figure 3.10 TMIGD3 i1 and i3 run at almost the same size

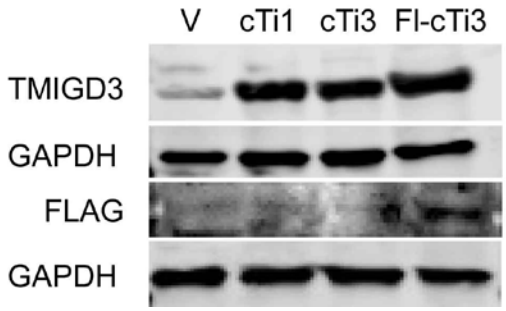

Figure 3.11 TMIGD3i1, but not TMIGD3i3, rescues increased sphere formation following knockdown of TMIGD3, similar to A3AR.

(A) Sphere formation assays using SJSA-1 cells with or without knockdown of TMIGD3 (*T6U*, *T3*) along with overexpression of TMIGD3 i1 (cTi1) or i3 (cTi3). Representative western blotting results below the graphs.

(B) Sphere formation assays using SJSA-1 cells with or without knockdown of A3AR along with overexpression of A3AR. Representative western blotting results below the graphs

Figure 3.11 TMIGD3 i1, but not TMIGD3 i3, rescues increased sphere formation following knockdown of TMIGD3, similar to A3AR

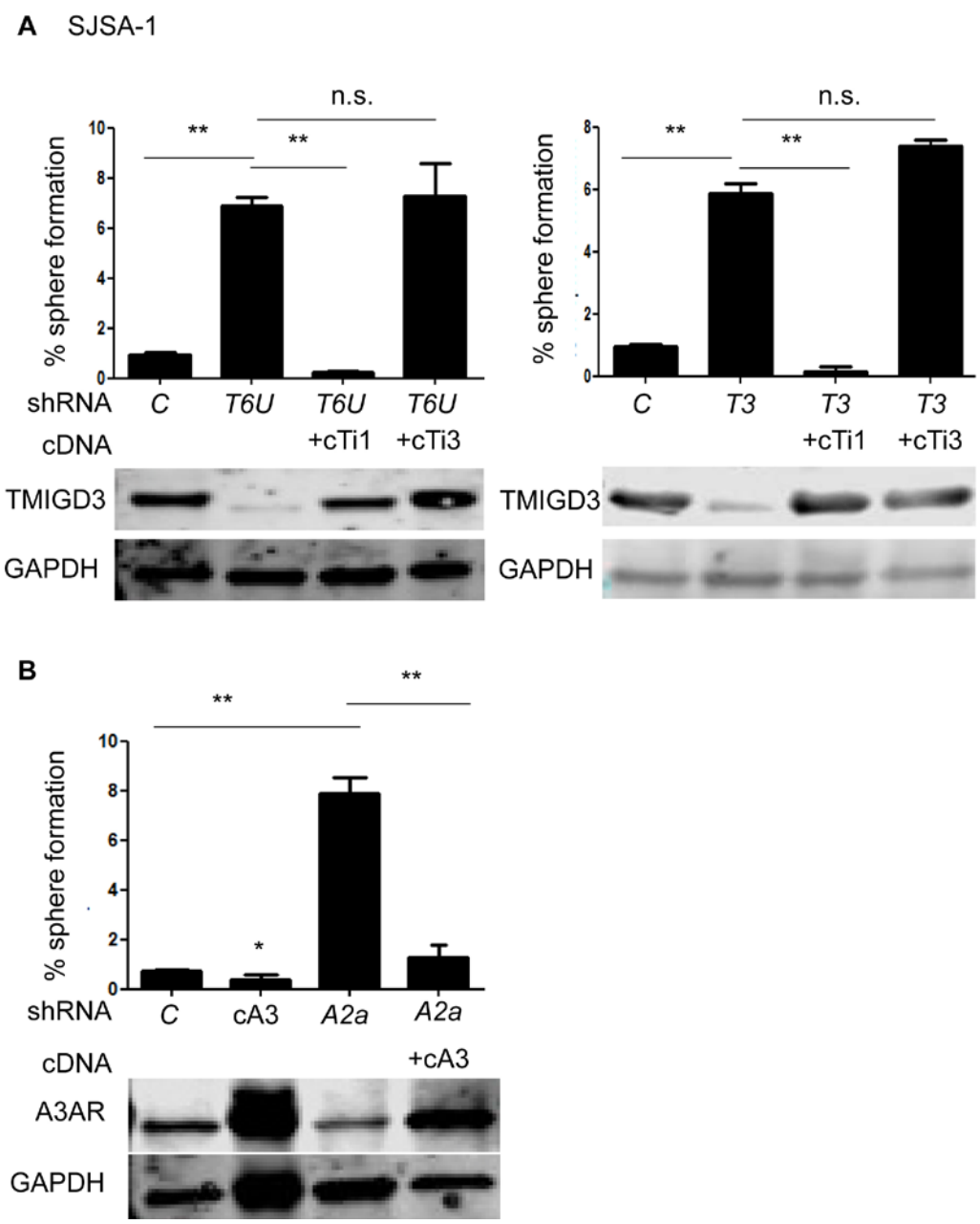

Figure 3.12 TMIGD3 i1, but not TMIGD3 i3, inhibits migration and tumor formation of OS, similar to A3AR.

(A) Transwell migration assays for 10 hours using SJSA-1 (left) and KHOS/NP (right) cells overexpressing V, cTi1, cTi3, and cA3. Graphs showing the relative migration to cell with vector control (top) and representative images (below). Error bars: means ± S.D. from 3 independent experiments. * $p<0.05$, ** $p<0.01$; Student's t-test

(B) Tumor growth assays in mice injected with SJSA-1 cells overexpressing V, cTi1, cTi3, and cA3 (n=5). Cells ($1x10^6$) were subcutaneously injected into nude mice, and tumor sizes were monitored twice a week for 18 days. Representative images of tumors next to the graph. ** $p<0.01$, n.s.: not significant; Two way-ANOVA.

Figure 3.12 TMIGD3i1, but not TMIGD3i3, inhibits migration and tumor formation of OS, similar to A3AR.

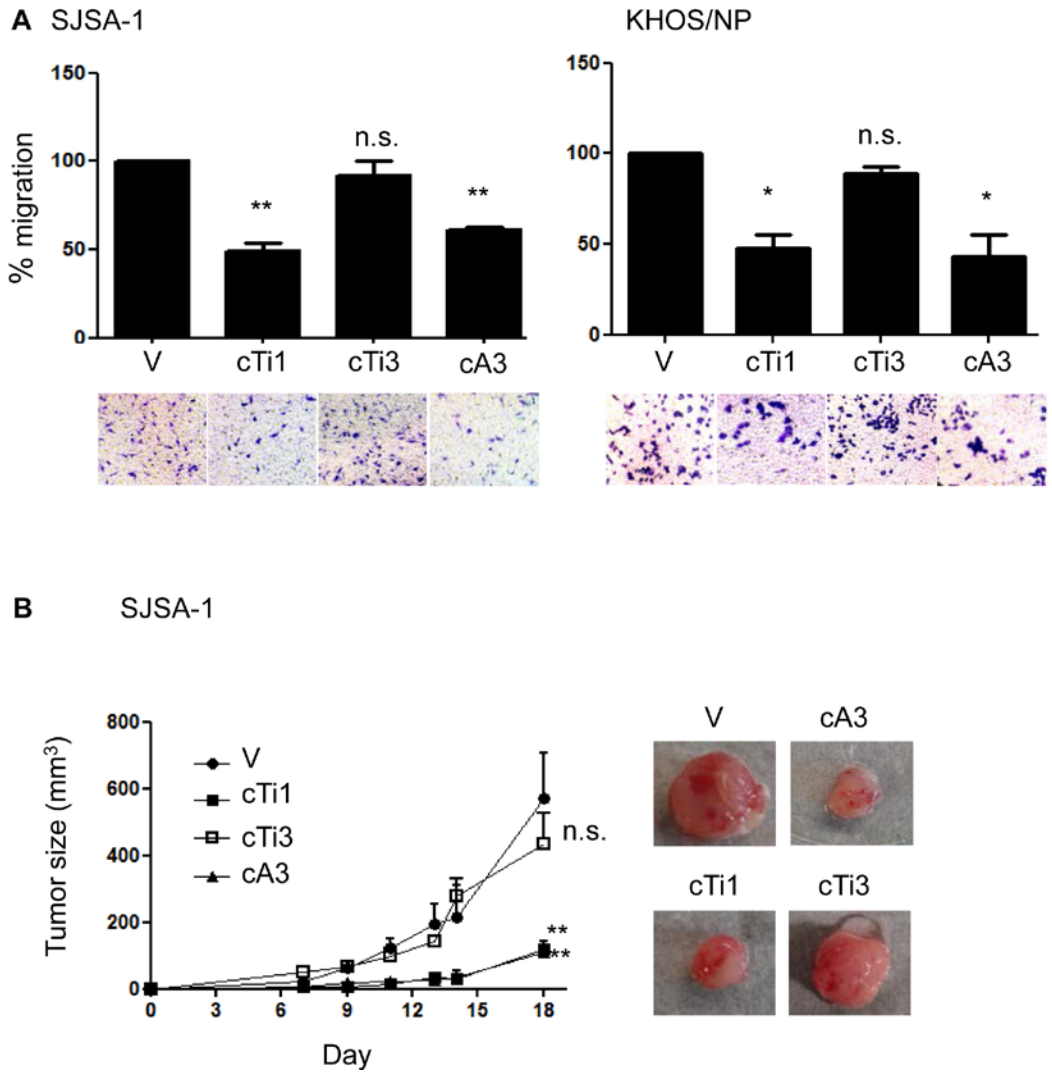

3.4 Discussion

Our study has shown that TMIGD3 and A3AR inhibit aggressive properties of OS including migration, proliferation, tumor formation, and metastasis. This is the first report illustrating a tumor suppressive role for the novel TMIGD3 protein. Also, this is the first study elucidating tumor inhibitory roles for A3AR in OS. Of the two isoforms for TMIGD3, TMIGD3 i1 and TMIGD3 i3, TMIGD3 i1 is crucial in the suppression of OS aggressive properties including proliferation, migration, and tumor formation. TMIGD3 i3 has a distinct N-terminal region and shares its C-terminal region with TMIGD3 i1, thus sharing no similarity with A3AR (Fig 3.2). Our web-based domain analyses using protein structure prediction sites, including PridictProtein server (https://www.predictprotein.org/) and SOSUI (http://harrier.nagahama-i-bio.ac.jp/sosui/sosui_submit.html) identified two transmembrane helices at the C-terminal region of TMIGD3 i1 (aa129-151 and aa291-313), in addition to 3 transmembrane helices within the first 117 amino acids sharing with A3AR, as well as a known Ig-like fold at the C-terminal region (aa167-256) (Fig. 4.1). Since TMIGD3 I1 and A3AR are involved in OS suppression, and not TMIGD3 i3, this postulates the hypothesis that the common N-terminal region between TMIGD3 i1 and A3AR plays an important role in the OS suppression. Future detailed domain mapping and mutational studies in the N-terminal region are required to address this hypothesis.

Since no commercially available antibody could discriminate between A3AR and TMIGD3, our study is the first one to examine the expression levels of TMIGD3 in normal and tumor tissues. We have generated a peptide antibody (PAb128) in exon T3 of TMIGD3, which recognizes both isoforms of i1 and i3. It should be noted that it is very

difficult to generate an antibody, which detects only TMIGD3 i1, since its N-terminal region is identical with A3AR, while its C-terminal region is identical with TMIGD3 i3. Moreover, despite the differences of predicted sizes of TMIGD3 i1 and i3 proteins, both run at almost the same size in SDS PAGE (Fig. 3.9). Even when using overexpression of TMIGD3 i3 tagged with FLAG, it runs at the same size as TMIGD3 i1 and non-tagged TMIGD3 i3 (Fig 3.10). Similar changes in predicted size vs actual size have been observed previously for TMIGD1 and TMIGD2, due to post-translational modifications linked with N- glycosylation [174,177]. Generation of an antibody detecting a specific region of TMIGD3 i3 (first exon) would be necessary to discriminate between these two isoforms. Nonetheless, protein expression of TMIGD3 in OS tissues is significantly lower than that in normal bone and lungs, similar to A3AR. Indeed, A3AR expression appears low in many types of cancer in the Human Protein ATLAS database (http://www.proteinatlas.org/ENSG00000121933-ADORA3/cancer). Since both *A3AR* and *TMIGD3 i1* genes are likely to be driven by the same promoter, expression of these proteins may be attenuated at the transcriptional levels. It would be important to determine how mRNA expression of these genes is regulated and the possible mechanisms behind its gene silencing. Interestingly, no significant differences in the expression of TMIGD3 and A3AR between primary and metastatic OS are found. This could be because TMIGD3 and A3AR expression may be lost during early stages of OS genesis. It is unfortunate that we could not obtain detailed patients' information; correlation studies between expression of TMIGD3 or A3AR with patient's prognosis or clinical stages need to be elucidated as a future study. Also, it should be noted that A3AR knockout mice are not tumor-prone, rather show increased inflammatory

response [178]. In order to examine the *in vivo* significance of TMIGD3 i1 and A3AR on tumor development, generating compound knockout mice of *TMIGD3 i1* and *A3AR* and a mouse model of cancer would be necessary.

CHAPTER 4

TMIGD3 AND A3AR SUPPRESS OS PROGRESSION THROUGH THE NF-κB PATHWAY

4.1 Introduction

4.1.1 Signaling pathways regulated by A3AR and their roles in pathogenesis of OS

A3ARs are associated with classic G-protein coupled secondary messenger pathways signaling through both Gi and Gq family of G proteins[121,179,180]. A3AR inhibits cAMP accumulation through the inhibition of adenylyl cyclase activity through the Gi protein and stimulate phospholipase C (PLC) through Gq protein coupling[181,182]. It should be noted that the potency of a GPCR to activate different signaling pathways depends on the physiological conditions prevalent in the cells [183].

4.1.1.1 <u>The NF-κB pathway</u>

The NF-κB pathway is involved in multiple malignancies [184] including OS [185,186], NF-κB regulates transcripts of a number of genes crucial for tumorigenesis including PDGF-1, TIMP 1 & 2, Bcl-2, Bax, XIAP, cyclin D1 and cMyc [187-193]. NF-κB is also associated with metastasis and prognosis in several types of sarcomas including OS[194-196]. Inhibition of the NF-κB pathway decreases cell growth, increases apoptosis, and increases sensitivity to radiation[197,198]

The NF-κB pathway is involved in proliferation and differentiation of OS cells[191,197,198]. Indeed, the NF-κB pathway is reported to have an antagonistic effect on the bone morphogenetic protein (BMP-2)-mediated osteoblast differentiation of mesenchymal stem cells[199-201]. Hyperactivation of NF-κB causes incomplete differentiation and hence causes the maintenance of a stem-like population, with the ability to give rise to a heterogeneous OS tumor [202,203]. It is shown that inhibition of

NF-κB, decreases the CSC population in culture [204]. Hence, targeting the NF-κB axis to diminish the most malignant subpopulation in the tumor could be a promising strategy. However, the mechanism behind how NF-κB regulates the stem-like population is still unexplored.

Well-characterized anti-inflammatory activity of A3AR is mediated through the NF-κB signaling pathway (Fig 4.2). A3AR activation suppresses TNFα production through the NF-κB pathway [205,206]. Also, activation of A3AR by its specific agonists induce apoptosis or growth suppression of several types of cancer, such as leukemia, lung cancer, bladder cancer, and melanoma, via inhibition of the β-catenin and NF-κB pathways [165,207-209]. Mechanistically, the activation of A3AR inhibits the activities of protein kinase A (PKA) and protein kinase B (PKB/Akt) [210,211] leading to decreased nuclear translocation of NF-κB. The A3AR-NF-κB axis is implicated in the suppression of tumor growth both *in vitro* and *in vivo* [207]. Also A3AR is a direct transcriptional target of NF-κB [212] which might explain the high expression of A3AR in certain tumors [213]. However, the physiological levels of adenosine are not adequate enough to activate A3AR in tumors since the affinity of A3AR for adenosine is very low[214]. Hence, activation of A3AR by its specific agonists and subsequent inhibition of NF-κB activity can be considered to be a potential anti-cancer therapy[215].

4.1.1.2 β-catenin pathway

The β-catenin pathway, a major player of cell survival and growth, is a target for mutations known to promote neoplastic transformation in humans and in mouse models [216]. Accumulation of nuclear and/or cytoplasmic β-catenin is observed in 70% of patient

OS samples [217]. Iwaya *et al*. also observe that LM8, highly metastatic OS cells, show stronger staining intensity of β-catenin compared to non-metastatic Dunn OS cells, suggesting the use of β-catenin as a biological marker for metastasis of OS [218]. The β-catenin pathway is associated with stem cell renewal and mesenchymal stem cell differentiation [219]. Treatment of OS cell lines and primary OS culture, with salinomycin causes inhibition of the stem–like population through this pathway. CSCs/TICs derived from OS cell lines treated with salinomycin, show decreased expression of β-catenin, activation of GSK-3β and subsequent downregulation of cyclinD1, a downstream target of this pathway [220,221]

However, the role of the β-catenin pathway in OS stem cells is ambiguous. As observed with the NF-κB pathway, the importance of the β-catenin pathway in osteoblast differentiation and proliferation is precedent and is required for maintenance of mesenchymal progenitor cells [222,223].

The connection between A3AR and the β-catenin pathway is also suggested in mediating the inhibitory effect of A3AR on tumor growth. The activation of A3AR decreases activities of PKA and PKB/Akt which leads to decrease in the phosphorylation and subsequent activation of GSK-3β. GSK-3β controls mammalian cell proliferation and survival by phosphorylating β-catenin, and prevents it from translocating to the nucleus, hence activating its downstream effectors such as cyclin D1 and cMyc and leading to tumor inhibition of colon carcinoma and prostate cancer [162,207]. Thus β-catenin activity is crucial for aggressive properties of OS and could play a role in the mechanism behind A3AR-mediated suppression of OS malignancy.

4.1.1.3 Erk pathway

Extracellular Receptor Kinase (Erk) proteins comprise a family of serine/threonine kinases that respond to growth stimuli, such as insulin and nerve growth factor (NGF) that cause their subsequent tyrosine phosphorylation. The role of Erk in inflammation and oncology is well established, which is also known more commonly as Mitogen-Activated Protein Kinase (MAPK). Erk activation by phosphorylation is orchestrated from Ras/Raf followed by MAPK/Erk Kinase (MEK) through a variety of stimuli including growth factors and cytokine receptors. MAPK/Erk signaling is associated with many characteristics of malignancy such as high mitotic index, increased matrix metalloproteinase production, Warburg effect, angiogenesis, and cytokine production[224-228]. Increased activity of MAPK signaling is correlated with poor prognosis and has therapeutic implications in different types of cancer[229-231].

The role of MAPK/Erk pathway in OS is not clearly understood. Higher expression levels of MAPK/Erk in OS, Ewing's sarcoma, and high-grade chondrosarcoma are reported [80,232,233]; hence several studies unveiling the potential therapeutic implication of this pathway in bone sarcomas are underway. Inhibition of the Erk activity leads to increased OS apoptosis, increased doxorubicin sensitivity, and inhibits migration and invasion in OS[80,232-234]. Erk inhibitors alone or in combination with other chemotherapeutic drugs inhibit OS growth showing prolonged survival in mice[233].

A3AR also influences the MAPK pathway. A3AR is shown to signal to Erk1/2 through the phophoinositide 3- kinase (PI3K) and MAP kinase (MEK) in human fetal astrocytes[214]. A3AR also mediates Erk1/2 phosphorylation in primary mouse microglia cells, as well as in pathological conditions such as colon carcinoma and glioblastoma [235]

[236,237]. However, in prostate cancer cells, A3AR appears to inhibit the Erk1/2 activity through adenylyl cyclase and PKA. Indeed, treatment of glioma cells with A3AR agonist, Cl-IB-MECA, inhibits Erk1/2 activities and induces caspase-dependent cell death. Similarly, in melanoma cells, A3AR fails to activate Erk through phosphorylation and in fact A3AR antagonists cause activation of the MEK activity. The activation of MEK activity through Ras/Raf pathway, could lead to increase in Erk activity, though the mechanism behind how A3AR directly causes activation of Ras/Raf pathway is not clear. Thus, the effects of A3AR on Erk 1/2 activities are controversial and cellular context dependent.

Our results demonstrate that knockdown of TMIGD3 or A3AR activates mainly the NF-κB pathway with minimal effects on the cellular localization of β-catenin and p-Erk1/2. TMIGD3 knockdown results in degradation of IκB followed by nuclear translocation of NF-κB, and increased expression of downstream targets cyclin D1 and cMyc as A3AR knockdown. Overexpression of TMIGD3 i1 or A3AR in cells downregulated for TMIGD3 or A3AR respectively, nullifies NF-κB nuclear translocation. These results suggest that both TMIGD3 i1 and A3AR may suppress malignant properties of OS by inhibiting NF-κB activity.

This is the first report demonstrating the roles of TMIGD3 i1, as well as A3AR, in the suppression of OS progression through the NF-κB pathway, thus opening new avenues as therapeutic targets for high grade OS.

4.2 Materials and Methods

Immunofluorescence

The cells were grown on poly-D-lysine/laminin-coated glass coverslips (BD Biosciences) in 24-well plates. Cells were fixed with 4% paraformaldehyde for 20 minutes and permeabilized with 0.3% Triton X-100 for 5 minutes. Following blocking in 1% BSA in PBS plus 0.3% Triton-X for 30 minutes at room temperature, cells were incubated with the following primary antibodies: p65 (8242S, Cell Signaling)), β-catenin (sc1496-R, Santa Cruz Biotechnology), p-Erk1/2 (4695S, Cell Signaling), IκB (4814S, Cell Signaling), GAPDH (H-12, Santa Cruz Biotechnology) at 4 °C overnight. After washing with PBS, cells were incubated with fluorescence-conjugated secondary antibodies at room temperature for 1 hour. Cells were mounted in the ProLong Gold Antifade Reagent with DAPI (Invitrogen) and analyzed using a Nikon epifluorescence microscope.

Q*uantitative Reverse Transcription PCR (qRT-PCR)*

RNAs isolated using the RNA-Quick MiniPrep (Zymo Research) was reversed transcribed to cDNA using M-MLV reverse transcriptase (Amresco), followed by TaqMan assays with ViiA7 (Life Technologies). TaqMan assay primers and probes were purchased from Life Technologies or Integrated DNA Technologies. The following assay numbers were used for probes: *Cyclin D1* (HS00277039_m1, Life Technologies), *cMyc* (HS00153408_m1, Life Technologies). The mRNA levels were normalized to those of *GAPDH* (Hs.PT.39a.22214836, IDT).

Signal analysis and luciferase assays

Cells were transfected with a NF-κB promoter-luciferase reporter plasmid (E849A, Promega) and luciferase assays were performed according to the manufacture's protocol using the Dual-Luciferase Reporter Assay System (Promega).

Cignal 45-Pathway Reporter Array was purchased from SABiosciences (CCA-901L) and luciferase assays were performed according to the manufacturer's protocol. Briefly, 50 µl Opti-MEM® was added to each well of the Cignal Finder Array plate coated with reporter assay constructs. Subsequently, 50 µl of Opti-MEM® containing 0.3 µl of Attractene Transfection Reagent (QIAGEN) was used for each individual transfection. Following a 20-minute incubation, 50 µl of a cell suspension containing 1-3 × 10^4 cells in Opti-MEM® with 10% of fetal bovine serum and 1% NEAA was added to each well. After 16 hours of transfection, the medium was changed to complete growth medium and further incubated for 36 hours, followed by luciferase assays using the Dual-Luciferase Reporter Assay System (Promega).

Western Blotting

Western Blotting was performed as described in Chapter 2 using the following antibodies: IκB (4814S, Cell Signaling), TMIGD3 (Pab128, generated against aa. 235 to aa. 248 CGIQRDFARDDMDF by GenScript), p65 (8242S, Cell Signaling), Lamin B (C-20, Santa Cruz Biotechnology), GAPDH (H-12, Santa Cruz Biotechnology) and Vinculin (10R-C105a, Fitzgerald)

Sphere formation assays and *in vivo* subcutaneous tumor formation assays were performed as described in Chapters 2 & 3.

4.3 Results

4.3.1 TMIGD3 knockdown induces nuclear translocation of NF-κB with minimal effects on β-catenin, and p-ERK1/2 as A3AR in OS

Our results demonstrated similar biological profiles between TMIGD3 i1 and A3AR. To mechanistically understand functional similarity of TMIGD3 i1 with A3AR, we first performed web-based domain analyses using protein structure prediction sites, including PridictProtein server (https://www.predictprotein.org/) and SOSUI (http://harrier.nagahama-i-bio.ac.jp/sosui/sosui_submit.html), which identified two transmembrane helices at the C-terminal region of TMIGD3 i1 (aa129-151 and aa291-313), in addition to 3 transmembrane helices within the first 117 amino acids sharing with A3AR, as well as a known Ig-like fold at the C-terminal region (aa167-256, Fig. 4.1). Given that A3AR is a GPCR with 7 transmembrane helices [238] and TMIGD3 i1 preserves a part of the A3AR structure, we questioned if TMIGD3 i1 could regulate signaling similar to A3AR, which is known to inhibit three major cancer-associated signaling including the NF-κB, β-catenin, and MAPK-Erk pathways (Fig. 4.2) [239,240]

To address this, we examined cellular localization of NF-κB (p65), β -catenin, and p-Erk1/2, since nuclear localization of these proteins is well correlated with their activities. We observed that knockdown of TMIGD3 (*T6U*) significantly increased nuclear localization of p65 with minimal effects on β-catenin and p-Erk1/2 localization in SJSA-1 cells, similar to A3AR knockdown by the *A2a* shRNA (Fig. 4.3A). We also confirmed increased NF-κB activity by p65 accumulation in the nuclear fraction (Fig. 4.3B).Overexpression of TMIGD3 i1 or A3AR nullified the increased nuclear localization of NF-κB (p65) by TMIGD3 or A3AR knockdown, respectively, suggesting that increase

in the NF-κB activities by the *T6U* and *A2a* shRNAs were not due to their off-target effects. (Fig. 4.4).

Figure 4.1 Predicted structure of TMIGD3 i1 and its comparison with A3AR.

Blue filled boxes indicate reported transmembrane helices. Blue boxes with oblique lines indicate predicted transmembrane helices. Three N-terminal transmembrane helices are common between TMIGD3 i1 and A3AR. Numbers indicate amino acid locations.

Figure 4.1 Predicted structure of TMIGD3 i1 and its comparison with A3AR.

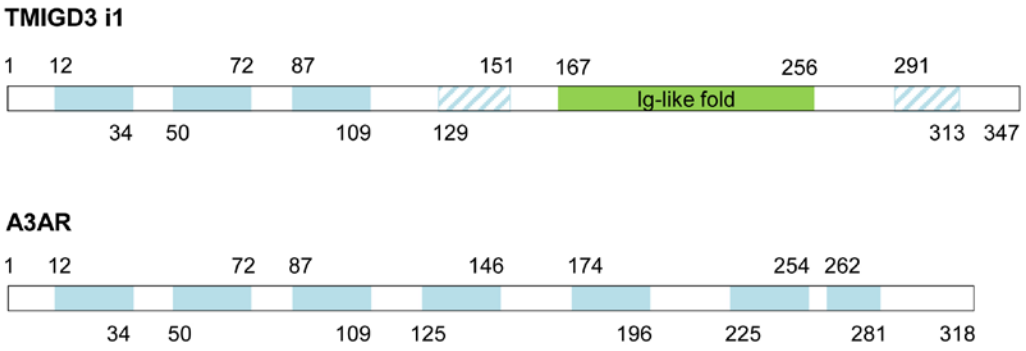

Figure 4.2 Cancer associated-signaling pathways regulated by A3AR. A3AR is previously known to regulate three major pathways including the NF-κB, β-catenin, and Erk pathways.

Figure 4.2 Cancer associated-signaling pathways regulated by A3AR.

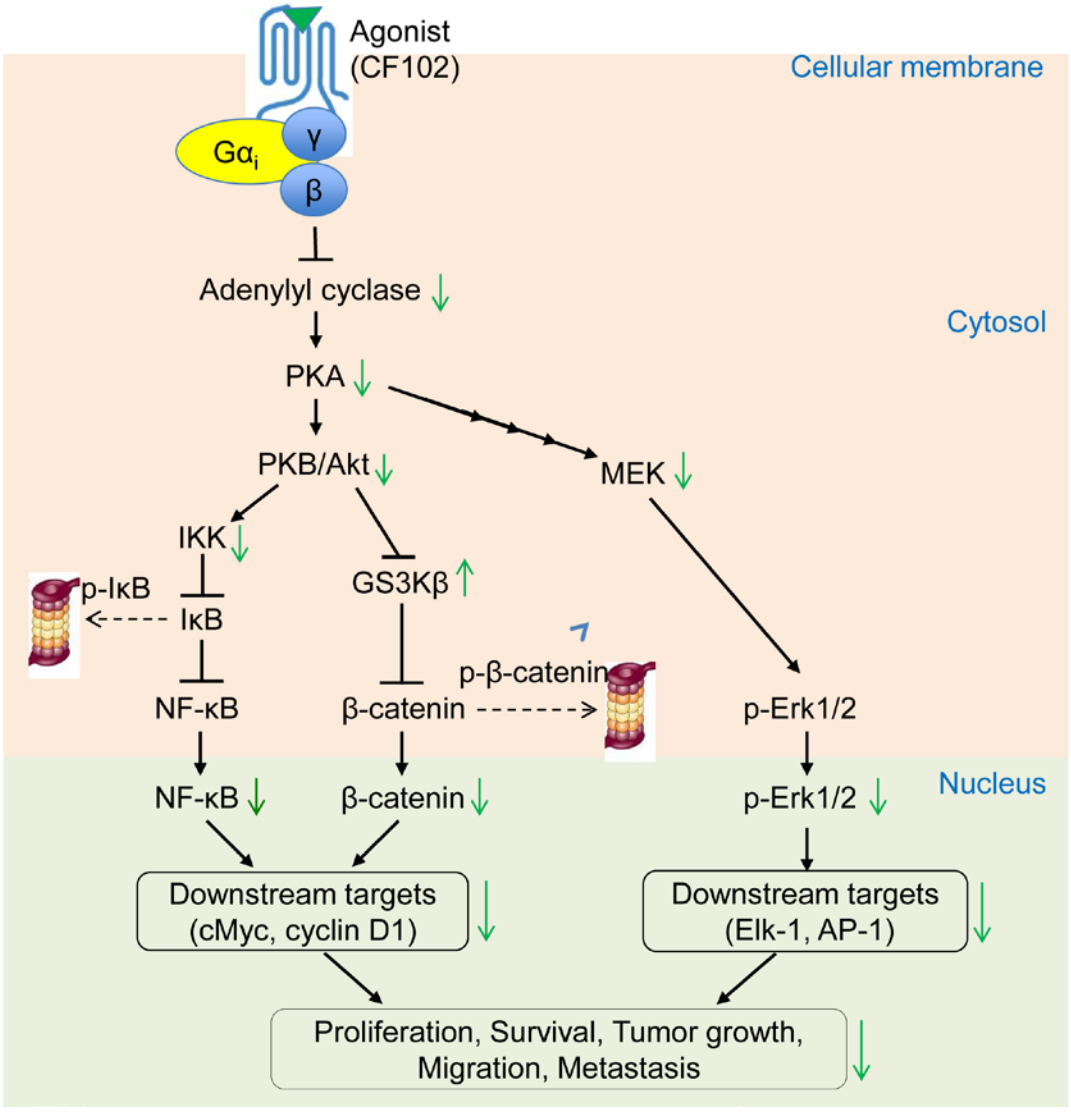

Figure 4.3 Knockdown of TMIGD3 causes nuclear translocation of NF-κB similar to A3AR.

(A) Immunofluorescence for NF-κB (p65), β-catenin, and p-Erk1/2 using SJSA-1 cells infected with lentiviral vectors encoding non-silencing c*ontrol* (*C*), *T6U*, or *A2a* shRNAs. Original magnification, x40.

(B) Immunoblots for p65, Lamin B and GAPDH, using nuclear and cytoplasmic extracts of SJSA-1 cells with or without downregulation of TMIGD3 (*T6U*) or A3AR (*A2a*).

Figure 4.3 Knockdown of TMIGD3 causes nuclear translocation of NF-κB similar to A3AR

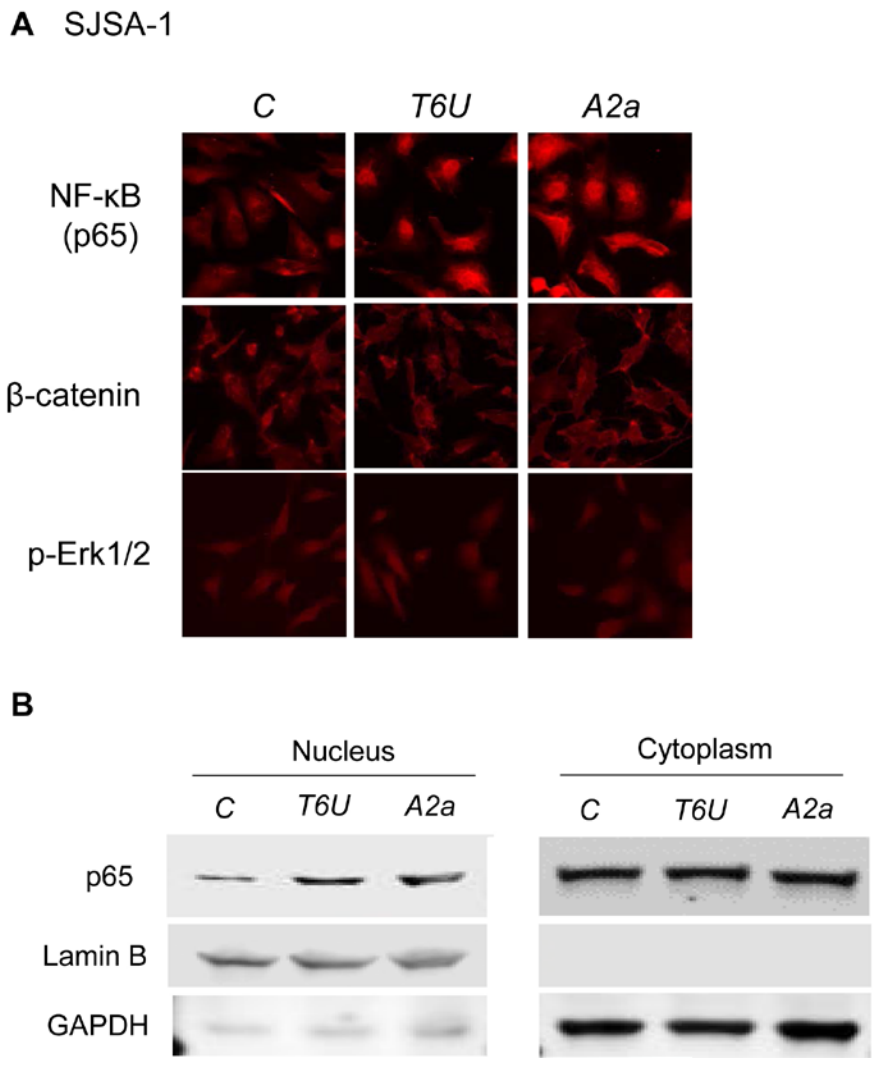

Figure 4.4 Overexpression of TMIGD3 i1 and A3AR nullifies the nuclear translocation of NF-κB induced by knockdown of TMIGD3 and A3AR, respectively.

Immunofluorescence for p65 using SJSA-1 cells downregulated for TMIGD3 (*T6U*) or A3AR (*A2a*) with or without overexpression of TMIGD3 i1 (cTi1) or A3AR (cA3), respectively.

.

Figure 4.4 Overexpression of TMIGD3 i1 and A3AR rescues the nuclear translocation of NF-κB following knockdown of TMIGD3 and A3AR respectively.

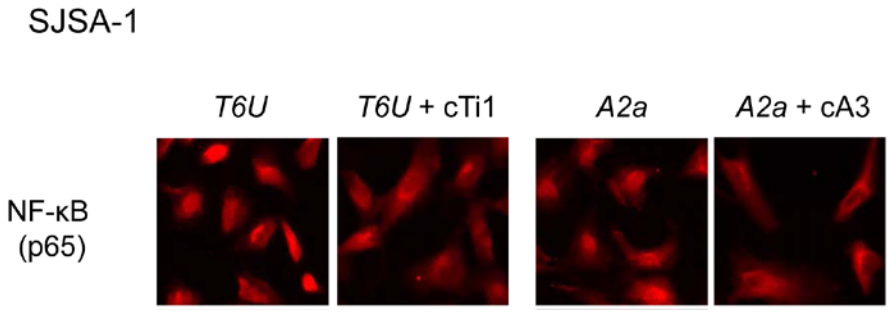

4.3.2 TMIGD3 knockdown results in degradation of IκB and increases activity of NF-κB *as A3AR in OS cells*

Knockdown of TMIGD3 and A3AR, both reduced levels of IκB, an inhibitor of NF-κB, as assessed by immunofluorescence (Fig. 4.5A, up) and western blotting (Fig. 4.5A, down). Knockdown of TMIGD3 also increased the transcriptional activity of NF-κB, similar to A3AR knockdown (Fig. 4.5B). To furthermore ensure increased NF-κB activity by knockdown of TMIGD3 or A3AR, we examined mRNA expression of NF-κB downstream targets, *cyclin D1* and *cMyc*, in SJSA-1 cells and found increase in the mRNA expression of these genes, as compared to the control cells (Fig. 4.6). These results suggest that both TMIGD3 i1 and A3AR may suppress malignant properties of OS by inhibiting NF-κB activity.

Figure 4.5 TMIGD3 knockdown results in degradation of IκB and increases activity of NF-κB, as A3AR, in OS cells.

(A) Immunofluorescence (up) and western blotting (below) for IκB in SJSA-1 cells: control (*C*), knockdown of TMIGD3 (*T6U*, *T3U*), A3AR (*A2a*). IκB levels were decreased following TMIGD3 and A3AR knockdown.

(B) Relative luciferase activity of *NF-κB* response element using SJSA-1 cells downregulated for TMIGD3 or A3AR. Graph showing relative luciferase activity (firefly/ renilla) normalized to that of SJSA-1 cells infected with non-silencing *control* lentiviral vector (*C*). Error bars: means ± S.D. ** $p<0.01$; Student's t-test.

Figure 4.5 TMIGD3 knockdown results in degradation of IκB and increases activity of NF-κB, as A3AR in OS cells

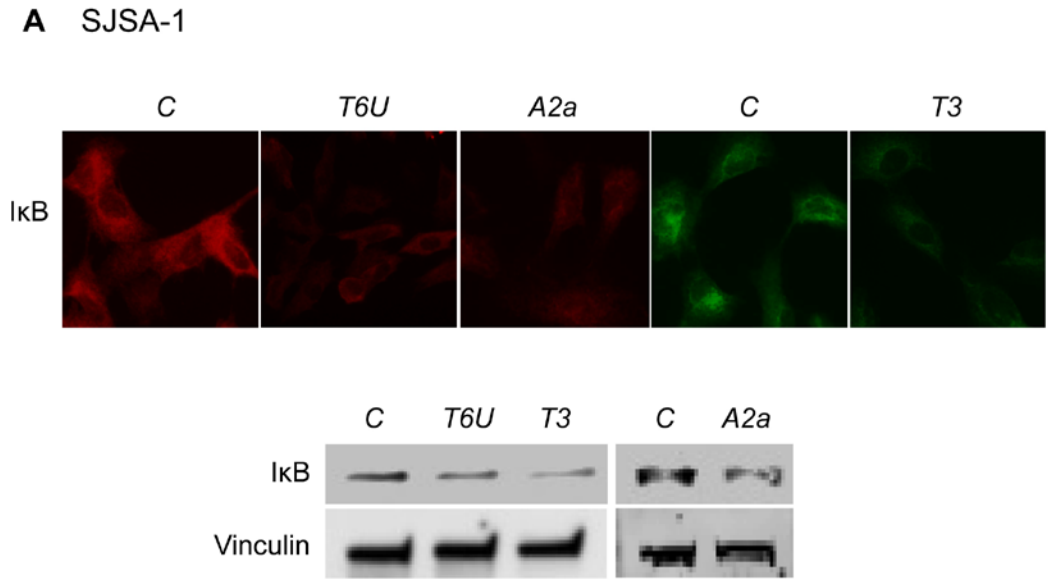

Figure 4.6 Knockdown of TMIGD3 and A3AR increases transcription of NF-κB downstream targets, *cyclin D1* and *cMyc*.

Quantitative RT-PCR for *cyclin D1* and *cMyc* using SJSA-1 downregulated for TMIGD3 (*T6U*, *T3*) or A3AR (*A2a*). Relative mRNA expression was standardized by that of *GAPDH* and normalized by values in non-silencing vector-infected cells (*C*). Data represents results from 3 independent experiments. Error bars: means ± S.D. * $p<0.05$; Student's t-test.

Figure 4.6 Knockdown of TMIGD3 and A3AR increases transcription of NF-κB downstream targets, *cyclin D1* and *c-Myc*

A SJSA-1

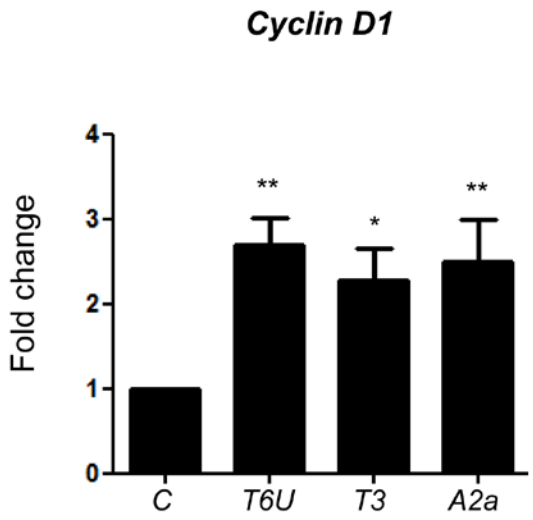

B SJSA-1

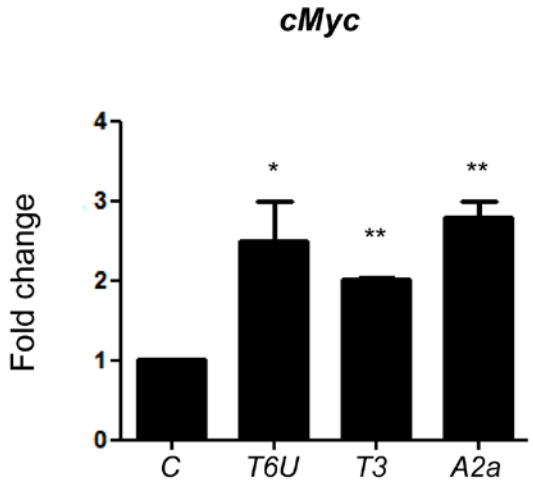

4.3.3 Malignant properties including sphere formation and tumor growth enhanced by TMIGD3 knockdown can be rescued by simultaneous knockdown of NF-κB (p65)

We therefore determined whether enhanced malignancy associated with TMIGD3 knockdown could be rescued by simultaneous knockdown of NF-κB/p65. Indeed, concomitant knockdown of p65 attenuated sphere formation and subcutaneous tumor growth of SJSA-1 cells enhanced by TMIGD3 knockdown (Fig .4.7A and B). It should be noted that the observed effects of p65 knockdown were partial, and not complete. These data suggest that suppressive effects of TMIGD3 i1 on the malignant properties of OS cells are regulated mainly, but not solely, through inhibition of NF-κB activity.

Figure 4.7 Sphere formation and tumor growth enhanced by TMIGD3 knockdown can be rescued by simultaneous knockdown of NF-κB.

(A) Sphere formation assays using SJSA-1 cells with or without knockdown of TMIGD3 (*T6U*) and/or NF-κB/p65 (*NF3*, *NF4*). Graph represents sphere forming potential from 3 independent experiments and representative western blotting for p65 and TMIGD3. * $p<0.05$; Student's t-test.

(B) Subcutaneous tumor formation assays using SJSA-1 cells with or without knockdown of TMIGD3 (*T6U*) and/or p65 (*NF4*). Graph showing tumor weight (g) and representative images of tumors at day 21,

Figure 4.7 Sphere formation and tumor growth enhanced by TMIGD3 knockdown can be rescued by simultaneous knockdown of NF-κB

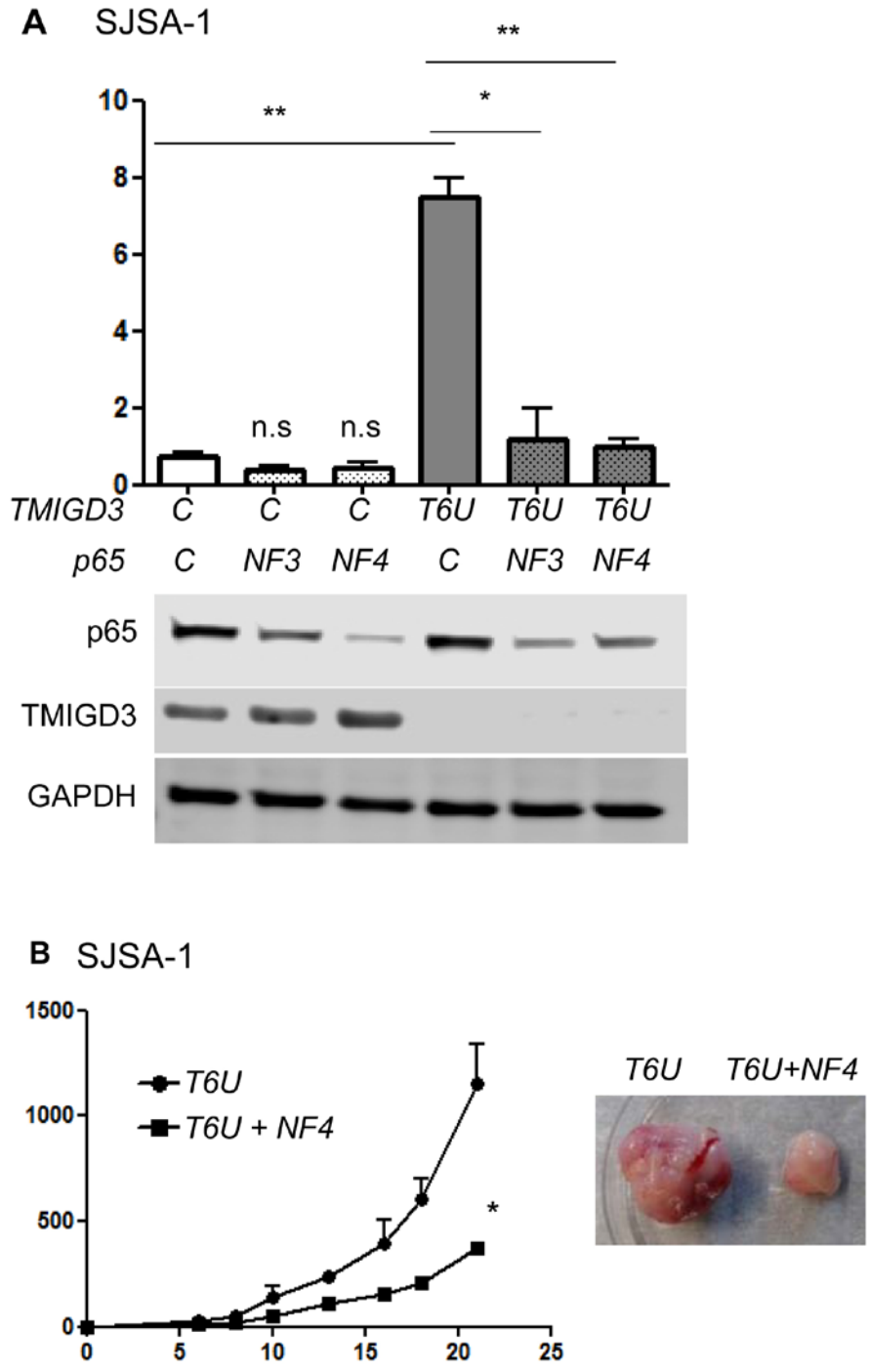

4.3.4 TMIGD3 i1 regulates both overlapping and non-overlapping pathways with A3AR. Our data suggest that there is a possibility that suppressive effects of TMIGD3 and A3AR on the malignant properties of OS cells could be regulated by differential pathways other than the NF-κB pathway. We compared signaling pathways altered by knockdown of either TMIGD3 or A3AR through an unbiased luciferase-based signal array experiment in SJSA-1 cells (Fig. 4.8). Firstly, we noted that knockdown of TMIGD3 and A3AR consistently showed increase in the NF-κB activity. Secondly, the activities of TCF/LEF (transcription factors for Wnt signaling) and Elk-1 (downstream of MAPK/Erk signaling) were either undetectable or unaffected by knockdown of TMIGD3 and A3AR, supporting the results in Fig. 4.3. And finally, there were distinct pathways altered by knockdown of these proteins (Fig. 4.8).

Figure 4.8 TMIGD3 i1 regulates both overlapping and non-overlapping pathways with A3AR.

Luciferase-based signal array experiments using SJSA-1 cells downregulated for TMIGD3 (*T6U*) or A3AR (*A2a*). Graph showing average of relative luciferase activity normalized to that of SJSA-1 cells infected with non-silencing *control* lentiviral vector from 2 independent experiments. Ud. Undetectable.

Figure 4.8 TMIGD3 i1 regulates both overlapping and non-overlapping pathways with A3AR.

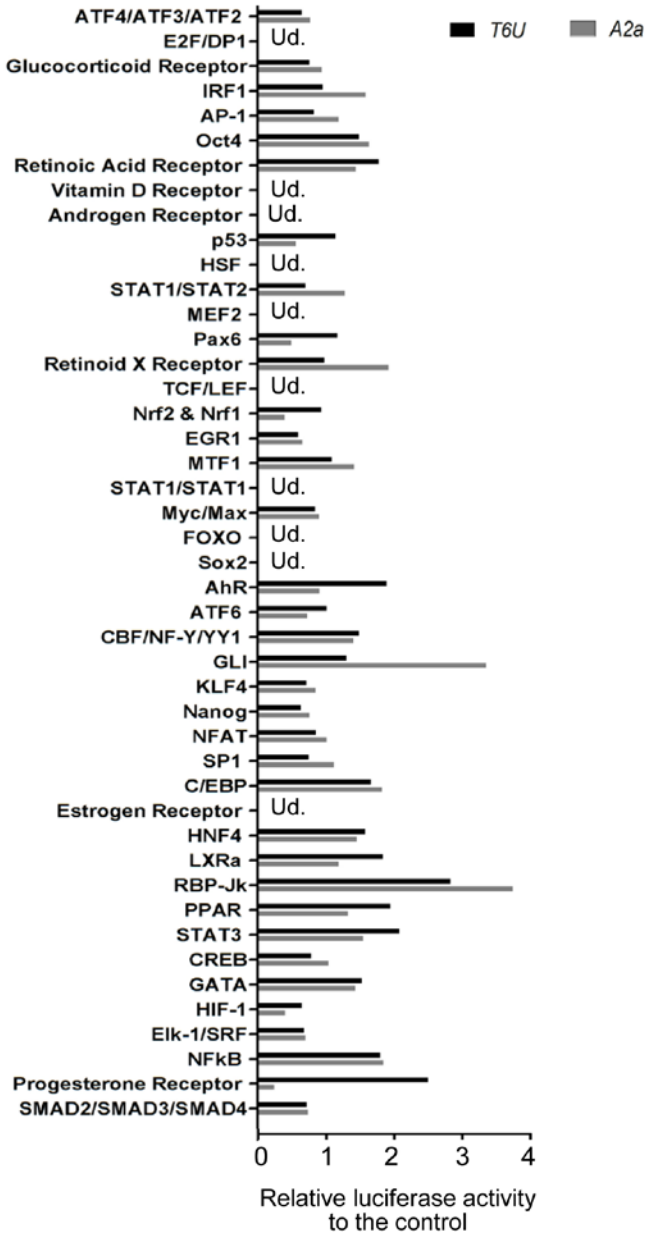

4.4 Discussion

TMIGD3 function is completely unknown. Based on the observation that it shares the N-terminal 117 aa with A3AR, and thus preserves part of the GPCR structure, we hypothesized that TMIGD3 signals through similar pathways as A3AR. Our data show that TMIGD3 i1 inhibits NF-κB activity, similar to A3AR. TMIGD3 knockdown does not alter activities of β-catenin and p-Erk1/2, similarly with A3AR. It remains unsolved whether TMIGD3 i1 plays roles in tumor suppression in other types of cancer or immune-inflammatory diseases, similar to A3AR.

Additionally, our unbiased luciferase-based pathway analyses indicate distinct signaling pathways regulated by TMIGD3 from A3AR that may further contribute towards OS suppression. These include retinoic acid X receptor, AhR (aryl hydrocarbon receptor), GLI and progesterone receptor. The detailed studies questioning the significance of these pathways in OS progression and their relationship to TMIGD3 i1 or A3AR should be further elaborated on in the near future.

Agonists for A3AR are currently under clinical trials for several diseases including hepatocellular carcinoma and rheumatoid arthritis[96,207,241]. Success of clinical trials may rely on the expression levels of A3AR and TMIGD3 i1 in OS tumors. Since our study suggests low expression of both A3AR and TMIGD3 in OS tissues, studies to restore the expression levels of A3AR and TMIGD3 i1 in tumors are required before treating tumors with agonists.

Deregulation in NF-κB pathway is a common event in many cancers, including solid and hematologic malignancies. NF-κB through its transcriptional activity increases

expression of genes that contribute toward increased cell proliferation, angiogenesis, metastasis, and tumor formation, some of the hallmarks of cancer. Genetic ablation in the NF-κB pathway in mouse models of cancer that leads to block in NF-κB activity, have clearly highlighted the role of NF-κB in the promotion of inflammation-influenced cancer. The roles of NF-κB in anti-apoptotic machinery thus promoting cell survival, chemotherapy resistance are well documented. Thus, inhibition of NF-κB pathway, may serve as a promising therapeutic target in multiple cancers to improve the efficacy of current conventional therapies. One of the clinically relevant examples is the use of Bortezomib, a proteasome inhibitor, in the treatment of multiple myeloma. Even though multiple signaling pathways may be affected by Bortezomib, decrease in cancer cell growth may be in due to inhibition of NF-κB activity. Thalidomide and its analogues, also active against multiple myeloma, induce apoptosis and growth arrest, in these cells through inhibition of IKK activity, and thus NF-κB activity. Proteasome mediated inhibition that led to suppression of NF-κB activity was also observed in T-cell leukemia. Specifically, small molecule inhibitor against IKK (PS-1145) was toxic for large B-cell lymphoma cells through suppression of NF-κB dependent genes. IKK inhibitors, BAY 11-7082 and AS602868 have also shown promising effects in leukemia via increased apoptosis. Another drug, sulfasalazine, NSAID, which is known to block NF-κB activation, shows inhibition of growth and apoptosis in glioblastoma cell lines.

NF-κB activity is associated with increased chemoresistance and progression of OS [191,197,198,242,243].NF-κB specific inhibitors, including pyrrolidine dithiocarbamate (PDTC), parthenolide (PARTH), and Bay 11-7085 (BAY) induced apoptosis and inhibited tumor growth of OS cells [244]. Moreover, enhanced anti-tumorigenic effects

were observed when NF-κB inhibitors were combined with a commonly used chemotherapeutic drug in OS, doxorubicin (also known as adriamycin, ADM) [244]. Kishida et al. also showed that parthenolide, inhibited lung metastases of a highly metastatic OS cell line, through inhibition of NF-κB activity[245]. Thus, targeting the NF-κB signaling could be a promising strategy for OS having low expression of A3AR or TMIGD3 i1.

CHAPTER 5:

PRELIMINARY RESULTS ELUCIDATING THE ROLE OF TMIGD3 IN STEM-LIKE PROPERTIES OF OS

5.1 Introduction

Tumors are comprised of a heterogeneous cell population [246]. Accumulating evidence indicates that a small subset of cancer cells within a tumor possess similar characteristics to normal stem cells and can generate phenotypically diverse cancer cells and form the bulk of the tumor [246]. This small subset of tumor cells are called cancer stem cells (CSCs) or tumor initiating cells (TICs) which have been demonstrated in different types of cancer, including breast cancer, central nervous system tumors, colon cancer, prostate cancer, pancreatic cancer, and hepatic cancer [247-255]. CSCs/TICs have high abilities of tumor initiation, multi-lineage differentiation, and sphere formation, as well as express stem cell-related transcription factors and cell surface markers [91], thereby being considered to be responsible for tumor recurrence, metastasis, and drug resistance [93,256]. Thus, it is important to discover strategies to target CSCs/TICs, which the current conventional therapies fail to do[52,53].

The manifestation of metastases at diagnosis is significantly associated with a poorer prognosis in patients [16]. Recent studies suggest that the molecular machinery responsible for cancer invasion and metastasis is similar to that involved in the activation, mobilization, and homing of normal stem cells [71,72,86,257,258]. Since non-CSCs/TICs cannot efficiently initiate tumors at secondary sites [73,75,257] and because CSCs/TICs share several molecular and biological properties with normal stem cells, CSCs/TICs have been proposed to be responsible for metastasis [257,259].

In many types of cancer, CSCs/TICs are enriched within spheres, which grow in serum- and anchorage-independent conditions[73,248,249,260,261]. Thus, sphere-forming ability is a hallmark of cancer cells possessing stem cell-like properties. Our lab and

others have demonstrated that both primary and established cells from OS, as well as other types of sarcomas, have the ability to grow in serum- and anchorage-independent conditions and form spheres [69,73,262]. As few as 200 cells from mouse OS spheres can efficiently initiate tumors in immunocompromised mice[73,257]. These spheres are also enriched with cells positive for stem cell transcription factors such as Oct-4 and also positive for mesenchymal stem cell markers Stro-1, CD117, CXCR4, and ABCG2 [263] [69,73,264]. Furthermore, $CD117^{+}Stro\text{-}1^{+}$ cells from both primary and established human OS cell lines show high metastatic and doxorubicin resistance, in addition to enrichment of cells positive for CXCR4 and ABCG2, each associated with metastasis and drug resistance, respectively [69,73]. *These results suggest that spheres as well as $CD117^{+}Stro\text{-}1^{+}$ cells, are enriched in OS CSCs/TICs.*

In Chapters 2 & 3, we identified a novel uncharacterized gene TMIGD3, whose knockdown increased the sphere forming ability of multiple OS cells. Interestingly, TMIGD3 i1 shares its N-terminal region with A3AR, a Gi-associated GPCR. Downregulation of TMIGD3 enhances OS malignancy *in vitro* as shown by increased proliferation and migration. Also, cells downregulated for TMIGD3 efficiently enhances primary tumor formation and metastasis of OS cells *in vivo*. We hence hypothesized that TMIGD3 regulates OS malignancy by influencing their stem-like properties. We show that downregulation of TMIGD3 increases stem cell transcription factor expression and tumor initiation efficiency, some of the key properties defining CSCs/TICs. Downregulation of TMIGD3 increases ALDH activity of OS cells. Thus, we have identified TMIGD3 as a novel regulator of stem-like properties of OS and could potentially serve as therapeutic target for treatment of high grade OS.

5.2 Materials and Methods

Quantitative RT-PCR for stem-related transcription factors

Methods of RNA isolation, cDNA synthesis, and RT-PCR were described in Chapter 4. The following Taqman assay primers and probes are used: *Oct-4* (Catalog #HS0999632_g1, Applied Biosystems), *Sox-2* (Catalog # HS01053049_S1, Applied Biosystems), *TMIGD3* (Catalog # Hs.PT.56a.2147158.9, Integrated DNA Technologies). The levels of mRNA were normalized with those of *GAPDH.*

Limited dilution tumor formation assay

Cells were dissociated using nonenzymatic cell dissociation solution (Sigma Biochemicals) into single-cell suspensions. Cells were counted (200 cells) using trypan blue staining (Thermo Fisher Scientific) and then suspended in 4.5 mg/ml of Matrigel (Corning) in HBSS. These cells were injected subcutaneously into flanks of NIH-III nude mice (Charles River). For orthotopic injections, cells were directly injected into the femurs of NOD-SCID IL2Rγ^{null} (NSG) mice (The Jackson Laboratories) as previously described [171]. For subcutaneous tumor formation, tumors were measured three dimensionally twice a week until day 50. For orthotopic injections, mice were monitored for ~4 months following injections or when the tumors reached ~2 cm in thigh diameter. The numbers of metastatic nodules in the lungs were counted and the weights of the primary tumors were measured.

ALDEFLUOR assay and collection of positive population for ALDH using fluorescence activated cell sorting (FACS)

The ALDEFLUOR assays were performed using the ALDEFLUOR kit (Stem Cell Technologies). Briefly, cells were dissociated into single suspensions following which they were suspended in ALDFLUOR assay buffer containing the ALDH substrate (BAAA) and efflux inhibitor, and incubated at 37^{o}C for 30 minutes. For every sample, as a negative control, an equal proportion of cells were treated with 1.5 mM of diethylaminobenzaldehyde (DEAB), an ALDH inhibitor. The gates for sorting were based on the negative control after which ALDEFLUOR positive cells were collected and the percentages were measured[265].

5.3 Results

5.3.1 Knockdown of TMIGD3 efficiently initiated tumors in vivo

Our previous results (Fig. 3.5 & 3.6) showed that TMIGD3 knockdown significantly enhanced tumor growth and metastasis. We hypothesized that TMIGD3 knockdown increases stem-like properties of OS cells, thereby initiating tumors *in vivo*. To test this hypothesis, we subcutaneously injected 200 SJSA-1 cells infected with lentiviral vectors encoding non-silencing control (*C*) or TMIGD3 (*T6U*) into flanks of nude mice. Indeed, only 200 SJSA-1 cells with TMIGD3 knockdown successfully gave rise to tumors, whereas control cells failed to do so (Fig. 5.1A). To test if TMIGD3 knockdown initiated tumor formation when placed in a bone microenvironment and to examine the metastatic potential of formed tumors, we also performed orthotropic tumor formation assays by injecting control or TMIGD3-downregulated SJSA-1 cells (200) into the femurs of NSG mice. All mice injected with cells with TMIGD3 knockdown gave rise to tumors whereas only 1 mouse with control cells formed a tumor. Moreover, the OS tumors formed with TMIGD3 knockdown metastasized to the lungs, but control OS tumors failed to do so (Fig. 5.1B).

Figure 5.1 Knockdown of TMIGD3 enhances tumor initiation.

(A) Subcutaneous tumor formation assays were performed using SJSA-1 cells (200 cells/mouse) expressing non-silencing shRNA (*C*) or TMIGD3 shRNA (*T6U*) (n=7). Tumors were measured three-dimensionally twice a week until day 50.

(B) Orthotopic (intrafemoral) tumor cell injection assays using SJSA-1 cells (200 cells/mouse) expressing non-silencing shRNA (*C*) or TMIGD3 shRNA (*T6U*) in NSG mice. Mice were monitored for tumor formation and were euthanized when thigh diameter reached ~2 cm or became moribund. Graph showing weights of primary tumors (left) and numbers of metastatic nodules (right). Representative images of primary tumors and lungs with metastatic nodules below the graphs and a table representing the numbers of tumor-bearing mice/numbers of mice examined.

Figure 5.1 Knockdown of TMIGD3 enhances tumor initiation

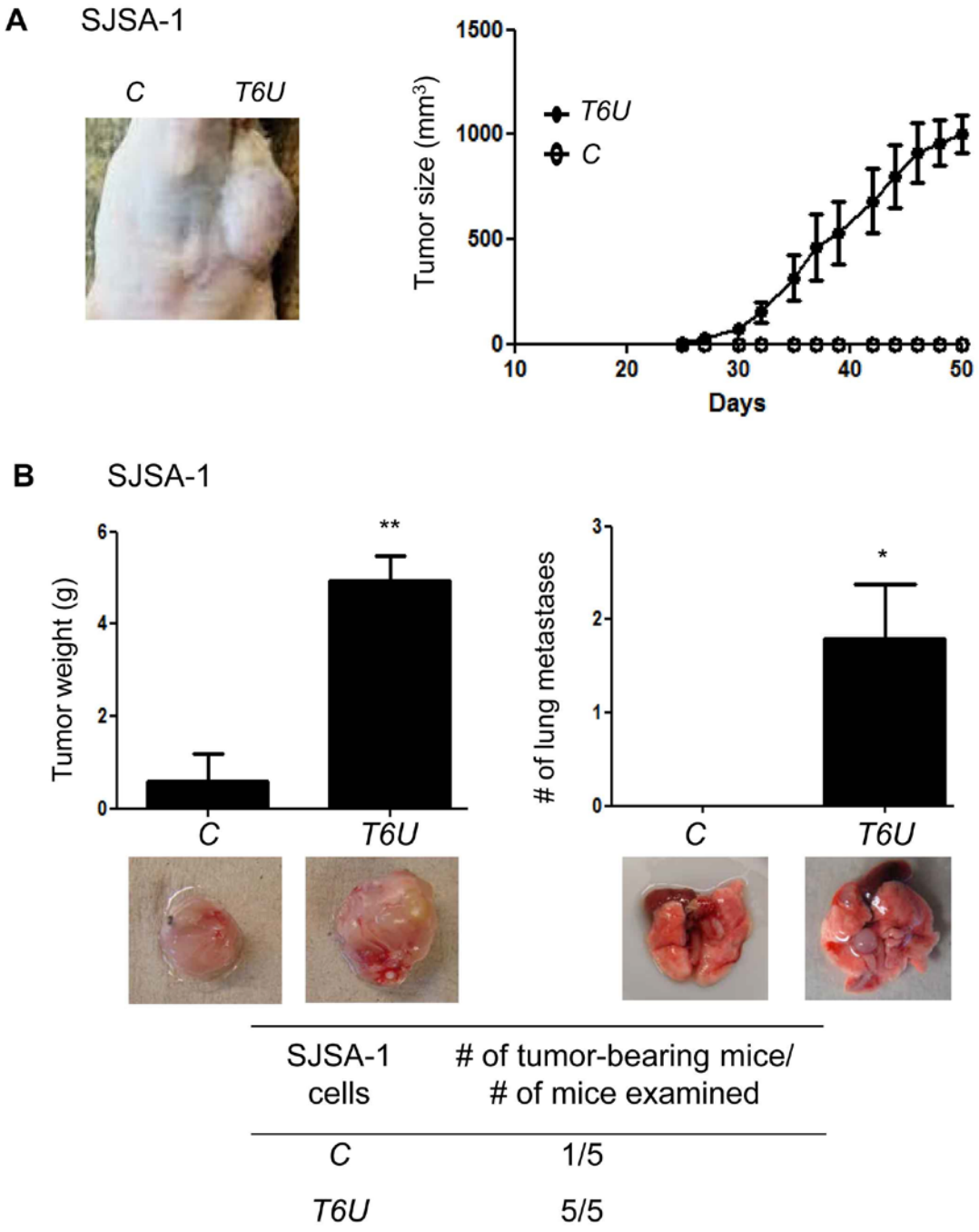

SJSA-1 cells	# of tumor-bearing mice/ # of mice examined
C	1/5
T6U	5/5

5.3.2 Downregulation of TMIGD3 increases expression of stem-cell transcription factors

High expression of Oct-4 and Sox-2, important pluripotent stem cell transcription factors, is well associated with stem-like properties of OS including self-renewability, sphere formation, and metastasis [71,72]. Our results showed that knockdown of TMIGD3 increased expression of *Oct-4* mRNA in SJSA-1 and Saos2 OS cells (Fig. 5.2A). Knockdown of TMIGD3 also enhanced expression of Sox-2 when compared to control (*C*) cells with non-silencing shRNA in SJSA-1 and Saos2 OS cells (Fig. 5.2 B). These results suggest that knockdown of TMIGD3 enhances expression of two crucial stem cell transcription factors, thus possibly could enhance stem-like properties in OS cells.

Figure 5.2 Knockdown of TMIGD3 increased mRNA expression of stem cell transcription factors.

(A, B) Quantitative RT-PCR for *Oct-4* and *Sox-2* using SJSA-1 and Saos2 cells with or without downregulation of TMIGD3 (*T6U, T3*). Relative mRNA expression was standardized by that of *GAPDH* and normalized by values in cells infected with a non-silencing *control* shRNA-encoding lentivirus (*C*). Data are from 3 independent experiments. Error bars: means ± S.D. * $p<0.05$, ** $p<0.01$; Student's t-test

Figure 5.2. Knockdown of TMIGD3 increased mRNA expression of stem cell transcription factors.

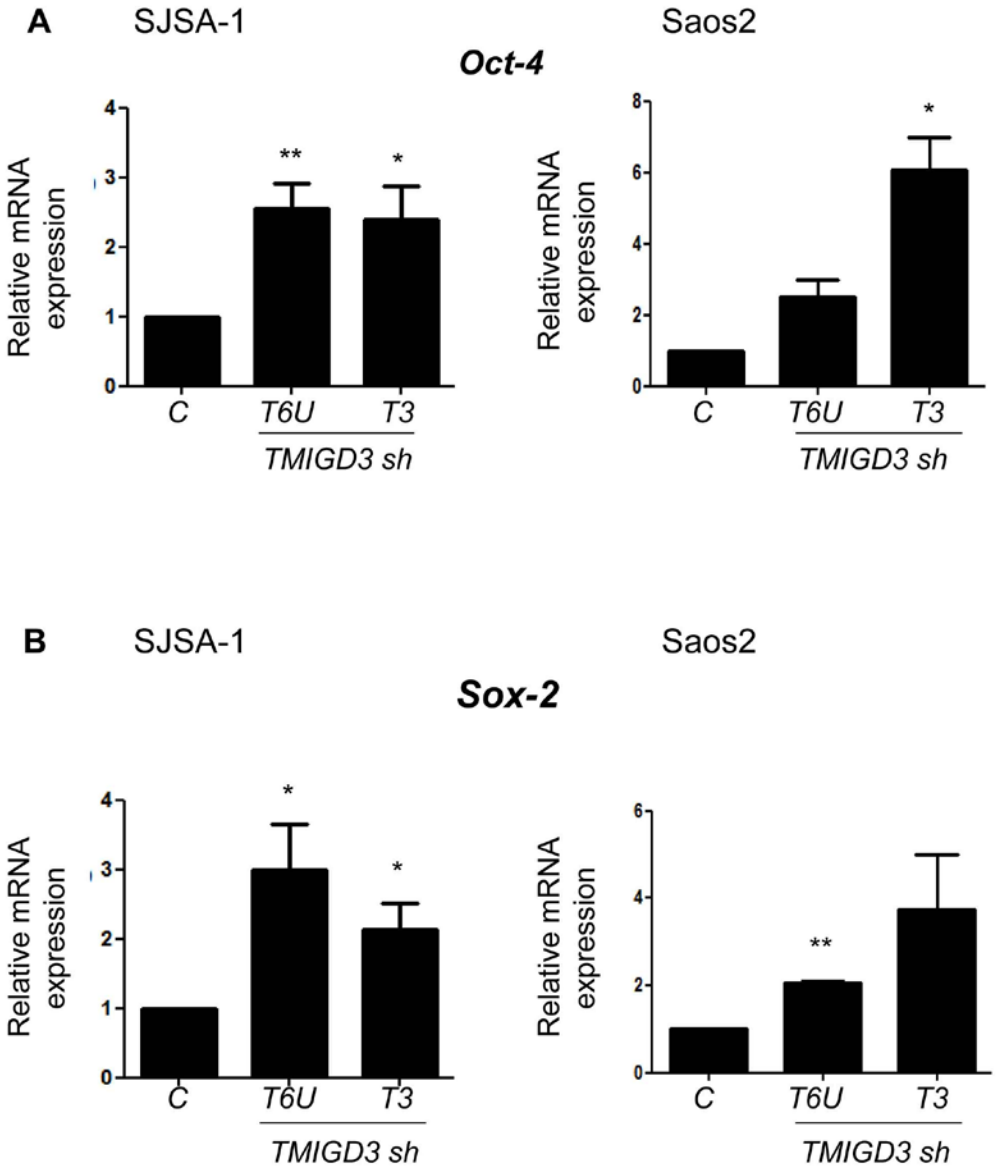

5.3.3 Decreased TMIGD3 expression is correlated with increased ALDH activity

Increased activity of aldehyde dehydrogenases (ALDHs), a group of enzymes that catalyze the oxidation of aldehydes and play roles in drug detoxification [266], is a property associated with normal stem cells including hematopoietic stem cells and neural progenitors. Hence, ALDH activity is associated with drug resistance and stem-like properties of cancer cells. Cancer cells possessing high ALDH activity ($ALDH^{High}$) frequently show enhanced tumor formation and sphere formation, and also express stem cell transcription factors including Oct-4, Nanog, and Sox-2[267].

To test if TMIGD3 knockdown was associated with increased ALDH activity, we performed ALDEFLUOR assays using SJSA-1, U2OS, and Saos2 OS cells with or without knockdown of TMIGD3. Knockdown of TMIGD3 increased the percentage of ALDEFLUOR-positive cells correlating with increased ALDH activity (Fig. 5.3A).

We also examined whether ALDH activity was negatively correlated with TMIGD3 expression. We hence examined *TMIGD3* mRNA expression in flow-sorted $ALDH^{Low}$ and $ALDH^{High}$ SJSA-1 and MG63 cells. As expected, $ALDH^{High}$ population had lower mRNA expression of *TMIGD3* than that in $ALDH^{Low}$ population in both the cell lines (Fig. 5.3B). Thus, these results suggest that decreased TMIGD3 expression is associated with increased ALDH activity, hence contributing towards the malignant and stem-like properties of OS cells.

Figure 5.3 Decreased TMIGD3 expression is correlated with increased ALDH activity.

(A) ALDEFLOUR assays measuring the ALDH activity. SJSA-1, U2OS, and Saos2 cells infected with lentiviral vectors encoding *non-silencing* (*C*) or TMIGD3 (*T3*) shRNAs were subjected to ALDEFLOUR assays, followed by flow cytometric analyses. Results were presented as percentage of cells positive for the substrate ALDEFLOUR.

(B) Quantitative RT-PCR for *TMIGD3* using $ALDH^{Low}$ and $ALDH^{High}$ SJSA-1 and MG63 cells.

Figure 5.3. Decreased TMIGD3 expression is correlated with increased ALDH activity

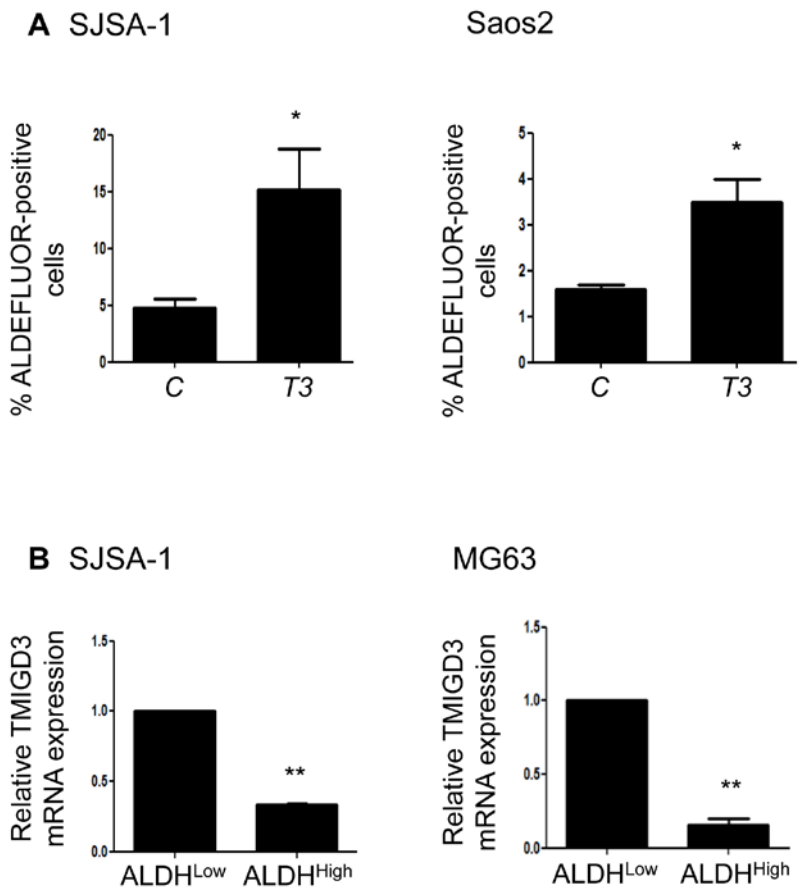

5.4 Discussion

Given that TMIGD3 inhibits sphere forming potential of OS cells, TMIGD3 could also regulate stem-like properties of OS. Indeed, knockdown of TMIGD3 results in increase in ALDH activity and the expression of stem cell transcription factors of Oct-4 and Sox-2, makers for OS CSCs/TICs [72]. Moreover, TMIGD3 knockdown cells show increase in tumor initiation and metastasis of OS cells. These preliminary results suggest the involvement of TMIGD3 in the stem-like properties of OS. Detailed examinations of self-renewability and multi-lineage differentiation potential are necessary to define the roles of TMIGD3 in the regulation of stemness of OS cells.

It would be interesting to examine whether TMIGD3 knockdown could increase the expression of other OS stem cell surface markers CD117, Stro-1, CD133, and Sca-1, as well as a metastasis-associated chemokine receptor CXCR4 and a drug-resistance associated drug transporter ABCG2. Co-expression analyses of TMIGD3 and stem cell markers in human OS tissues should be performed in future. Furthermore, it will be important to examine if high ALDH activity is associated with low expression of TMIGD3 and if TMIGD3 ^{Low} OS cell population has high tumor initiating potential or self-renewability from fresh OS biopsies. Toward this, it is crucial to have an antibody that detects extracellular region of TMIGD3 and hence allows for sorting of live cells. We can explore if our generated antibody for TMIGD3 could serve this purpose.

Since A3AR also inhibits sphere forming potential, it would be important to determine whether A3AR could also regulate stemness in OS, similar to TMIGD3 in the future.

CHAPTER 6

CONCLUSIONS AND SUMMARY

OS is the most common non-hematologic deadly malignancy affecting children and adolescents with a dismal survival rate especially for patients who manifest metastases and disease relapse [268,87,88]. Even though certain molecular pathways are associated with OS development and progression, the exact mechanisms underlying the full spectrum of the disease remain elusive. Also, there is a great paucity in the availability of directed therapies for OS that could target the most aggressive properties of the disease including chemoresistance and metastases. Hence, a detailed understanding of the molecular mechanisms underlying these aggressive properties, as well as discovery of novel therapies that target these mechanisms, are an absolute requirement for the cure of OS.

Sphere formation assay was first described in 1992 when Reynolds *et al* cultured cells with stem-like properties from the adult brain as free floating spheres called neurospheres [269]. This technique was further adapted to study adult stem cells including the nerve, prostate, and mammary stem cells[261,270,271]. Then, it finally paved its way as a functional assay to study malignant properties of cancer cells[57,272]. The ability of cells to survive under nutrient-deprived, anchorage-independent conditions and form spheres defines a symbol of malignant properties of cancer cells. To understand the regulatory mechanisms underlying malignant properties of OS, we screened a human whole-genome shRNA library using SJSA-1 OS cells harboring poor sphere forming potential and identified a novel uncharacterized protein, TMIGD3, as a factor whose downregulation increased sphere forming potential of these cells.

TMIGD3 shares its N-terminal region with A3AR, hence referred to as an isoform of A3AR (A3AR i1). However, the function of TMIGD3 is not described in literature,

whereas the functional importance of A3AR (precisely A3AR i2) in inflammatory response and cancer progression is well established. Specifically, A3AR is a Gi/Gq protein-associated G-protein coupled receptor and it belongs to a family of adenosine receptors including A1 and A2AR that regulate a variety of cellular functions[120,273]. Activation of A3AR by its agonist leads to inhibition of adenylyl cyclase and cyclic AMP formation, which then converges into various signaling pathways in context-dependent manners [214].

Our study is the first to elucidate the roles of TMIGD3 and A3AR in aggressive properties of OS. We found that knockdown of TMIGD3 and A3AR enhanced sphere formation, migration, proliferation, tumor formation, and metastasis of OS cells. Also, detailed analyses of the isoforms of TMIGD3 revealed that of the two isoforms, TMIGD3 i1 and TMIGD3 i3, TMIGD3 i1 was crucial in the suppression of aggressive properties of OS including proliferation, migration, and tumor formation. Our data suggests the significance of the N-terminal region, the common region between TMIGD3 i1 and A3AR, in the regulation of malignant properties of OS. Detailed mapping of the N-terminal domain and subsequent functional assays to test the malignancy will help us identify the region crucial for suppression of OS malignancy.

We performed expression analyses of TMIGD3 and A3AR using human OS tissues with a newly generated peptide antibody for TMIGD3 and commercially available antibody for A3AR. Our generated TMIGD3 antibody against exon T3 does not discriminate the two isoforms. The expression levels of TMIGD3 (both i1 and i3) and A3AR were lower in primary and metastatic OS tissues when compared to normal bone and normal lung tissues. This is the first study describing the protein expression of

TMIGD3 and A3AR in OS. Correlation of TMIGD3 and A3AR expression with OS prognosis or other clinical factors should be performed in the future.

We suspect that there might be certain post-translational modifications present in TMIGD3 since we detected both the isoforms i1 and i3 it at levels higher than their predicted sizes. Similar differences in predicted size vs actual size have been observed previously for TMIGD1 and TMIGD2, due to their post-translational modifications linked with N- glycosylation[174,177]. We are aware that in future a TMIGD3 i3 specific antibody should be generated, since it has a unique N-terminal region. This could help us further delineate the differences between TMIGD3 i1 and i3 in clinical samples.

A3AR was previously demonstrated to suppress tumor progression through the inhibition of major signaling pathways including the β-catenin, NF-κB and Erk pathways[162]. We queried the involvement of TMIGD3 through these pathways to inhibit OS malignancy. Indeed, TMIGD3 inhibited NF-κB activation, similar to A3AR. We did not observe any obvious effects of TMIGD3 knockdown on the β-catenin and Erk activities, similarly with A3AR. This suggests that both TMIGD3 and A3AR may influence malignant properties of OS mainly via the NF-κB but not β-catenin and Erk activities in OS and indicates that an overlapping function of TMIGD3 with A3AR is present for inhibition of OS malignancy. The deregulation of NF-κB pathway is linked with several pathologies including cancer progression [274-276]. Given the low expression of TMIGD3 and A3AR in human OS tissues, targeting the NF-κB activity associated with increased chemoresistance and progression of OS could be a promising strategy for OS [191,197,198,242,243].

Additionally, since TMIGD3 inhibited sphere forming potential, a hallmark of stem-like properties, we explored the role of TMIGD3 in stem-like properties of OS. Our preliminary results demonstrated that knockdown of TMIGD3 resulted in increase in ALDH activity and the expression of stem cell transcription factors Oct-4 and Sox-2, as well as tumor initiation and metastasis. These results suggest the involvement of TMIGD3 in the stem-like properties of OS.

In summary, our study delineated the roles of TMIGD3, as well as A3AR, as novel players involved in the suppression of OS progression. Most importantly reduced expression of these proteins enhanced OS metastasis in orthotopic mouse models, one of the deadly characteristics responsible for the poor prognosis of OS patients. Hence, targeted therapies aiming at these two proteins could greatly improve the life of OS patients in the future.

CHAPTER 7

FUTURE DIRECTIONS

Our IHC analyses using OS tissues revealed low expression levels of TMIGD3 and A3AR in both primary and metastatic OS tissues, suggesting that TMIGD3 and A3AR expression might be silenced during early stage of OS genesis. Indeed, A3AR expression appears low in many types of cancer in the Human Protein ATLAS database (http://www.proteinatlas.org/ENSG00000121933-ADORA3/cancer). Correlation studies between expression of these proteins and patient's prognosis or clinical stages need to be elucidated as a future study.

Since TMIGD3 and A3AR share the first exon, these two genes are most likely driven by the same promoter. This could explain why both protein levels are reduced in OS, which could be due to promoter silencing. Hence, studies examining epigenetic modifications of these genes including DNA methylation and histone modifications will help us address the possible mechanisms behind silencing of the expression of these genes. Interestingly, our preliminary studies suggest that treatment of aggressive OS cell lines that have low TMIGD3 and A3AR expression at basal levels (Saos2-LM7, MG63, KHOS/NP) with a DNA methylation inhibitor 5-aza-2-deoxycytidine and a histone deacetylase inhibitor Trichostatin A increases mRNA expression of both TMIGD3 and A3AR (data not shown). Additionally, it is possible that some physiological stress including hypoxia and nutrition deprivation in the tumor milieu could cause epigenetic silencing of TMIGD3 and A3AR. Although A3AR agonists are under clinical trials for hepatocellular carcinoma[241], efficacy of A3AR agonists could be dependent on the expression levels of A3AR in tumors. Hence, it would be important to find strategies to restore the expression levels of A3AR before treatment with its agonists. More

importantly, methods or agonists that efficiently activate the TMIGD3 signaling and its expression should be looked into in the future.

Another important remaining question is whether TMIGD3 i1 plays roles in tumor suppression of different types of cancer or immune-inflammatory diseases, similar to A3AR. Although we expect TMIGD3 i1 to function similarly to A3AR, we observed that there are unique TMIGD3 pathways that do not overlap with A3AR. Such pathways should be explored in the future, which could further help us develop targeted therapies towards the treatment of high grade OS. Since robust metastases are observed following TMIGD3 knockdown in both orthotopic and intravenous tail vein assays, it would be intriguing to study the role of these differential regulators that specifically contribute towards increased metastasis following TMIGD3 knockdown.

Additionally, the roles of TMIGD3 i1 and A3AR in stem-like properties of other sarcomas should also be examined, since all sarcomas are of mesenchymal origin. Further studies elucidating the roles of these proteins in self-renewability and multi-lineage differentiation in different cancer types are required to establish TMIGD3 and A3AR as negative regulators of stem-like properties. Therapies targeting these proteins might diminish not only malignant properties, but also stem-like properties of many cancer types including OS.

It should be noted that *A3AR* knockout mice are not tumor-prone, rather show increased inflammatory response [172,178]. In order to examine the *in vivo* significance of TMIGD3 i1 and A3AR on tumor development, generating compound knockout mice of *TMIGD3 i1* and *A3AR* and a mouse model of cancer would be necessary.

..

CHAPTER 8

REFERENCES

1 Burningham, Z., Hashibe, M., Spector, L. & Schiffman, J. D. The epidemiology of sarcoma. *Clin Sarcoma Res* **2**, 14, doi:10.1186/2045-3329-2-14 (2012).
2 McKenna, R. J., Schwinn, C. P. & Higinbotham, N. L. Osteogenic sarcoma in children. *CA Cancer J Clin* **16**, 26-28 (1966).
3 Haddox, C. L. *et al.* Osteosarcoma in pediatric patients and young adults: a single institution retrospective review of presentation, therapy, and outcome. *Sarcoma* **2014**, 402509, doi:10.1155/2014/402509 (2014).
4 Morrow, J. J. & Khanna, C. Osteosarcoma Genetics and Epigenetics: Emerging Biology and Candidate Therapies. *Critical reviews in oncogenesis* **20**, 173-197 (2015).
5 Geller, D. S. & Gorlick, R. Osteosarcoma: a review of diagnosis, management, and treatment strategies. *Clin Adv Hematol Oncol* **8**, 705-718 (2010).
6 Link, M. P. *et al.* The effect of adjuvant chemotherapy on relapse-free survival in patients with osteosarcoma of the extremity. *N Engl J Med* **314**, 1600-1606, doi:10.1056/NEJM198606193142502 (1986).
7 Cade, S. Osteogenic sarcoma; a study based on 133 patients. *Journal of the Royal College of Surgeons of Edinburgh* **1**, 79-111 (1955).
8 Tjalma, R. A. Canine bone sarcoma: estimation of relative risk as a function of body size. *Journal of the National Cancer Institute* **36**, 1137-1150 (1966).
9 Fraumeni, J. F., Jr. Stature and malignant tumors of bone in childhood and adolescence. *Cancer* **20**, 967-973 (1967).
10 Cotterill, S. J., Wright, C. M., Pearce, M. S. & Craft, A. W. Stature of young people with malignant bone tumors. *Pediatr Blood Cancer* **42**, 59-63, doi:10.1002/pbc.10437 (2004).
11 Ottaviani, G. & Jaffe, N. The epidemiology of osteosarcoma. *Cancer treatment and research* **152**, 3-13, doi:10.1007/978-1-4419-0284-9_1 (2009).
12 Nishida, Y. *et al.* Osteosarcoma in the elderly over 60 years: a multicenter study by the Japanese Musculoskeletal Oncology Group. *J Surg Oncol* **100**, 48-54, doi:10.1002/jso.21287 (2009).
13 Thorpe, W. P., Reilly, J. J. & Rosenberg, S. A. Prognostic significance of alkaline phosphatase measurements in patients with osteogenic sarcoma receiving chemotherapy. *Cancer* **43**, 2178-2181 (1979).
14 Link, M. P. *et al.* Adjuvant chemotherapy of high-grade osteosarcoma of the extremity. Updated results of the Multi-Institutional Osteosarcoma Study. *Clin Orthop Relat Res*, 8-14 (1991).
15 Clark, J. C., Dass, C. R. & Choong, P. F. A review of clinical and molecular prognostic factors in osteosarcoma. *J Cancer Res Clin Oncol* **134**, 281-297, doi:10.1007/s00432-007-0330-x (2008).
16 Marina, N., Gebhardt, M., Teot, L. & Gorlick, R. Biology and therapeutic advances for pediatric osteosarcoma. *The oncologist* **9**, 422-441 (2004).
17 Gronthos, S. *et al.* Differential cell surface expression of the STRO-1 and alkaline phosphatase antigens on discrete developmental stages in primary cultures of human bone cells. *J Bone Miner Res* **14**, 47-56, doi:10.1359/jbmr.1999.14.1.47 (1999).

18 Mutsaers, A. J. & Walkley, C. R. Cells of origin in osteosarcoma: mesenchymal stem cells or osteoblast committed cells? *Bone* **62**, 56-63, doi:10.1016/j.bone.2014.02.003 (2014).
19 Roodman, G. D. Cell biology of the osteoclast. *Exp Hematol* **27**, 1229-1241 (1999).
20 Kinpara, K., Mogi, M., Kuzushima, M. & Togari, A. Osteoclast differentiation factor in human osteosarcoma cell line. *Journal of immunoassay* **21**, 327-340, doi:10.1080/01971520009349540 (2000).
21 Tanaka, S., Nakamura, K., Takahasi, N. & Suda, T. Role of RANKL in physiological and pathological bone resorption and therapeutics targeting the RANKL-RANK signaling system. *Immunological reviews* **208**, 30-49, doi:10.1111/j.0105-2896.2005.00327.x (2005).
22 Broadhead, M. L., Clark, J. C., Myers, D. E., Dass, C. R. & Choong, P. F. The molecular pathogenesis of osteosarcoma: a review. *Sarcoma* **2011**, 959248, doi:10.1155/2011/959248 (2011).
23 Logue, J. P. & Cairnduff, F. Radiation induced extraskeletal osteosarcoma. *Br J Radiol* **64**, 171-172, doi:10.1259/0007-1285-64-758-171 (1991).
24 Le Vu, B. *et al.* Radiation dose, chemotherapy and risk of osteosarcoma after solid tumours during childhood. *International journal of cancer. Journal international du cancer* **77**, 370-377 (1998).
25 Kumar, A. S. R. a. S. *Transformation of nontumorigenic osteoblast-like human osteosarcoma cells byhexavalent chromates: alteration of morphology, induction of anchorage-independence and proteolytic function*. Vol. 13 2021–2027 (1992).
26 Dutra, F. R. & Largent, E. J. Osteosarcoma induced by beryllium oxide. *The American journal of pathology* **26**, 197-209 (1950).
27 Brandt-Rauf, P. W. *et al.* Serum oncoproteins and growth factors in asbestosis and silicosis patients. *International journal of cancer. Journal international du cancer* **50**, 881-885 (1992).
28 Klein, R. M. & Norman, A. Diagnostic procedures for Paget's disease. Radiologic, pathologic, and laboratory testing. *Endocrinology and metabolism clinics of North America* **24**, 437-450 (1995).
29 Hamdy, R. C. Clinical features and pharmacologic treatment of Paget's disease. *Endocrinology and metabolism clinics of North America* **24**, 421-436 (1995).
30 Laurin, N., Brown, J. P., Morissette, J. & Raymond, V. Recurrent mutation of the gene encoding sequestosome 1 (SQSTM1/p62) in Paget disease of bone. *Am J Hum Genet* **70**, 1582-1588, doi:10.1086/340731 (2002).
31 Smith, J., Botet, J. F. & Yeh, S. D. Bone sarcomas in Paget disease: a study of 85 patients. *Radiology* **152**, 583-590, doi:10.1148/radiology.152.3.6235535 (1984).
32 Wuyts, W., Schmale, G. A., Chansky, H. A. & Raskind, W. H. in *GeneReviews(R)* (eds R. A. Pagon *et al.*) (1993).
33 Gokgoz, N. *et al.* Comparison of p53 mutations in patients with localized osteosarcoma and metastatic osteosarcoma. *Cancer* **92**, 2181-2189 (2001).
34 Deshpande, A. & Hinds, P. W. The retinoblastoma protein in osteoblast differentiation and osteosarcoma. *Current molecular medicine* **6**, 809-817 (2006).
35 Hansen, M. F. *et al.* Osteosarcoma and retinoblastoma: a shared chromosomal mechanism revealing recessive predisposition. *Proc Natl Acad Sci U S A* **82**, 6216-6220 (1985).

36 Larsen, N. B. & Hickson, I. D. RecQ Helicases: Conserved Guardians of Genomic Integrity. *Adv Exp Med Biol* **767**, 161-184, doi:10.1007/978-1-4614-5037-5_8 (2013).
37 Wang, L. L. *et al.* Association between osteosarcoma and deleterious mutations in the RECQL4 gene in Rothmund-Thomson syndrome. *Journal of the National Cancer Institute* **95**, 669-674 (2003).
38 Siitonen, H. A. *et al.* Molecular defect of RAPADILINO syndrome expands the phenotype spectrum of RECQL diseases. *Hum Mol Genet* **12**, 2837-2844, doi:10.1093/hmg/ddg306 (2003).
39 Rosen, R. S., Cimini, R. & Coblentz, D. Werner's syndrome. *Br J Radiol* **43**, 193-198, doi:10.1259/0007-1285-43-507-193 (1970).
40 Lauper, J. M., Krause, A., Vaughan, T. L. & Monnat, R. J., Jr. Spectrum and risk of neoplasia in Werner syndrome: a systematic review. *PLoS One* **8**, e59709, doi:10.1371/journal.pone.0059709 (2013).
41 German, J. Bloom's syndrome. XX. The first 100 cancers. *Cancer Genet Cytogenet* **93**, 100-106 (1997).
42 Bridge, J. A. *et al.* Cytogenetic findings in 73 osteosarcoma specimens and a review of the literature. *Cancer Genet Cytogenet* **95**, 74-87 (1997).
43 Sandberg, A. A. & Bridge, J. A. Updates on the cytogenetics and molecular genetics of bone and soft tissue tumors: osteosarcoma and related tumors. *Cancer Genet Cytogenet* **145**, 1-30 (2003).
44 Smida, J. *et al.* Genomic alterations and allelic imbalances are strong prognostic predictors in osteosarcoma. *Clinical cancer research : an official journal of the American Association for Cancer Research* **16**, 4256-4267, doi:10.1158/1078-0432.CCR-10-0284 (2010).
45 Helman, L. J. & Meltzer, P. Mechanisms of sarcoma development. *Nat Rev Cancer* **3**, 685-694, doi:10.1038/nrc1168 (2003).
46 Nevins, J. R., Leone, G., DeGregori, J. & Jakoi, L. Role of the Rb/E2F pathway in cell growth control. *J Cell Physiol* **173**, 233-236, doi:10.1002/(SICI)1097-4652(199711)173:2<233::AID-JCP27>3.0.CO;2-F (1997).
47 Nielsen, G. P., Burns, K. L., Rosenberg, A. E. & Louis, D. N. CDKN2A gene deletions and loss of p16 expression occur in osteosarcomas that lack RB alterations. *The American journal of pathology* **153**, 159-163, doi:10.1016/S0002-9440(10)65556-3 (1998).
48 Ta, H. T., Dass, C. R., Choong, P. F. & Dunstan, D. E. Osteosarcoma treatment: state of the art. *Cancer Metastasis Rev* **28**, 247-263, doi:10.1007/s10555-009-9186-7 (2009).
49 Berman, S. D. *et al.* Metastatic osteosarcoma induced by inactivation of Rb and p53 in the osteoblast lineage. *Proc Natl Acad Sci U S A* **105**, 11851-11856 (2008).
50 Walkley, C. R. *et al.* Conditional mouse osteosarcoma, dependent on p53 loss and potentiated by loss of Rb, mimics the human disease. *Genes Dev* **22**, 1662-1676, doi:10.1101/gad.1656808 (2008).
51 Haydon, R. C., Luu, H. H. & He, T. C. Osteosarcoma and osteoblastic differentiation: a new perspective on oncogenesis. *Clin Orthop Relat Res* **454**, 237-246, doi:10.1097/BLO.0b013e31802b683c (2007).

52 Vermeulen, L., de Sousa e Melo, F., Richel, D. J. & Medema, J. P. The developing cancer stem-cell model: clinical challenges and opportunities. *The Lancet. Oncology* **13**, e83-89, doi:10.1016/S1470-2045(11)70257-1 (2012).
53 Himelstein, B. P., Asada, N., Carlton, M. R. & Collins, M. H. Matrix metalloproteinase-9 (MMP-9) expression in childhood osseous osteosarcoma. *Medical and pediatric oncology* **31**, 471-474 (1998).
54 Nguyen, L. V., Vanner, R., Dirks, P. & Eaves, C. J. Cancer stem cells: an evolving concept. *Nature reviews. Cancer* **12**, 133-143, doi:10.1038/nrc3184 (2012).
55 Greaves, M. & Maley, C. C. Clonal evolution in cancer. *Nature* **481**, 306-313, doi:10.1038/nature10762 (2012).
56 Nowell, P. C. The clonal evolution of tumor cell populations. *Science* **194**, 23-28 (1976).
57 Clevers, H. The cancer stem cell: premises, promises and challenges. *Nat Med* **17**, 313-319, doi:10.1038/nm.2304 (2011).
58 Dela Cruz, F. S. Cancer stem cells in pediatric sarcomas. *Front Oncol* **3**, 168, doi:10.3389/fonc.2013.00168 (2013).
59 Di Fiore, R. *et al.* Genetic and molecular characterization of the human osteosarcoma 3AB-OS cancer stem cell line: a possible model for studying osteosarcoma origin and stemness. *J Cell Physiol* **228**, 1189-1201, doi:10.1002/jcp.24272 (2013).
60 Gibbs, C. P., Jr., Levings, P. P. & Ghivizzani, S. C. Evidence for the osteosarcoma stem cell. *Curr Orthop Pract* **22**, 322-326, doi:10.1097/BCO.0b013e318221aee8 (2011).
61 Martins-Neves, S. R. *et al.* Therapeutic implications of an enriched cancer stem-like cell population in a human osteosarcoma cell line. *BMC Cancer* **12**, 139, doi:10.1186/1471-2407-12-139 (2012).
62 Bae, K. M. *et al.* Expression of pluripotent stem cell reprogramming factors by prostate tumor initiating cells. *J Urol* **183**, 2045-2053, doi:10.1016/j.juro.2009.12.092 (2010).
63 Bussolati, B., Bruno, S., Grange, C., Ferrando, U. & Camussi, G. Identification of a tumor-initiating stem cell population in human renal carcinomas. *FASEB J* **22**, 3696-3705, doi:10.1096/fj.08-102590 (2008).
64 Chiou, S. H. *et al.* Positive correlations of Oct-4 and Nanog in oral cancer stem-like cells and high-grade oral squamous cell carcinoma. *Clinical cancer research : an official journal of the American Association for Cancer Research* **14**, 4085-4095, doi:10.1158/1078-0432.CCR-07-4404 (2008).
65 Liu, T. *et al.* Establishment and characterization of multi-drug resistant, prostate carcinoma-initiating stem-like cells from human prostate cancer cell lines 22RV1. *Mol Cell Biochem* **340**, 265-273, doi:10.1007/s11010-010-0426-5 (2010).
66 Lapidot, T. *et al.* A cell initiating human acute myeloid leukaemia after transplantation into SCID mice. *Nature* **367**, 645-648, doi:10.1038/367645a0 (1994).
67 Ischenko, I., Seeliger, H., Schaffer, M., Jauch, K. W. & Bruns, C. J. Cancer stem cells: how can we target them? *Curr Med Chem* **15**, 3171-3184 (2008).
68 Tang, C., Ang, B. T. & Pervaiz, S. Cancer stem cell: target for anti-cancer therapy. *FASEB J* **21**, 3777-3785, doi:10.1096/fj.07-8560rev (2007).
69 Gibbs, C. P. *et al.* Stem-like cells in bone sarcomas: implications for tumorigenesis. *Neoplasia* **7**, 967-976 (2005).

70 Fujii, H. *et al.* Sphere-forming stem-like cell populations with drug resistance in human sarcoma cell lines. *Int J Oncol* **34**, 1381-1386 (2009).
71 Levings, P. P. *et al.* Expression of an exogenous human Oct-4 promoter identifies tumor-initiating cells in osteosarcoma. *Cancer Res* **69**, 5648-5655, doi:10.1158/0008-5472.CAN-08-3580 (2009).
72 Basu-Roy, U. *et al.* Sox2 maintains self renewal of tumor-initiating cells in osteosarcomas. *Oncogene* **31**, 2270-2282, doi:10.1038/onc.2011.405 (2012).
73 Adhikari, A. S. *et al.* CD117 and Stro-1 identify osteosarcoma tumor-initiating cells associated with metastasis and drug resistance. *Cancer Res* **70**, 4602-4612, doi:10.1158/0008-5472.CAN-09-3463 (2010).
74 Tirino, V. *et al.* Detection and characterization of CD133+ cancer stem cells in human solid tumours. *PLoS One* **3**, e3469, doi:10.1371/journal.pone.0003469 (2008).
75 Murase, M. *et al.* Side population cells have the characteristics of cancer stem-like cells/cancer-initiating cells in bone sarcomas. *Br J Cancer* **101**, 1425-1432, doi:10.1038/sj.bjc.6605330 (2009).
76 Honoki, K. *et al.* Possible involvement of stem-like populations with elevated ALDH1 in sarcomas for chemotherapeutic drug resistance. *Oncol Rep* **24**, 501-505 (2010).
77 Burger, P. E. *et al.* High aldehyde dehydrogenase activity: a novel functional marker of murine prostate stem/progenitor cells. *Stem cells* **27**, 2220-2228, doi:10.1002/stem.135 (2009).
78 Ma, I. & Allan, A. L. The role of human aldehyde dehydrogenase in normal and cancer stem cells. *Stem cell reviews* **7**, 292-306, doi:10.1007/s12015-010-9208-4 (2011).
79 Wang, L., Park, P., Zhang, H., La Marca, F. & Lin, C. Y. Prospective identification of tumorigenic osteosarcoma cancer stem cells in OS99-1 cells based on high aldehyde dehydrogenase activity. *Int J Cancer* **128**, 294-303, doi:10.1002/ijc.25331 (2011).
80 Yu, Y., Luk, F., Yang, J. L. & Walsh, W. R. Ras/Raf/MEK/ERK pathway is associated with lung metastasis of osteosarcoma in an orthotopic mouse model. *Anticancer Res* **31**, 1147-1152 (2011).
81 Tabone, M. D. *et al.* Osteosarcoma recurrences in pediatric patients previously treated with intensive chemotherapy. *Journal of clinical oncology : official journal of the American Society of Clinical Oncology* **12**, 2614-2620 (1994).
82 Heare, T., Hensley, M. A. & Dell'Orfano, S. Bone tumors: osteosarcoma and Ewing's sarcoma. *Current opinion in pediatrics* **21**, 365-372, doi:10.1097/MOP.0b013e32832b1111 (2009).
83 Liu, B., Ma, W., Jha, R. K. & Gurung, K. Cancer stem cells in osteosarcoma: recent progress and perspective. *Acta Oncol* **50**, 1142-1150, doi:10.3109/0284186X.2011.584553 (2011).
84 Ladanyi, M. *et al.* MDM2 gene amplification in metastatic osteosarcoma. *Cancer Res* **53**, 16-18 (1993).
85 Lai, R., Wang, Z. & Zhe, X. [Detection of MDM 2 and p 53 genes in rhabdomyosarcoma by in situ hybridization]. *Zhonghua Bing Li Xue Za Zhi* **27**, 127-129 (1998).
86 Ladanyi, M. *et al.* MDM2 and CDK4 gene amplification in Ewing's sarcoma. *J Pathol* **175**, 211-217, doi:10.1002/path.1711750209 (1995).
87 Gorlick, R. *et al.* Biology of childhood osteogenic sarcoma and potential targets for therapeutic development: meeting summary. *Clin Cancer Res* **9**, 5442-5453 (2003).

88 Siegel, H. J. & Pressey, J. G. Current concepts on the surgical and medical management of osteosarcoma. *Expert Rev Anticancer Ther* **8**, 1257-1269, doi:10.1586/14737140.8.8.1257 (2008).
89 Hindupur, S. K. *et al.* Identification of a novel AMPK-PEA15 axis in the anoikis-resistant growth of mammary cells. *Breast Cancer Res* **16**, 420, doi:10.1186/s13058-014-0420-z (2014).
90 Liao, J. *et al.* Ovarian cancer spheroid cells with stem cell-like properties contribute to tumor generation, metastasis and chemotherapy resistance through hypoxia-resistant metabolism. *PLoS One* **9**, e84941, doi:10.1371/journal.pone.0084941 (2014).
91 Marotta, L. L. & Polyak, K. Cancer stem cells: a model in the making. *Curr Opin Genet Dev* **19**, 44-50 (2009).
92 Malanchi, I. & Huelsken, J. Cancer stem cells: never Wnt away from the niche. *Curr Opin Oncol* **21**, 41-46 (2009).
93 Reya, T., Morrison, S. J., Clarke, M. F. & Weissman, I. L. Stem cells, cancer, and cancer stem cells. *Nature* **414**, 105-111, doi:10.1038/35102167 (2001).
94 Bjerkvig, R., Tysnes, B. B., Aboody, K. S., Najbauer, J. & Terzis, A. J. Opinion: the origin of the cancer stem cell: current controversies and new insights. *Nat Rev Cancer* **5**, 899-904 (2005).
95 Burnett, L. A. *et al.* Testicular expression of Adora3i2 in Adora3 knockout mice reveals a role of mouse A3Ri2 and human A3Ri3 adenosine receptors in sperm. *J Biol Chem* **285**, 33662-33670, doi:10.1074/jbc.M110.156075 (2010).
96 Borea, P. A. *et al.* The A3 adenosine receptor: history and perspectives. *Pharmacol Rev* **67**, 74-102, doi:10.1124/pr.113.008540 (2015).
97 Fishman, P. *et al.* Adenosine receptors and cancer. *Handb Exp Pharmacol*, 399-441, doi:10.1007/978-3-540-89615-9_14 (2009).
98 Aghaei, M., Karami-Tehrani, F., Panjehpour, M., Salami, S. & Fallahian, F. Adenosine induces cell-cycle arrest and apoptosis in androgen-dependent and -independent prostate cancer cell lines, LNcap-FGC-10, DU-145, and PC3. *Prostate* **72**, 361-375, doi:10.1002/pros.21438 (2012).
99 Jacobson, K. A. & Gao, Z. G. Adenosine receptors as therapeutic targets. *Nat Rev Drug Discov* **5**, 247-264, doi:10.1038/nrd1983 (2006).
100 Rivas, M. & Santisteban, P. TSH-activated signaling pathways in thyroid tumorigenesis. *Molecular and cellular endocrinology* **213**, 31-45, doi:10.1016/j.mce.2003.10.029 (2003).
101 Warrington, N. M., Sun, T. & Rubin, J. B. Targeting brain tumor cAMP: the case for sex-specific therapeutics. *Frontiers in pharmacology* **6**, 153, doi:10.3389/fphar.2015.00153 (2015).
102 Fajardo, A. M., Piazza, G. A. & Tinsley, H. N. The role of cyclic nucleotide signaling pathways in cancer: targets for prevention and treatment. *Cancers* **6**, 436-458, doi:10.3390/cancers6010436 (2014).
103 Fredriksson, R., Lagerstrom, M. C., Lundin, L. G. & Schioth, H. B. The G-protein-coupled receptors in the human genome form five main families. Phylogenetic analysis, paralogon groups, and fingerprints. *Molecular pharmacology* **63**, 1256-1272, doi:10.1124/mol.63.6.1256 (2003).

104 Lagerstrom, M. C. & Schioth, H. B. Structural diversity of G protein-coupled receptors and significance for drug discovery. *Nat Rev Drug Discov* **7**, 339-357, doi:10.1038/nrd2518 (2008).
105 Svoboda, P. *et al.* Biochemistry of transmembrane signaling mediated by trimeric G proteins. *Physiol Res* **53 Suppl 1**, S141-152 (2004).
106 Oldham, W. M. & Hamm, H. E. Structural basis of function in heterotrimeric G proteins. *Q Rev Biophys* **39**, 117-166, doi:10.1017/S0033583506004306 (2006).
107 Bridges, T. M. & Lindsley, C. W. G-protein-coupled receptors: from classical modes of modulation to allosteric mechanisms. *ACS Chem Biol* **3**, 530-541, doi:10.1021/cb800116f (2008).
108 Jacoby, E., Bouhelal, R., Gerspacher, M. & Seuwen, K. The 7 TM G-protein-coupled receptor target family. *ChemMedChem* **1**, 761-782, doi:10.1002/cmdc.200600134 (2006).
109 De Vries, L., Zheng, B., Fischer, T., Elenko, E. & Farquhar, M. G. The regulator of G protein signaling family. *Annu Rev Pharmacol Toxicol* **40**, 235-271, doi:10.1146/annurev.pharmtox.40.1.235 (2000).
110 Smrcka, A. V., Hepler, J. R., Brown, K. O. & Sternweis, P. C. Regulation of polyphosphoinositide-specific phospholipase C activity by purified Gq. *Science* **251**, 804-807 (1991).
111 Pierce, K. L., Premont, R. T. & Lefkowitz, R. J. Seven-transmembrane receptors. *Nat Rev Mol Cell Biol* **3**, 639-650, doi:10.1038/nrm908 (2002).
112 Pitcher, J. A., Freedman, N. J. & Lefkowitz, R. J. G protein-coupled receptor kinases. *Annu Rev Biochem* **67**, 653-692, doi:10.1146/annurev.biochem.67.1.653 (1998).
113 Lefkowitz, R. J. Seven transmembrane receptors: something old, something new. *Acta Physiol (Oxf)* **190**, 9-19, doi:10.1111/j.1365-201X.2007.01693.x (2007).
114 DeWire, S. M., Ahn, S., Lefkowitz, R. J. & Shenoy, S. K. Beta-arrestins and cell signaling. *Annu Rev Physiol* **69**, 483-510, doi:10.1146/annurev.ph.69.013107.100021 (2007).
115 Krupnick, J. G. & Benovic, J. L. The role of receptor kinases and arrestins in G protein-coupled receptor regulation. *Annu Rev Pharmacol Toxicol* **38**, 289-319, doi:10.1146/annurev.pharmtox.38.1.289 (1998).
116 Goodman, O. B., Jr. *et al.* Role of arrestins in G-protein-coupled receptor endocytosis. *Adv Pharmacol* **42**, 429-433 (1998).
117 Fredholm, B. B. *et al.* Towards a revised nomenclature for P1 and P2 receptors. *Trends in pharmacological sciences* **18**, 79-82 (1997).
118 Auchampach, J. A. & Gross, G. J. Adenosine A1 receptors, KATP channels, and ischemic preconditioning in dogs. *Am J Physiol* **264**, H1327-1336 (1993).
119 Germack, R., Griffin, M. & Dickenson, J. M. Activation of protein kinase B by adenosine A1 and A3 receptors in newborn rat cardiomyocytes. *J Mol Cell Cardiol* **37**, 989-999, doi:10.1016/j.yjmcc.2004.08.001 (2004).
120 Fredholm, B. B., AP, I. J., Jacobson, K. A., Klotz, K. N. & Linden, J. International Union of Pharmacology. XXV. Nomenclature and classification of adenosine receptors. *Pharmacol Rev* **53**, 527-552 (2001).
121 Palmer, T. M., Benovic, J. L. & Stiles, G. L. Agonist-dependent phosphorylation and desensitization of the rat A3 adenosine receptor. Evidence for a G-protein-coupled receptor kinase-mediated mechanism. *J Biol Chem* **270**, 29607-29613 (1995).

122 Antonioli, L., Pacher, P., Vizi, E. S. & Hasko, G. CD39 and CD73 in immunity and inflammation. *Trends Mol Med* **19**, 355-367, doi:10.1016/j.molmed.2013.03.005 (2013).
123 Antonioli, L. *et al.* Adenosine deaminase in the modulation of immune system and its potential as a novel target for treatment of inflammatory disorders. *Curr Drug Targets* **13**, 842-862 (2012).
124 Baldwin, S. A. *et al.* The equilibrative nucleoside transporter family, SLC29. *Pflugers Arch* **447**, 735-743, doi:10.1007/s00424-003-1103-2 (2004).
125 Londos, C., Cooper, D. M. & Wolff, J. Subclasses of external adenosine receptors. *Proc Natl Acad Sci U S A* **77**, 2551-2554 (1980).
126 Muller, C. E., Geis, U., Grahner, B., Lanzner, W. & Eger, K. Chiral pyrrolo[2,3-d]pyrimidine and pyrimido[4,5-b]indole derivatives: structure-activity relationships of potent, highly stereoselective A1-adenosine receptor antagonists. *J Med Chem* **39**, 2482-2491, doi:10.1021/jm960011w (1996).
127 Dixon, A. K., Gubitz, A. K., Sirinathsinghji, D. J., Richardson, P. J. & Freeman, T. C. Tissue distribution of adenosine receptor mRNAs in the rat. *Br J Pharmacol* **118**, 1461-1468 (1996).
128 Salvatore, C. A., Jacobson, M. A., Taylor, H. E., Linden, J. & Johnson, R. G. Molecular cloning and characterization of the human A3 adenosine receptor. *Proc Natl Acad Sci U S A* **90**, 10365-10369 (1993).
129 Lasley, R. D. Adenosine receptors and membrane microdomains. *Biochimica et biophysica acta* **1808**, 1284-1289, doi:10.1016/j.bbamem.2010.09.019 (2011).
130 Mustafa, S. J., Morrison, R. R., Teng, B. & Pelleg, A. Adenosine receptors and the heart: role in regulation of coronary blood flow and cardiac electrophysiology. *Handbook of experimental pharmacology*, 161-188, doi:10.1007/978-3-540-89615-9_6 (2009).
131 Sheth, S., Brito, R., Mukherjea, D., Rybak, L. P. & Ramkumar, V. Adenosine receptors: expression, function and regulation. *International journal of molecular sciences* **15**, 2024-2052, doi:10.3390/ijms15022024 (2014).
132 Spychala, J. Tumor-promoting functions of adenosine. *Pharmacol Ther* **87**, 161-173 (2000).
133 Blay, J., White, T. D. & Hoskin, D. W. The extracellular fluid of solid carcinomas contains immunosuppressive concentrations of adenosine. *Cancer Res* **57**, 2602-2605 (1997).
134 Hasko, G., Linden, J., Cronstein, B. & Pacher, P. Adenosine receptors: therapeutic aspects for inflammatory and immune diseases. *Nat Rev Drug Discov* **7**, 759-770, doi:10.1038/nrd2638 (2008).
135 Burnstock, G. Purinergic signaling and vascular cell proliferation and death. *Arterioscler Thromb Vasc Biol* **22**, 364-373 (2002).
136 Serra, S. *et al.* CD73-generated extracellular adenosine in chronic lymphocytic leukemia creates local conditions counteracting drug-induced cell death. *Blood* **118**, 6141-6152, doi:10.1182/blood-2011-08-374728 (2011).
137 Feng, L. *et al.* Vascular CD39/ENTPD1 directly promotes tumor cell growth by scavenging extracellular adenosine triphosphate. *Neoplasia* **13**, 206-216 (2011).
138 Jackson, S. W. *et al.* Disordered purinergic signaling inhibits pathological angiogenesis in cd39/Entpd1-null mice. *The American journal of pathology* **171**, 1395-1404, doi:10.2353/ajpath.2007.070190 (2007).

139 Pennycooke, M., Chaudary, N., Shuralyova, I., Zhang, Y. & Coe, I. R. Differential expression of human nucleoside transporters in normal and tumor tissue. *Biochem Biophys Res Commun* **280**, 951-959, doi:10.1006/bbrc.2000.4205 (2001).
140 Ohana, G., Bar-Yehuda, S., Barer, F. & Fishman, P. Differential effect of adenosine on tumor and normal cell growth: focus on the A3 adenosine receptor. *J Cell Physiol* **186**, 19-23, doi:10.1002/1097-4652(200101)186:1<19::AID-JCP1011>3.0.CO;2-3 (2001).
141 Mirza, A. *et al.* RNA interference targeting of A1 receptor-overexpressing breast carcinoma cells leads to diminished rates of cell proliferation and induction of apoptosis. *Cancer biology & therapy* **4**, 1355-1360 (2005).
142 Khoo, H. E. *et al.* Differential expression of adenosine A1 receptors in colorectal cancer and related mucosa. *Cancer Lett* **106**, 17-21 (1996).
143 Lin, Z. *et al.* Adenosine A1 receptor, a target and regulator of estrogen receptoralpha action, mediates the proliferative effects of estradiol in breast cancer. *Oncogene* **29**, 1114-1122, doi:10.1038/onc.2009.409 (2010).
144 Colquhoun, A. & Newsholme, E. A. Inhibition of human tumour cell proliferation by analogues of adenosine. *Cell Biochem Funct* **15**, 135-139, doi:10.1002/(SICI)1099-0844(19970601)15:2<135::AID-CBF733>3.0.CO;2-G (1997).
145 Johnston, J. B. *et al.* Diminished adenosine A1 receptor expression on macrophages in brain and blood of patients with multiple sclerosis. *Ann Neurol* **49**, 650-658 (2001).
146 Gimenez-Llort, L. *et al.* Mice lacking the adenosine A1 receptor are anxious and aggressive, but are normal learners with reduced muscle strength and survival rate. *Eur J Neurosci* **16**, 547-550 (2002).
147 Synowitz, M. *et al.* A1 adenosine receptors in microglia control glioblastoma-host interaction. *Cancer Res* **66**, 8550-8557, doi:10.1158/0008-5472.CAN-06-0365 (2006).
148 Yang, H. *et al.* Reduced expression of Toll-like receptor 4 inhibits human breast cancer cells proliferation and inflammatory cytokines secretion. *Journal of experimental & clinical cancer research : CR* **29**, 92, doi:10.1186/1756-9966-29-92 (2010).
149 Saito, M., Yaguchi, T., Yasuda, Y., Nakano, T. & Nishizaki, T. Adenosine suppresses CW2 human colonic cancer growth by inducing apoptosis via A(1) adenosine receptors. *Cancer letters* **290**, 211-215, doi:10.1016/j.canlet.2009.09.011 (2010).
150 Gessi, S. *et al.* Pharmacological and biochemical characterization of A3 adenosine receptors in Jurkat T cells. *Br J Pharmacol* **134**, 116-126, doi:10.1038/sj.bjp.0704254 (2001).
151 Hillion, J. *et al.* Coaggregation, cointernalization, and codesensitization of adenosine A2A receptors and dopamine D2 receptors. *J Biol Chem* **277**, 18091-18097, doi:10.1074/jbc.M107731200 (2002).
152 Merighi, S. *et al.* Pharmacological and biochemical characterization of adenosine receptors in the human malignant melanoma A375 cell line. *Br J Pharmacol* **134**, 1215-1226, doi:10.1038/sj.bjp.0704352 (2001).
153 Etique, N., Grillier-Vuissoz, I., Lecomte, J. & Flament, S. Crosstalk between adenosine receptor (A2A isoform) and ERalpha mediates ethanol action in MCF-7 breast cancer cells. *Oncology reports* **21**, 977-981 (2009).

154 Zhao, Z. Q. *et al.* Adenosine attenuates reperfusion-induced apoptotic cell death by modulating expression of Bcl-2 and Bax proteins. *Journal of molecular and cellular cardiology* **33**, 57-68, doi:10.1006/jmcc.2000.1275 (2001).
155 Cassada, D. C. *et al.* An adenosine A2A agonist, ATL-146e, reduces paralysis and apoptosis during rabbit spinal cord reperfusion. *Journal of vascular surgery* **34**, 482-488, doi:10.1067/mva.2001.117996 (2001).
156 Merighi, S. *et al.* Adenosine receptors as mediators of both cell proliferation and cell death of cultured human melanoma cells. *J Invest Dermatol* **119**, 923-933, doi:10.1046/j.1523-1747.2002.00111.x (2002).
157 Yasuda, Y., Saito, M., Yamamura, T., Yaguchi, T. & Nishizaki, T. Extracellular adenosine induces apoptosis in Caco-2 human colonic cancer cells by activating caspase-9/-3 via A(2a) adenosine receptors. *Journal of gastroenterology* **44**, 56-65, doi:10.1007/s00535-008-2273-7 (2009).
158 Fredholm, B. B., Irenius, E., Kull, B. & Schulte, G. Comparison of the potency of adenosine as an agonist at human adenosine receptors expressed in Chinese hamster ovary cells. *Biochemical pharmacology* **61**, 443-448 (2001).
159 Ma, D. F. *et al.* Hypoxia-inducible adenosine A2B receptor modulates proliferation of colon carcinoma cells. *Hum Pathol* **41**, 1550-1557, doi:10.1016/j.humpath.2010.04.008 (2010).
160 Panjehpour, M. & Karami-Tehrani, F. An adenosine analog (IB-MECA) inhibits anchorage-dependent cell growth of various human breast cancer cell lines. *Int J Biochem Cell Biol* **36**, 1502-1509, doi:10.1016/j.biocel.2003.12.001 (2004).
161 Madi, L. *et al.* A3 adenosine receptor activation in melanoma cells: association between receptor fate and tumor growth inhibition. *J Biol Chem* **278**, 42121-42130, doi:10.1074/jbc.M301243200 (2003).
162 Fishman, P. *et al.* An agonist to the A3 adenosine receptor inhibits colon carcinoma growth in mice via modulation of GSK-3 beta and NF-kappa B. *Oncogene* **23**, 2465-2471, doi:10.1038/sj.onc.1207355 (2004).
163 Fishman, P. *et al.* Adenosine acts as an inhibitor of lymphoma cell growth: a major role for the A3 adenosine receptor. *Eur J Cancer* **36**, 1452-1458 (2000).
164 Aghaei, M., Panjehpour, M., Karami-Tehrani, F. & Salami, S. Molecular mechanisms of A3 adenosine receptor-induced G1 cell cycle arrest and apoptosis in androgen-dependent and independent prostate cancer cell lines: involvement of intrinsic pathway. *J Cancer Res Clin Oncol* **137**, 1511-1523, doi:10.1007/s00432-011-1031-z (2011).
165 Fishman, P. *et al.* Evidence for involvement of Wnt signaling pathway in IB-MECA mediated suppression of melanoma cells. *Oncogene* **21**, 4060-4064, doi:10.1038/sj.onc.1205531 (2002).
166 Chung, H. *et al.* The antitumor effect of LJ-529, a novel agonist to A3 adenosine receptor, in both estrogen receptor-positive and estrogen receptor-negative human breast cancers. *Mol Cancer Ther* **5**, 685-692, doi:10.1158/1535-7163.MCT-05-0245 (2006).
167 Morello, S. *et al.* Cl-IB-MECA inhibits human thyroid cancer cell proliferation independently of A3 adenosine receptor activation. *Cancer biology & therapy* **7**, 278-284 (2008).

168 Jajoo, S., Mukherjea, D., Watabe, K. & Ramkumar, V. Adenosine A(3) receptor suppresses prostate cancer metastasis by inhibiting NADPH oxidase activity. *Neoplasia* **11**, 1132-1145 (2009).
169 Agarwal, N. *et al.* MTBP suppresses cell migration and filopodia formation by inhibiting ACTN4. *Oncogene* **32**, 462-470, doi:10.1038/onc.2012.69 (2013).
170 Chen, Y. *et al.* Combined integrin phosphoproteomic analyses and small interfering RNA--based functional screening identify key regulators for cancer cell adhesion and migration. *Cancer Res* **69**, 3713-3720, doi:10.1158/0008-5472.CAN-08-2515 (2009).
171 Sasaki, H., Iyer, S. V., Sasaki, K., Tawfik, O. W. & Iwakuma, T. An improved intrafemoral injection with minimized leakage as an orthotopic mouse model of osteosarcoma. *Anal Biochem* **486**, 70-74, doi:10.1016/j.ab.2015.06.030 (2015).
172 Gallagher, R. *et al.* Clinicopathologic correlation of vitamin D receptor expression with retinoid X receptor and MIB-1 expression in primary and metastatic osteosarcoma. *Ann Diagn Pathol*, doi:10.1016/j.anndiagpath.2012.01.001 (2012).
173 Bi, Q. *et al.* MTBP inhibits migration and metastasis of hepatocellular carcinoma. *Clin Exp Metastasis* **32**, 301-311, doi:10.1007/s10585-015-9706-5 (2015).
174 Arafa, E. *et al.* TMIGD1 is a novel adhesion molecule that protects epithelial cells from oxidative cell injury. *The American journal of pathology* **185**, 2757-2767, doi:10.1016/j.ajpath.2015.06.006 (2015).
175 Roberts, D. L., O'Dwyer, S. T., Stern, P. L. & Renehan, A. G. Global gene expression in pseudomyxoma peritonei, with parallel development of two immortalized cell lines. *Oncotarget* **6**, 10786-10800, doi:10.18632/oncotarget.3198 (2015).
176 Janakiram, M., Chinai, J. M., Zhao, A., Sparano, J. A. & Zang, X. HHLA2 and TMIGD2: new immunotherapeutic targets of the B7 and CD28 families. *Oncoimmunology* **4**, e1026534, doi:10.1080/2162402X.2015.1026534 (2015).
177 Rahimi, N., Rezazadeh, K., Mahoney, J. E., Hartsough, E. & Meyer, R. D. Identification of IGPR-1 as a novel adhesion molecule involved in angiogenesis. *Molecular biology of the cell* **23**, 1646-1656, doi:10.1091/mbc.E11-11-0934 (2012).
178 Salvatore, C. A. *et al.* Disruption of the A(3) adenosine receptor gene in mice and its effect on stimulated inflammatory cells. *J Biol Chem* **275**, 4429-4434 (2000).
179 Merighi, S. *et al.* A glance at adenosine receptors: novel target for antitumor therapy. *Pharmacol Ther* **100**, 31-48 (2003).
180 Gessi, S. *et al.* Adenosine receptor targeting in health and disease. *Expert Opin Investig Drugs* **20**, 1591-1609, doi:10.1517/13543784.2011.627853 (2011).
181 Abbracchio, M. P. *et al.* G protein-dependent activation of phospholipase C by adenosine A3 receptors in rat brain. *Molecular pharmacology* **48**, 1038-1045 (1995).
182 Ramkumar, V., Stiles, G. L., Beaven, M. A. & Ali, H. The A3 adenosine receptor is the unique adenosine receptor which facilitates release of allergic mediators in mast cells. *J Biol Chem* **268**, 16887-16890 (1993).
183 Fredholm, B. B. *et al.* Structure and function of adenosine receptors and their genes. *Naunyn Schmiedebergs Arch Pharmacol* **362**, 364-374 (2000).
184 Rayet, B. & Gelinas, C. Aberrant rel/nfkb genes and activity in human cancer. *Oncogene* **18**, 6938-6947, doi:10.1038/sj.onc.1203221 (1999).
185 Webster, G. A. & Perkins, N. D. Transcriptional cross talk between NF-kappaB and p53. *Mol Cell Biol* **19**, 3485-3495 (1999).

186 Gudkov, A. V., Gurova, K. V. & Komarova, E. A. Inflammation and p53: A Tale of Two Stresses. *Genes Cancer* **2**, 503-516, doi:10.1177/1947601911409747 (2011).
187 Catz, S. D. & Johnson, J. L. Transcriptional regulation of bcl-2 by nuclear factor kappa B and its significance in prostate cancer. *Oncogene* **20**, 7342-7351, doi:10.1038/sj.onc.1204926 (2001).
188 Grimm, T. *et al.* EBV latent membrane protein-1 protects B cells from apoptosis by inhibition of BAX. *Blood* **105**, 3263-3269, doi:10.1182/blood-2004-07-2752 (2005).
189 Fichera, A. *et al.* Epidermal growth factor receptor signaling is required for microadenoma formation in the mouse azoxymethane model of colonic carcinogenesis. *Cancer Res* **67**, 827-835, doi:10.1158/0008-5472.CAN-05-3343 (2007).
190 Ko, H. M. *et al.* Nuclear factor kappaB dependency of platelet-activating factor-induced angiogenesis. *Cancer Res* **62**, 1809-1814 (2002).
191 Andela, V. B., Schwarz, E. M., Puzas, J. E., O'Keefe, R. J. & Rosier, R. N. Tumor metastasis and the reciprocal regulation of prometastatic and antimetastatic factors by nuclear factor kappaB. *Cancer Res* **60**, 6557-6562 (2000).
192 Millet, I. *et al.* Inhibition of NF-kappaB activity and enhancement of apoptosis by the neuropeptide calcitonin gene-related peptide. *J Biol Chem* **275**, 15114-15121 (2000).
193 Joyce, D. *et al.* NF-kappaB and cell-cycle regulation: the cyclin connection. *Cytokine Growth Factor Rev* **12**, 73-90 (2001).
194 Andela, V. B. *et al.* Malignant reversion of a human osteosarcoma cell line, Saos-2, by inhibition of NFkappaB. *Biochem Biophys Res Commun* **297**, 237-241 (2002).
195 Asai, T. *et al.* VCP (p97) regulates NFkappaB signaling pathway, which is important for metastasis of osteosarcoma cell line. *Jpn J Cancer Res* **93**, 296-304 (2002).
196 Valkov, A. *et al.* The prognostic impact of TGF-beta1, fascin, NF-kappaB and PKC-zeta expression in soft tissue sarcomas. *PLoS One* **6**, e17507, doi:10.1371/journal.pone.0017507 (2011).
197 Eliseev, R. A. *et al.* Increased radiation-induced apoptosis of Saos2 cells via inhibition of NFkappaB: a role for c-Jun N-terminal kinase. *J Cell Biochem* **96**, 1262-1273, doi:10.1002/jcb.20607 (2005).
198 Eliseev, R. A. *et al.* Smad7 mediates inhibition of Saos2 osteosarcoma cell differentiation by NFkappaB. *Exp Cell Res* **312**, 40-50 (2006).
199 Stein, G. S. *et al.* Runx2 control of organization, assembly and activity of the regulatory machinery for skeletal gene expression. *Oncogene* **23**, 4315-4329, doi:10.1038/sj.onc.1207676 (2004).
200 Balint, E. *et al.* Phenotype discovery by gene expression profiling: mapping of biological processes linked to BMP-2-mediated osteoblast differentiation. *J Cell Biochem* **89**, 401-426, doi:10.1002/jcb.10515 (2003).
201 Chen, D., Zhao, M. & Mundy, G. R. Bone morphogenetic proteins. *Growth Factors* **22**, 233-241, doi:10.1080/08977190412331279890 (2004).
202 Mohseny, A. B. *et al.* Osteosarcoma originates from mesenchymal stem cells in consequence of aneuploidization and genomic loss of Cdkn2. *J Pathol* **219**, 294-305, doi:10.1002/path.2603 (2009).

203 Tang, N., Song, W. X., Luo, J., Haydon, R. C. & He, T. C. Osteosarcoma development and stem cell differentiation. *Clin Orthop Relat Res* **466**, 2114-2130, doi:10.1007/s11999-008-0335-z (2008).
204 Zuch, D. *et al.* Targeting radioresistant osteosarcoma cells with parthenolide. *J Cell Biochem* **113**, 1282-1291, doi:10.1002/jcb.24002 (2012).
205 Lee, J. Y. *et al.* Activation of adenosine A3 receptor suppresses lipopolysaccharide-induced TNF-alpha production through inhibition of PI 3-kinase/Akt and NF-kappaB activation in murine BV2 microglial cells. *Neurosci Lett* **396**, 1-6, doi:10.1016/j.neulet.2005.11.004 (2006).
206 Lee, H. S., Chung, H. J., Lee, H. W., Jeong, L. S. & Lee, S. K. Suppression of inflammation response by a novel A(3) adenosine receptor agonist thio-Cl-IB-MECA through inhibition of Akt and NF-kappaB signaling. *Immunobiology* **216**, 997-1003, doi:10.1016/j.imbio.2011.03.008 (2011).
207 Fishman, P. *et al.* Targeting the A3 adenosine receptor for cancer therapy: inhibition of prostate carcinoma cell growth by A3AR agonist. *Anticancer Res* **23**, 2077-2083 (2003).
208 Kim, H. *et al.* A3 adenosine receptor antagonist, truncated Thio-Cl-IB-MECA, induces apoptosis in T24 human bladder cancer cells. *Anticancer Res* **30**, 2823-2830 (2010).
209 Mlejnek, P. & Dolezel, P. Induction of apoptosis by A3 adenosine receptor agonist N-(3-iodobenzyl)-adenosine-5'-N-methylcarboxamide in human leukaemia cells: a possible involvement of intracellular mechanism. *Acta Physiol (Oxf)* **199**, 171-179, doi:10.1111/j.1748-1716.2010.02087.x (2010).
210 Lindholm, P. F., Bub, J., Kaul, S., Shidham, V. B. & Kajdacsy-Balla, A. The role of constitutive NF-kappaB activity in PC-3 human prostate cancer cell invasive behavior. *Clin Exp Metastasis* **18**, 471-479 (2000).
211 Zhong, H., Voll, R. E. & Ghosh, S. Phosphorylation of NF-kappa B p65 by PKA stimulates transcriptional activity by promoting a novel bivalent interaction with the coactivator CBP/p300. *Mol Cell* **1**, 661-671 (1998).
212 Madi, L. *et al.* Overexpression of A3 adenosine receptor in peripheral blood mononuclear cells in rheumatoid arthritis: involvement of nuclear factor-kappaB in mediating receptor level. *J Rheumatol* **34**, 20-26 (2007).
213 Madi, L. *et al.* The A3 adenosine receptor is highly expressed in tumor versus normal cells: potential target for tumor growth inhibition. *Clinical cancer research : an official journal of the American Association for Cancer Research* **10**, 4472-4479, doi:10.1158/1078-0432.CCR-03-0651 (2004).
214 Schulte, G. & Fredholm, B. B. Signaling pathway from the human adenosine A(3) receptor expressed in Chinese hamster ovary cells to the extracellular signal-regulated kinase 1/2. *Molecular pharmacology* **62**, 1137-1146 (2002).
215 Bar-Yehuda, S. *et al.* Agonists to the A3 adenosine receptor induce G-CSF production via NF-kappaB activation: a new class of myeloprotective agents. *Exp Hematol* **30**, 1390-1398 (2002).
216 Polakis, P. Wnt signaling and cancer. *Genes Dev* **14**, 1837-1851 (2000).
217 Haydon, R. C. *et al.* Cytoplasmic and/or nuclear accumulation of the beta-catenin protein is a frequent event in human osteosarcoma. *Int J Cancer* **102**, 338-342, doi:10.1002/ijc.10719 (2002).

218 Iwaya, K. *et al.* Cytoplasmic and/or nuclear staining of beta-catenin is associated with lung metastasis. *Clin Exp Metastasis* **20**, 525-529 (2003).
219 Ling, L., Nurcombe, V. & Cool, S. M. Wnt signaling controls the fate of mesenchymal stem cells. *Gene* **433**, 1-7, doi:10.1016/j.gene.2008.12.008 (2009).
220 Tang, Q. L. *et al.* Salinomycin inhibits osteosarcoma by targeting its tumor stem cells. *Cancer Lett* **311**, 113-121, doi:10.1016/j.canlet.2011.07.016 (2011).
221 Cai, Y., Cai, T. & Chen, Y. Wnt pathway in osteosarcoma, from oncogenic to therapeutic. *J Cell Biochem* **115**, 625-631, doi:10.1002/jcb.24708 (2014).
222 Macsai, C. E., Foster, B. K. & Xian, C. J. Roles of Wnt signalling in bone growth, remodelling, skeletal disorders and fracture repair. *J Cell Physiol* **215**, 578-587, doi:10.1002/jcp.21342 (2008).
223 Stevens, J. R. *et al.* Wnt10b deficiency results in age-dependent loss of bone mass and progressive reduction of mesenchymal progenitor cells. *J Bone Miner Res* **25**, 2138-2147, doi:10.1002/jbmr.118 (2010).
224 Bayley, J. P. & Devilee, P. The Warburg effect in 2012. *Curr Opin Oncol* **24**, 62-67, doi:10.1097/CCO.0b013e32834deb9e (2012).
225 Eves, E. M. & Rosner, M. R. MAP kinase regulation of the mitotic spindle checkpoint. *Methods Mol Biol* **661**, 497-505, doi:10.1007/978-1-60761-795-2_31 (2010).
226 Lee, H. G. *et al.* Actin and ERK1/2-CEBPbeta signaling mediates phagocytosis-induced innate immune response of osteoprogenitor cells. *Biomaterials* **32**, 9197-9206, doi:10.1016/j.biomaterials.2011.08.059 (2011).
227 Mielgo, A. *et al.* A MEK-independent role for CRAF in mitosis and tumor progression. *Nat Med* **17**, 1641-1645, doi:10.1038/nm.2464 (2011).
228 Zeng, Q. *et al.* Crosstalk between tumor and endothelial cells promotes tumor angiogenesis by MAPK activation of Notch signaling. *Cancer Cell* **8**, 13-23, doi:10.1016/j.ccr.2005.06.004 (2005).
229 McGlynn, L. M. *et al.* Ras/Raf-1/MAPK pathway mediates response to tamoxifen but not chemotherapy in breast cancer patients. *Clinical cancer research : an official journal of the American Association for Cancer Research* **15**, 1487-1495, doi:10.1158/1078-0432.CCR-07-4967 (2009).
230 Atmaca, A. *et al.* Prognostic impact of phosphorylated mitogen-activated protein kinase expression in patients with metastatic gastric cancer. *Oncology* **80**, 130-134, doi:10.1159/000329063 (2011).
231 Pelloski, C. E. *et al.* Prognostic associations of activated mitogen-activated protein kinase and Akt pathways in glioblastoma. *Clinical cancer research : an official journal of the American Association for Cancer Research* **12**, 3935-3941, doi:10.1158/1078-0432.CCR-05-2202 (2006).
232 Sasaki, K., Hitora, T., Nakamura, O., Kono, R. & Yamamoto, T. The role of MAPK pathway in bone and soft tissue tumors. *Anticancer Res* **31**, 549-553 (2011).
233 Noh, K. *et al.* Targeting inflammatory kinase as an adjuvant treatment for osteosarcomas. *J Bone Joint Surg Am* **93**, 723-732, doi:10.2106/JBJS.J.00302 (2011).
234 Huang, C. Y. *et al.* Stromal cell-derived factor-1/CXCR4 enhanced motility of human osteosarcoma cells involves MEK1/2, ERK and NF-kappaB-dependent pathways. *J Cell Physiol* **221**, 204-212, doi:10.1002/jcp.21846 (2009).

235 Chang, S. H. *et al.* Elevated inorganic phosphate stimulates Akt-ERK1/2-Mnk1 signaling in human lung cells. *Am J Respir Cell Mol Biol* **35**, 528-539, doi:10.1165/rcmb.2005-0477OC (2006).
236 Gessi, S. *et al.* Adenosine receptors in colon carcinoma tissues and colon tumoral cell lines: focus on the A(3) adenosine subtype. *J Cell Physiol* **211**, 826-836, doi:10.1002/jcp.20994 (2007).
237 Merighi, S. *et al.* Adenosine modulates vascular endothelial growth factor expression via hypoxia-inducible factor-1 in human glioblastoma cells. *Biochemical pharmacology* **72**, 19-31, doi:10.1016/j.bcp.2006.03.020 (2006).
238 Moro, S., Bacilieri, M., Deflorian, F. & Spalluto, G. G protein-coupled receptors as challenging druggable targets: insights from in silico studies. *New Journal of Chemistry* **30**, 301-308, doi:10.1039/B516389G (2006).
239 Martin, L., Pingle, S. C., Hallam, D. M., Rybak, L. P. & Ramkumar, V. Activation of the adenosine A3 receptor in RAW 264.7 cells inhibits lipopolysaccharide-stimulated tumor necrosis factor-alpha release by reducing calcium-dependent activation of nuclear factor-kappaB and extracellular signal-regulated kinase 1/2. *J Pharmacol Exp Ther* **316**, 71-78, doi:10.1124/jpet.105.091868 (2006).
240 Tsuchiya, A. & Nishizaki, T. Anticancer effect of adenosine on gastric cancer via diverse signaling pathways. *World J Gastroenterol* **21**, 10931-10935, doi:10.3748/wjg.v21.i39.10931 (2015).
241 Stemmer, S. M. *et al.* CF102 for the treatment of hepatocellular carcinoma: a phase I/II, open-label, dose-escalation study. *Oncologist* **18**, 25-26, doi:10.1634/theoncologist.2012-0211 (2013).
242 Wang, C. Y., Cusack, J. C., Jr., Liu, R. & Baldwin, A. S., Jr. Control of inducible chemoresistance: enhanced anti-tumor therapy through increased apoptosis by inhibition of NF-kappaB. *Nat Med* **5**, 412-417, doi:10.1038/7410 (1999).
243 Higgins, K. A. *et al.* Antisense inhibition of the p65 subunit of NF-kappa B blocks tumorigenicity and causes tumor regression. *Proc Natl Acad Sci U S A* **90**, 9901-9905 (1993).
244 Tang, Q. L. *et al.* Glycogen synthase kinase-3beta, NF-kappaB signaling, and tumorigenesis of human osteosarcoma. *Journal of the National Cancer Institute* **104**, 749-763, doi:10.1093/jnci/djs210 (2012).
245 Kishida, Y., Yoshikawa, H. & Myoui, A. Parthenolide, a natural inhibitor of Nuclear Factor-kappaB, inhibits lung colonization of murine osteosarcoma cells. *Clinical cancer research : an official journal of the American Association for Cancer Research* **13**, 59-67, doi:10.1158/1078-0432.CCR-06-1559 (2007).
246 Shackleton, M., Quintana, E., Fearon, E. R. & Morrison, S. J. Heterogeneity in cancer: cancer stem cells versus clonal evolution. *Cell* **138**, 822-829, doi:10.1016/j.cell.2009.08.017 (2009).
247 Yang, Z. F. *et al.* Significance of CD90+ cancer stem cells in human liver cancer. *Cancer Cell* **13**, 153-166, doi:10.1016/j.ccr.2008.01.013 (2008).
248 Singh, S. K. *et al.* Identification of human brain tumour initiating cells. *Nature* **432**, 396-401 (2004).
249 Al-Hajj, M., Wicha, M. S., Benito-Hernandez, A., Morrison, S. J. & Clarke, M. F. Prospective identification of tumorigenic breast cancer cells. *Proc Natl Acad Sci U S A* **100**, 3983-3988 (2003).

250 Ricci-Vitiani, L. *et al.* Identification and expansion of human colon-cancer-initiating cells. *Nature* **445**, 111-115 (2007).
251 Collins, A. T., Berry, P. A., Hyde, C., Stower, M. J. & Maitland, N. J. Prospective identification of tumorigenic prostate cancer stem cells. *Cancer Res* **65**, 10946-10951 (2005).
252 Adikrisna, R. *et al.* Identification of Pancreatic Cancer Stem Cells and Selective Toxicity of Chemotherapeutic Agents. *Gastroenterology*, doi:10.1053/j.gastro.2012.03.054 (2012).
253 Li, C. *et al.* Identification of pancreatic cancer stem cells. *Cancer Res* **67**, 1030-1037 (2007).
254 Kleinsmith, L. J. & Pierce, G. B., Jr. Multipotentiality of Single Embryonal Carcinoma Cells. *Cancer Res* **24**, 1544-1551 (1964).
255 Shimada, H. *et al.* Histopathologic prognostic factors in neuroblastic tumors: definition of subtypes of ganglioneuroblastoma and an age-linked classification of neuroblastomas. *J Natl Cancer Inst* **73**, 405-416 (1984).
256 Al-Hajj, M. & Clarke, M. F. Self-renewal and solid tumor stem cells. *Oncogene* **23**, 7274-7282, doi:10.1038/sj.onc.1207947 (2004).
257 Adhikari, A. S., Agarwal, N. & Iwakuma, T. Metastatic potential of tumor-initiating cells in solid tumors. *Front Biosci* **16**, 1927-1938, doi:3831 [pii] (2011).
258 Iwakuma, T. *et al.* Mtbp haploinsufficiency in mice increases tumor metastasis. *Oncogene* **27**, 1813-1820 (2008).
259 Zhang, L. & Hill, R. P. Hypoxia enhances metastatic efficiency by up-regulating Mdm2 in KHT cells and increasing resistance to apoptosis. *Cancer Res* **64**, 4180-4189, doi:10.1158/0008-5472.CAN-03-3038 (2004).
260 Hemmati, H. D. *et al.* Cancerous stem cells can arise from pediatric brain tumors. *Proc Natl Acad Sci U S A* **100**, 15178-15183, doi:10.1073/pnas.2036535100 (2003).
261 Singh, S. K. *et al.* Identification of a cancer stem cell in human brain tumors. *Cancer Res* **63**, 5821-5828 (2003).
262 Welm, B. E. *et al.* Sca-1(pos) cells in the mouse mammary gland represent an enriched progenitor cell population. *Dev Biol* **245**, 42-56 (2002).
263 Lin, G. *et al.* Tissue distribution of mesenchymal stem cell marker Stro-1. *Stem Cells Dev* **20**, 1747-1752, doi:10.1089/scd.2010.0564 (2011).
264 Beyer Nardi, N. & da Silva Meirelles, L. Mesenchymal stem cells: isolation, in vitro expansion and characterization. *Handb Exp Pharmacol*, 249-282 (2006).
265 Ginestier, C. *et al.* ALDH1 is a marker of normal and malignant human mammary stem cells and a predictor of poor clinical outcome. *Cell Stem Cell* **1**, 555-567, doi:10.1016/j.stem.2007.08.014 (2007).
266 Pors, K. & Moreb, J. S. Aldehyde dehydrogenases in cancer: an opportunity for biomarker and drug development? *Drug Discov Today* **19**, 1953-1963, doi:10.1016/j.drudis.2014.09.009 (2014).
267 Xu, X. *et al.* Aldehyde dehydrogenases and cancer stem cells. *Cancer Lett* **369**, 50-57, doi:10.1016/j.canlet.2015.08.018 (2015).
268 Cormier, J. N. & Pollock, R. E. Soft tissue sarcomas. *CA Cancer J Clin* **54**, 94-109 (2004).
269 Reynolds, B. A. & Weiss, S. Generation of neurons and astrocytes from isolated cells of the adult mammalian central nervous system. *Science* **255**, 1707-1710 (1992).

270 Dontu, G. *et al.* In vitro propagation and transcriptional profiling of human mammary stem/progenitor cells. *Genes Dev* **17**, 1253-1270, doi:10.1101/gad.1061803 (2003).
271 Shi, X., Gipp, J. & Bushman, W. Anchorage-independent culture maintains prostate stem cells. *Dev Biol* **312**, 396-406, doi:10.1016/j.ydbio.2007.09.042 (2007).
272 Hirschhaeuser, F. *et al.* Multicellular tumor spheroids: An underestimated tool is catching up again. *J Biotechnol* **148**, 3-15 (2010).
273 Ralevic, V. & Burnstock, G. Receptors for purines and pyrimidines. *Pharmacol Rev* **50**, 413-492 (1998).
274 Ghosh, S. & Karin, M. Missing pieces in the NF-kappaB puzzle. *Cell* **109 Suppl**, S81-96 (2002).
275 Silverman, N. & Maniatis, T. NF-kappaB signaling pathways in mammalian and insect innate immunity. *Genes Dev* **15**, 2321-2342, doi:10.1101/gad.909001 (2001).
276 Sasaki, Y., Schmidt-Supprian, M., Derudder, E. & Rajewsky, K. Role of NFkappaB signaling in normal and malignant B cell development. *Adv Exp Med Biol* **596**, 149-154 (2007).